THE UNIVERSITY OF HULL

A Computational Framework for Similarity Estimation and Stimulus Reconstruction of Hodgkin-Huxley Neural Responses

being a Thesis submitted for the Degree of

Doctor of Philosophy

in the University of Hull

by

Mayur Sarangdhar

M.Res. Computer Science and Artificial Intelligence, University of Sussex, 2005

B.E. Computer Engineering, University of Mumbai, 2004

November 2010

To my grandparents

Narayan Dinanath Sarangdhar

&

Shalini Narayan Sarangdhar

"Almost everything you do will seem insignificant, but it is important that you do it"

-Mahatma Gandhi

Acknowledgements

I am deeply indebted to Dr. Chandrasekhar Kambhampati for being a humble and excellent mentor who gave me the opportunity to pursue my academic dream of a PhD. Under his expert tutelage and vision, I have been able to take critical decisions that have helped during the course of my research. His constant encouragement, motivation and openness to discussions gave me a great deal of scientific freedom of expression. This thesis would not have been possible without the much-needed inspiration at regular intervals provided by him.

I would like to thank Dr. Darryl N Davis for his expert suggestions and feedback during my presentations and meetings. I owe him tons of gratitude for arranging Conference funds and hardship grants, both of which were needed during the course of my PhD.

I have dedicated this thesis to my grandparents Narayan Dinanath Sarangdhar and Shalini Narayan Sarangdhar. This dedication is a tiny drop in the ocean of gratitude towards my grandparents, who have nurtured, cared and sacrificed a lot for me since I was a child. I am indebted to my academically brilliant brother Mithun for being there for our grandparents, while I am away. My mum, Disha, is the source of positivity that encouraged self-belief in me as a child. Today, her philosophical teachings on morals and values have helped me to be on the path of righteousness. She has constantly strived for Mithun and I to have the best possible education – I cannot find the words to express my heartfelt indebtedness. My humble dad Milind, has given me the best possible comfort as a child. His coaching has

helped me win accolades in cricket in both India and the UK. I thank him for making me the person I am, his notions of humility have been the hardest to emulate.

Dr. Gowri D Nayak, a molecular biologist, has been there with me throughout this academic journey. She is my source of inspiration and aspiration, without her it would not have been possible to come this far. An excellent and patient person, she has helped me balance the content of this thesis and deserves a special mention for her help on the anatomy of a neuron. I am extremely pleased to have met her before I embarked on this journey- in her, I have a guide, a light, a friend, a peer and a confidante.

During the course of this academic journey, I have met some wonderful people – David R Glover, a cricket purist, who made lab-demonstrations very enjoyable; Helen M El-Sharkawy, who bakes lovely cakes and along with Joan L Hopper, Colleen B Nicholson, Jo Clappison and Amanda J Millson keeps the Computer Science Department working efficiently.

My fellow lab-mates Zurinahni Zainol, Julius Nganji, Nabil Abu Hashish, Nongnuch Poolsawad, and the ever-jolly Hossein Miri (Joshua) make the DRIS lab a very enjoyable place. I would like to thank Woakil U Ahamed and Nan Hu, the senior members in the lab for making me feel relaxed when I started my PhD. Shawulu H Nggada and Amer Dheedan deserve special thanks for making lab-demonstrations a unique experience. Special thanks to Karen Pearce, Atib Chowdhury and Laura J Wilson for giving me some of the best memories at the Brynmor Jones Library. My friends Chinmai, Rashmi, Sharada, Sai, Amit, Sonal, Harshad, Shweta and Sanket have made my PhD experience special.

I would also like to thank the University of Hull and University of Sussex Libraries for providing books and journal articles and access to a huge repository of information.

Abstract

Periodic stimuli are known to induce chaotic oscillations in the squid giant axon for a certain range of frequencies, a behaviour modelled by the Hodgkin-Huxley equations. In the presence of chaotic oscillations, similarity between neural responses depends on their temporal nature as firing times and amplitudes together reflect the true dynamics of the neuron. This thesis presents a method to estimate similarity between neural responses exhibiting chaotic oscillations by using both amplitude fluctuations and firing times. It is observed that identical stimuli have similar effect on the neural dynamics and therefore, as the temporal inputs to the neuron are identical, the occurrence of similar dynamical patterns result in a high estimate of similarity, which correlates with the observed temporal similarity.

The information about a neural activity is encoded in a neural response and usually the underlying stimulus that triggers the activity is unknown. Thus, this thesis also presents a numerical solution to reconstruct stimuli from Hodgkin-Huxley neural responses while retrieving the neural dynamics. The stimulus is reconstructed by first retrieving the maximal conductances of the ion channels and then solving the Hodgkin-Huxley equations for the stimulus. The results show that the reconstructed stimulus is a good approximation of the original stimulus, while the retrieved the neural dynamics, which represent the voltage-dependent changes in the ion channels, help to understand the changes in neural biochemistry. As high non-linearity of neural dynamics renders analytical inversion of a neuron an arduous task, a numerical approach provides a local solution to the problem of stimulus reconstruction and neural dynamics retrieval.

Keywords

chaotic oscillations, Hodgkin-Huxley neuron, neural dynamics retrieval, similarity estimation, stimulus reconstruction

Relevant Publications

The following papers have been published during the period of research. They inform the thesis and form a part of it.

- Sarangdhar M, Kambhampati C (2010). Chaotic Oscillations in Hodgkin-Huxley Neural Dynamics: Stimulus Reconstruction and Neural Dynamics Retrieval. *In Electrical Engineering and Applied Computing* (Article in print).

- Kambhampati C, Sarangdhar M, Poolsawad N (2010). Dysphonia Measures in Parkinson's Disease and their use in prediction of its progression. *International Conference on Knowledge Engineering and Ontology Development* (Article in print).

- Sarangdhar M, Kambhampati C (2010). A numerical model for neural stimulus reconstruction. *Engineering Letters* (Article in print).

- Sarangdhar M, Kambhampati C (2010). Quantification of Similarity using Amplitudes and Firing times of a Hodgkin-Huxley Neuron. *In Electrical Engineering and Applied Computing* (Article in print).

- Sarangdhar M, Kambhampati C (2010). Stimulus Reconstruction from a Hodgkin-Huxley Neural Response- A Numerical Solution. *In World Congress on Engineering 2010: The 2010 International Conference of Systems Biology and Bioengineering*, London, U.K. 30 June-2 July 2010, Vol. 1, pp. 627-632.

- Sarangdhar M, Kambhampati C (2010). Chaotic Oscillations in a Hodgkin-Huxley Neuron – Quantifying Similarity Estimation of Neural Responses *In World Congress on Engineering 2010: The 2010 International Conference of Systems Biology and Bioengineering*, London, U.K. 30 June-2 July 2010, Vol. 1, pp. 589-594.

- Sarangdhar M, Kambhampati C (2009). Spiking Neurons and Synaptic Stimuli - Neural Response Comparison using Coincidence-Factor. *In Advances in Electrical Engineering and Computational Science*. Edited by Gelman L, Balkan N, Ao S. Published by Springer, Volume 39, pp. 681-690.

- Sarangdhar M, Kambhampati C (2008). Spiking Neurons and Synaptic Stimuli: Determining the Fidelity of Coincidence-Factor in Neural Response Comparison. *Engineering Letters*, Volume 16 Issue 4, pp. 512-517.

- Sarangdhar M, Kambhampati C (2008). Spiking Neurons: Is coincidence-factor enough to compare responses with fluctuating membrane voltage? *In World Congress on Engineering 2008 : The 2008 International Conference of Systems Biology and Bioengineering*, London, U.K. 2-4 July 2008, Vol. 2, pp. 1640-1645.

Table of Contents

Table of Figures

List of Tables

1 Introduction

1.1 Background

The human nervous system is the most complex and delicate of all body systems and is composed of two parts, a) the Central Nervous System (CNS) and b) the Peripheral Nervous System (PNS). The CNS comprises of all the nerves in the brain and the spinal cord and covers all the nerves from the brain to the tailbone. Given the organ weight to body weight ratio of 2%, the average human brain is the most efficient organ considering the vast amount of work done by it. The PNS represents the nerves spreading out from the brain and the spinal cord, which connect the CNS to the limbs and organs (Brazier, 1977). The nervous system is a collection of nerve cells commonly known as neurons that are its fundamental and constitutional elements, which process information throughout the body.

1.1.1 Neuroscience: The Early Years

The earliest recorded observations of a neuron are around 1863-1869 by Otto Friedrich Karl Deiters using chromic acid and carmine red (Nicholls *et. al.*, 1992). The anatomical studies of Deiters however, were limited due to the lack of localised staining methods. Thus the processes, the projections or outgrowths of the neuron emanating from the neural cell body, were not identified until advancement in physiology. In the year 1873, Italian physician Camillo Golgi discovered a nervous tissue staining technique, which consisted of staining the neural membrane by silver chromate particles using a reaction between silver nitrate and potassium dichromate. Golgi aptly named the staining technique '*the black reaction*' as it resulted in a deep black deposit on the neuron against a well-contrasted yellow background. This staining technique (now known as Golgi staining) aided the identification of the neural soma, axons and the dendrites. In 1888, the

Spanish anatomist Santiago Ramón y Cajal (1899) revealed the existence of neurons as functional units of the nervous system.

The formal identification of the neuron by Ramón y Cajal impressed German anatomist Waldeyer-Hartz and in the year 1891 led to the formulation of the '*neuron doctrine*' – a fundamental idea that the nervous system is made up of discrete individual cells. Waldeyer-Hartz coined the term '*neuron*'. The neuron doctrine was based on Ramón y Cajal's conclusion about the propagation of signals in neuronal networks. Ramón y Cajal defined the '*Law of Dynamic Polarisation*', which stated that neural signals always propagated from the dendrites to the axons and then to the dendrites or soma of other neurons (Sabbatini, 2003). The principal tenets of the neuron doctrine defined the neuron as

1) the structural and functional unit of the nervous system;

2) an individual cell. The neurons were identified as discrete anatomical structures;

3) having three parts: the dendrites, soma (cell body) and axon. The interneuronal connections were possible due to axon branches making close contacts with the dendrites or the soma of other neurons;

4) a unidirectional unit. The conduction takes place in the direction from the dendrites to the soma and then to the branches of the axon.

Golgi and Ramón y Cajal shared the 1906 Nobel Prize in Physiology or Medicine in recognition for their work on the structure of the nervous system. By the early twentieth century, the anatomy of the neuron was well defined, with Ramón y Cajal describing the '*spines*' on the dendrites as a potential requirement for interneuronal communication. Around 1918, the British physiologist Charles Scott Sherrington identified these dendritic spines as receptors of synapses in dendrites and was awarded the 1932 Nobel Prize in Physiology or Medicine.

1.1.2 Neuroscience: 20th Century and Beyond

Since the pioneering work of Ramón y Cajal and the establishment of the neuron doctrine, twentieth century neuroscience focused on the physiology of neuron function. The physiological properties of the neuron were yet unidentified and required the study of isolated neurons. By 1940, physiologists were able to isolate individual neurons for functional studies and it was firmly established that electrical stimulation of a nerve cell produced a response (Brazier, 1977; Nicholls *et. al.*, 1992; Kingsley, 2000). To understand the neural response and identify the physiology of neural spiking required laboured laboratory-based work, which defined the next phase of research.

During the next decade, significant advances were made towards understanding the neuron as a logical model. Warren McCulloch and Walter Pitts (1943) suggested a simplistic neuron model with a linear threshold gate, which gave a binary output as a function of weighted inputs. Donald Hebb (1949) described the basic mechanism for synaptic plasticity to explain associative learning in a network of neurons. While these logical models were important to the formation of '*Neural Networks*' and '*Hebbian Learning*', the biochemistry and physiology of neural spiking was still unknown.

In 1952, two British physiologists Alan Lloyd Hodgkin and Andrew Fielding Huxley isolated a squid's giant axon and through their experiments explained the formation of a neural response. Hodgkin and Huxley described the elegant biophysics of a neuron in a series of mathematical equations that led to the first computational model of a neuron. Their meticulous study involved effective measurements of the various ion concentrations within the neuron and the extracellular fluid to define the state of equilibrium of a neuron. They discovered that a change in neural biophysics due to electrical excitability caused a shift from the equilibrium and resulted in the neuron firing a spike. The spiking of the neuron was identified as a physiological change in the membrane potential due to influx-efflux of ions across the cell membrane. Hodgkin and Huxley were the first to demonstrate the physiology of a neural spike using mathematical equations that defined the neural

dynamics (the influx-efflux of ions) of the cell membrane (Hodgkin and Huxley, 1952). The Australian neurophysiologist John Carew Eccles, through his work on the synapse (electrical or chemical stimulation of a nerve cell) contributed greatly towards the understanding the phenomenon of neural spiking (Eccles, 1964). In recognition for their research, Hodgkin, Huxley and Eccles shared the 1963 Nobel Prize in Physiology or Medicine.

The physiology of the neuron, documented by Hodgkin and Huxley in the form of ordinary differential equations, gave rise to '*Computational Neuroscience*'. With the advent of computational techniques to solve ordinary differential equations, the work of Hodgkin and Huxley was transformed into a computational neural model. This model, known as the Hodgkin-Huxley neuron model (described in detail in Chapter 2) is a well-known representation of a biological neuron that shows the fundamental physiological changes in ionic concentrations during a neural spike. These changes, referred to as the '*neural dynamics*' of the initiation and propagation of a neural spike are adopted in the spiking mechanism of the recent computational models like the Morris-Lecar (Morris and Lecar, 1981), FitzHugh-Nagumo (FitzHugh, 1961; Nagumo *et. al.*, 1961), Wilson model of neocortical neuron (Wilson, 1999b), and the Hindmarsh-Rose (Hindmarsh and Rose, 1984). The work of Hodgkin and Huxley was derived from physiological observations in their laboratory; hence, the Hodgkin-Huxley model is physiologically relevant.

1.2 Motivation

The term '*computational neuroscience*' identifies the ability to simulate a neuron model and predict a neural response to a stimulus, while contributing to classical neuroscience, computational biology and computational neurophysiology (Trappenberg, 2002). This ability to predict a neural response is physiologically precise in comparison with neurophysiological experiments, which has brought together computer scientists, physiologists and biologists to form a truly interdisciplinary field of study. While laboratory based experiments take weeks for completion, these *in silico* experiments

(computational simulations) take significantly less time. In addition to accurate predictions, computational simulations offer the advantage of flexible adjustment of environment variables to gather a broad range of data. On the other hand, laboratory-based measurement of neural responses at various ion concentrations require weeks of neuronal culturing and preparation of individual cultures for experiments.

Philip Strange (1992) explains that an imbalance in the neural biochemistry is responsible for various neural disorders like Parkinson's disease (PD), Huntington's disease, Alzheimer's disease (AD), schizophrenia, affective disorders like depression and mania, and anxiety. In addition, previous research suggests that there is a possible link between degeneration of motor neurons and the glutamate transporters in the brain, which cause changes in chemical concentrations (Brooks, 1986; Foran and Trotti, 2009). Hence, it is conceivable that the basis of a neural disorder is due to dysfunction at a neuronal level. Neural disorders are often clinically diagnosed using studies on body fluid and blood cells, biopsy of samples of the brain, post-mortem brain examination, imaging of living brains, neurophysiological testing or behavioural studies of drugs with defined biochemical properties. However, the clinical diagnosis is usually post-symptomatic and post onset of a disorder. The motivation for this research arises from the existing knowledge of neural modelling, the computational ability to predict a neural response and the objective of aiding clinicians and biologists to understand neural disorders in more physiological detail.

The biophysical properties of a neuron define the ionic basis of a neural spike, which represent neural function. These spikes present vast information to the clinicians about the state of a neuron, i.e. the nature of spiking activity, the strength of the stimulus or whether they deviate from normalcy (as in the Electroencephalogram, EEG). *Estimating the similarity between neural spikes therefore helps to identify distinct neural responses caused by different stimuli*. Since observations like the EEG convey information on neural

spiking patterns, studying the stimulus-response relationship and understanding neural response similarity can offer some insight into neural processing.

These neural spikes, however, do not describe the physiological state of the neuron or the nature of stimuli that evoke neural responses, which is often unknown. To understand neural disorders, retrieving information about the neural stimulus and the biochemistry will be beneficial. The exact physiological changes in a neuron can be traced using computational neural modelling that can recreate the neural biophysics and the external stimulus from a neural response. Using a phenomenological neural model such as the Hodgkin-Huxley for studying this objective can help to provide an understanding of the biophysical changes in neural disorders.

This thesis contributes towards a general foundation for recreating neural biophysics and the external stimulus with a view towards enhancing our understanding of neural functions. Identifying biochemical changes in a particular neural disorder using a computational study of neural biophysics will help in identifying the onset and remains a future objective.

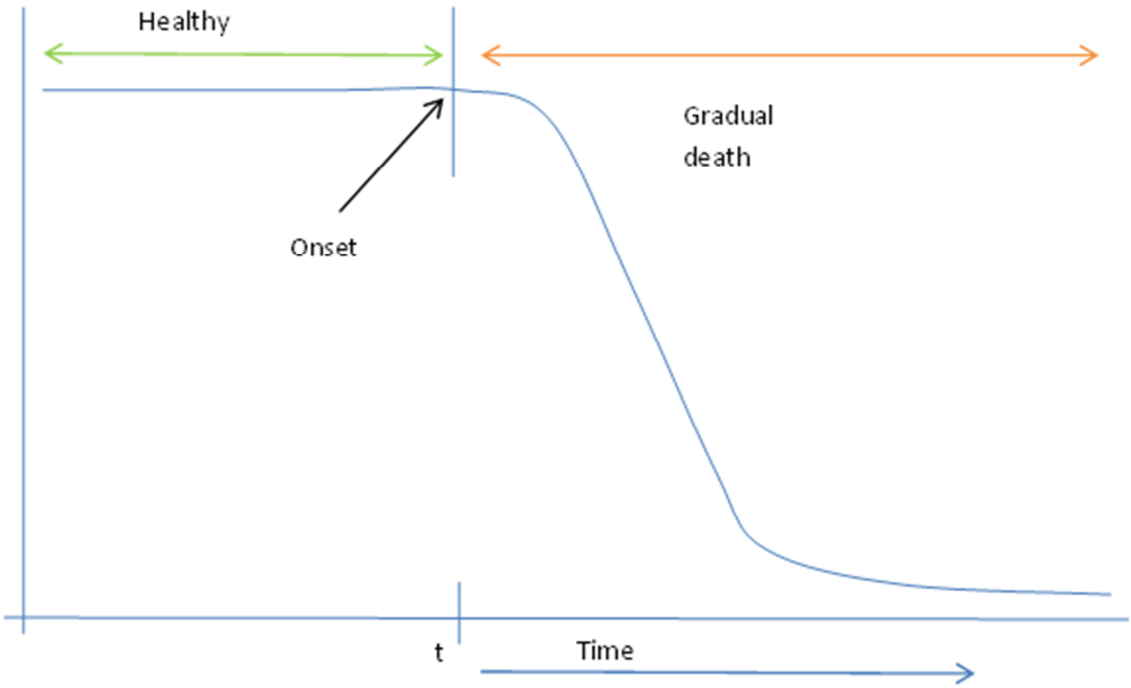

Figure 1.1: Understanding the onset of neural degeneration.

Fig. 1.1 represents transition of a neuron from a healthy state towards gradual decay. This transition in commonly observed for individual neurons in most disorders like Motor Neuron Diseases (MND), PD and AD. At disease onset, when the biochemistry of a neuron starts to drift from normalcy, it is reflected by a change in neural spiking and its function, which can be observed in the neural dynamics (Strange, 1992). Studying such neural responses and recreating the neural biophysics can contribute towards understanding and predicting onset of neural disorders. Currently, post-onset restorative neurology aims to transplant embryonic neurons using stem cells to replace decaying neurons (Nogradi and Szabo, 2009; Silani *et. al.*, 2004). The computational ability to identify the early onset can help prolong the life of a neuron by determining biochemical changes that initiate degeneration.

1.3 Aims and Objectives of this Research

The classification of neural responses based on similarity provides important information about neural stimulation to the clinicians. Populations of neurons, under similar stimulation, exhibit identical biophysics and display highly correlated firing patterns. This unique stimulus-response relationship is also observed for individual neurons (Davies *et. al.*, 2006, Chechik *et. al.*, 2006).

A neural response is dependent on the temporal nature of the stimulus indicating that a variation in the shape or form of the stimulus results in a change in the firing pattern of a neuron. For instance, two similar neurons stimulated by non-identical stimuli generate responses that are distinct and stimulus-dependent (fig 1.2-1.3). This stimulus-dependent nature of a neural response is physiologically relevant to neural spiking and is the basis of all neural activities. The dependence of neural responses on the temporal nature of stimulation is shown in fig. 1.4. *Stimulus 1* and *Stimulus 2* are two distinct stimuli that stimulate identical neurons *Neuron 1* and *Neuron 2*. Due to the nature of each stimulus, the corresponding neuron is excited at different times, thus creating independent neuronal dynamics.

The vertical line in fig. 1.4 shows that at a specific time *t*, *Stimulus 1* is at its peak while *Stimulus 2* is around its lowest value. The strength of the *Stimulus 1* is maximum therefore the chances of the *Neuron 1* depolarization are higher while *Neuron 2* will be hyperpolarized due to a weak external stimulus, thus the neuronal dynamics would differ for either neuron. The corresponding responses of the two neurons at time *t* therefore, will be non-identical and conversely, identical stimuli will result in similar neural responses.

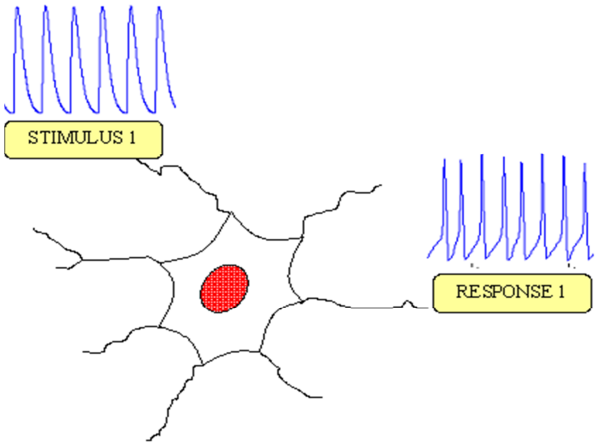

Figure 1.2: Neuron 1 stimulated by Stimulus 1 evokes a response exhibiting neural spikes.

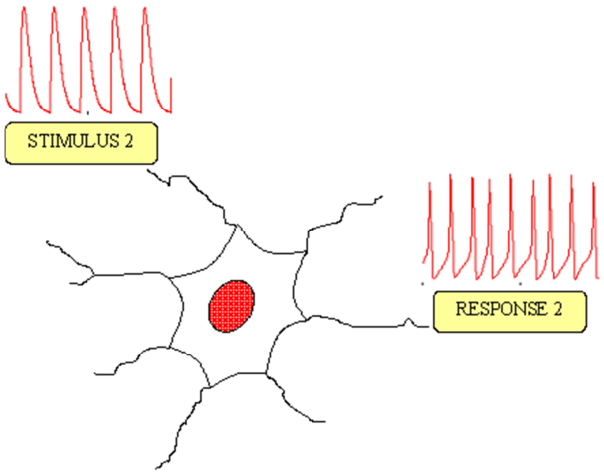

Figure 1.3: Neuron 2 stimulated by Stimulus 2 evokes a response non-identical to Neuron 1.

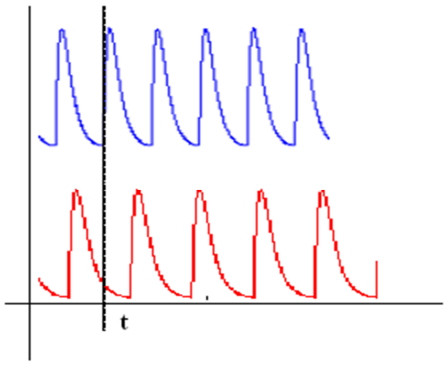

Figure 1.4: The temporal influence of distinct stimuli, Stimulus 1 – blue and Stimulus 2 - red

Classification of neural responses requires similarity estimation of individual neural spikes to differentiate identical from non-identical spikes. For individual neurons, similarity measures that aid this classification rely either on firing times of neural spikes, the time at which a neuron depolarizes, or the rate at which a neuron fires (Joeken and Schwegler, 1995; Kistler *et. al.*, 1997). On the other hand, *spike- sorting* is implemented to associate neural spikes to a specific neuron within a population of neurons (Herbst *et. al.*, 2008). This thesis considers an individual bipolar neuron (Hodgkin-Huxley neuron); and therefore, a similarity measure rather than a spike-sorting algorithm is required to identify similarity between neural responses.

One of the main objectives of this research is to understand whether similarity estimation of neural responses is physiologically plausible and mathematically accurate. An accurate estimate of similarity between neural response pairs helps to understand the effect of corresponding stimulation. Neural stimulation plays an active role in neural excitability and the nature of this stimulation is vital to neural firing. A change in stimulation reflects in neural excitability and is observed in corresponding neural responses. The relationship between neural excitability and external stimulation is governed by the neural dynamics whose retrieval from neural responses defines the next objective.

As discussed in section 1.2, this thesis aims to combine computational and mathematical knowledge with physiology and medicine to provide an approach to reconstruct the unknown stimulus of a neuron. More specifically, this thesis aims to retrieve the stimulus

and time-dependent changes in a neuron from its response. The temporal changes in a neuron represent its depolarizing and hyperpolarizing states, the opening and closing of ion channels and the conductance of ionic gates. The ability to retrieve this information from a neural response can be beneficial towards intrinsic studies in neurology and neural disorders.

1.3.1 Summary of Aims and Objectives

To summarise, the four major aims and their corresponding objectives are listed below

1) To study the effect of distinct temporal nature of stimuli on neural responses of a bipolar neuron by
    - Identifying the similarity between neural responses using an existing similarity measure
    - Understanding the effect of temporal pattern of neural responses on similarity estimation
2) To develop a similarity measure that estimates similarity between neural responses from the understanding of temporal patterns
    - To assess the accuracy and quantify the estimated similarity
3) To perform comparison of this similarity measure with an existing classification approach
    - To assess the applicability of this similarity measure to model validation
4) Reconstruct unknown stimuli from the existing knowledge of a bipolar neuron model
    - To understand time-dependent changes in ion channels and retrieve the neural biophysics during the neural stimulus reconstruction

- To demonstrate how a change in neural biochemistry reflects on the neural biophysics

1.4 Thesis Outline

The thesis is organised with a view of providing the required and necessary information to understand the chapters and their content. Considering the vast interdisciplinary knowledge in the field of computational neuroscience, this thesis hopes contribute a differential increment, but nevertheless a significant one. Certainly, in this regard, some of the questions pertaining to a broader arena and applications are beyond the scope of this thesis and the interested reader is directed to rich and valuable resources of information, these are cited in the chapters.

Each chapter introduces the problem and explains the motivation behind the research, followed by a literature review and revisiting existing approaches, if any, a problem definition, the approach and results ending with a chapter summary. The organisation of the chapters follows the aims and objectives defined in section 1.3 and are interlinked to provide a flow of information.

1.4.1 Chapter Outlines

The breakdown of the chapters is as follows

Chapter 2 introduces the reader to the biological neuron, the anatomy and the physiology with precise information on the neuron function. The reader is provided with a brief account of the internal structure of a neuron, neural biochemistry, neuron signalling and communication via synapses and neurotransmitters. The physiology of neural spiking is explained in detail considering the neural biophysics and external stimulation. With the advent of computational ability, the transition to computational modelling including mathematical equations, neural dynamics and physiological relevance is described in detail. A short account of existing computational models is given to provide the reader with an in depth information on physiological relevance in neural modelling.

Chapter 3 describes the effect of temporal nature of stimulus on a neural response, its dynamics and similarity estimation. The chapter explains the need for a new similarity measure in view of certain inconsistencies observed in an existing similarity measure. The experimental results demonstrate how nature of a stimulus affects the neural dynamics and it response. The results presented in the chapter are physiologically relevant and corroborate with the observations of physiologists. The existing similarity measure, has inconsistencies due to implicit assumptions about the neural dynamics, this chapter suggests possible changes to improve similarity estimation.

Chapter 4 describes the changes necessary for accurate similarity estimation and formulates a new similarity measure, which considers the temporal variations in the neural responses. To assess consistency, the similarity between neural responses generated by various types of stimuli is estimated using this similarity measure. The chapter exemplifies comparison between these similarity estimates and that of Chapter 3 to determine the efficiency of the similarity measure. The results of comparison are detailed in this chapter.

Chapter 5 describes the possibility of applying this similarity measure to validate computational neuron models, neural responses with minimal temporal variations and the efficiency of a similarity measure to capture absolute difference between two neural responses. This chapter introduces a detailed Integrate and Fire neuron model and describes validating its neural responses using the similarity measure. This chapter further describes a concept of energy content and its application to a neural response and its relationship with similarity measures.

Chapter 6 describes the reconstruction of unknown neural stimuli and neural dynamics from known neural responses. Chapters 3-5 establish the difference in neural responses in relation to a change in stimulation and the ability to reconstruct the stimulation can help to understand physiological changes in neuron. The chapter provides an account of the

existing approaches to reconstructions and their limitations followed by a detailed algorithm to reconstruct neural stimuli and dynamics, which is supported by well-illustrated results that aim to contribute towards the motivation of this research.

Chapter 7 summarises the thesis by highlighting the important results and discusses stimulating areas and possibilities of future work.

The author has intentionally kept the thesis precise and attached additional related work as Appendices with Appendix A describing the software platform, design, implementation, testing and algorithms used in each chapter and Appendix B describing a sample test case cluster formation.

2 The Neuron: From Physiology to a Computational Model

2.1 Introduction

The brain consists of many nerve cells that are well-defined tiny regions in the brain. De Wilde estimates that the human brain has approximately 10^{11} such nerve cells (De Wilde, 1997). Neurons are specialised cells and exhibit characteristics common to all cells. They have a nucleus and cytoplasm that is bound by a distinct cell membrane. The cytoplasm contains intracellular organelles like the endoplasmic reticulum, Golgi bodies, mitochondria, peroxisomes, ribosomes, endosomes, lysosomes and lipofuscin bodies (Kingsley, 2000; Levitan and Kaczmarek, 1997). A typical neuron has three anatomically distinct parts: the soma or the cell body, which represents the central part of the neuron, and the two different types of protrusions of the soma, the dendrite and the axon (fig. 2.1).

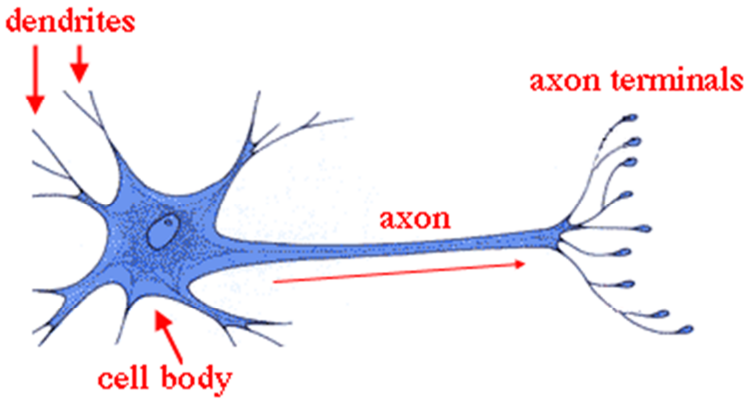

Figure 2.1: A typical neuron with its dendrites, the soma (cell body) and the axon (EruptingMind, 2010).

Neurons are generally classified based on the number of processes (projections or outgrowths of the neuron) they exhibit. Unipolar neurons have a single process, bipolar neurons exhibit two processes and multipolar neurons have more than two processes (fig.

2.2). Multipolar neurons are the most common type of neurons in the human nervous system while true bipolar neurons in the adult mammal are associated with the first, second and eighth cranial nerves. On the other hand, true unipolar neurons are common in invertebrates but are not present in the adult mammalian nervous system, which contains *pseudounipolar* neurons instead, where the single process originating from the neuron almost immediately divides into two (Kingsley, 2000).

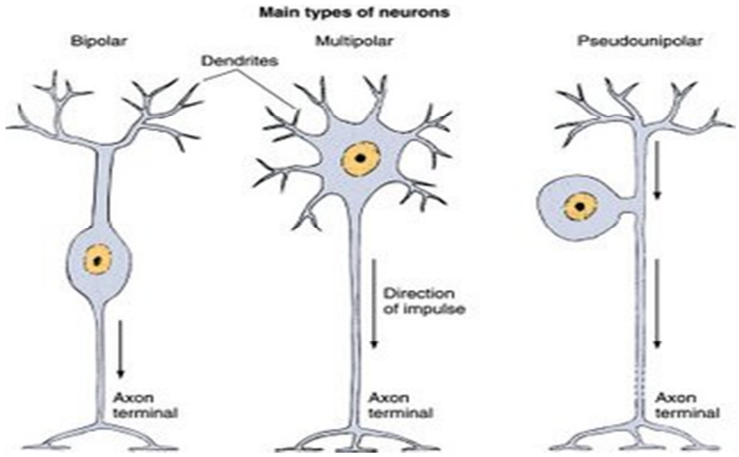

Figure 2.2: The classification of neurons based on the number of processes of the soma (Hollet, 2008).

2.2 Anatomy of the Neuron

The neurons are the principal cells of the nervous system. The anatomy of a typical neuron is described below

2.2.1 The Soma

The soma (fig. 2.3), a compact and globular structure, is the central part of the neuron and it contains the ultrastructural organelles that perform many of the cell's metabolic functions as well as those necessary for protein synthesis. The soma mostly has the same cellular components as a secretory cell and produces an extensive variety of proteins. The nucleus and the nucleolus are the most prominent structures within the soma and the DNA is mostly in the extended form allowing for its transcription. As neurons produce an extraordinary amount of proteins, the soma consists of a larger number of ribosomes, which synthesise soluble proteins that will remain within the cell. Along with this, the soma also contains a complex set of internal membranes where the newly synthesised

proteins undergo modifications necessary to generate functional proteins. The internal membrane complex encompasses the rough endoplasmic reticulum (rER) which is studded with ribosomes on its cytosolic surface and is involved in the synthesis of proteins destined for export or secretion. On synthesis, the precursor protein is extruded through the membrane into the lumen of the rER. From here, the proteins are carried in small membrane-bound transport vesicles to the luminal cavity of the membrane-limited organelle-the Golgi complex. The precursor proteins undergo various modifications within the rER and Golgi complex, including addition of carbohydrate moieties and proteolytic cleavage to release functional proteins. The proteins are finally carried to their destinations by membrane-bound vesicles that pinch off from the Golgi complex and are transported to the various locations within the neuron or even down the axon. More modifications of the proteins may occur within these transport vesicles depending on the structure and destination of the proteins (Kingsley, 2000; Nicholls *et. al.*, 1992).

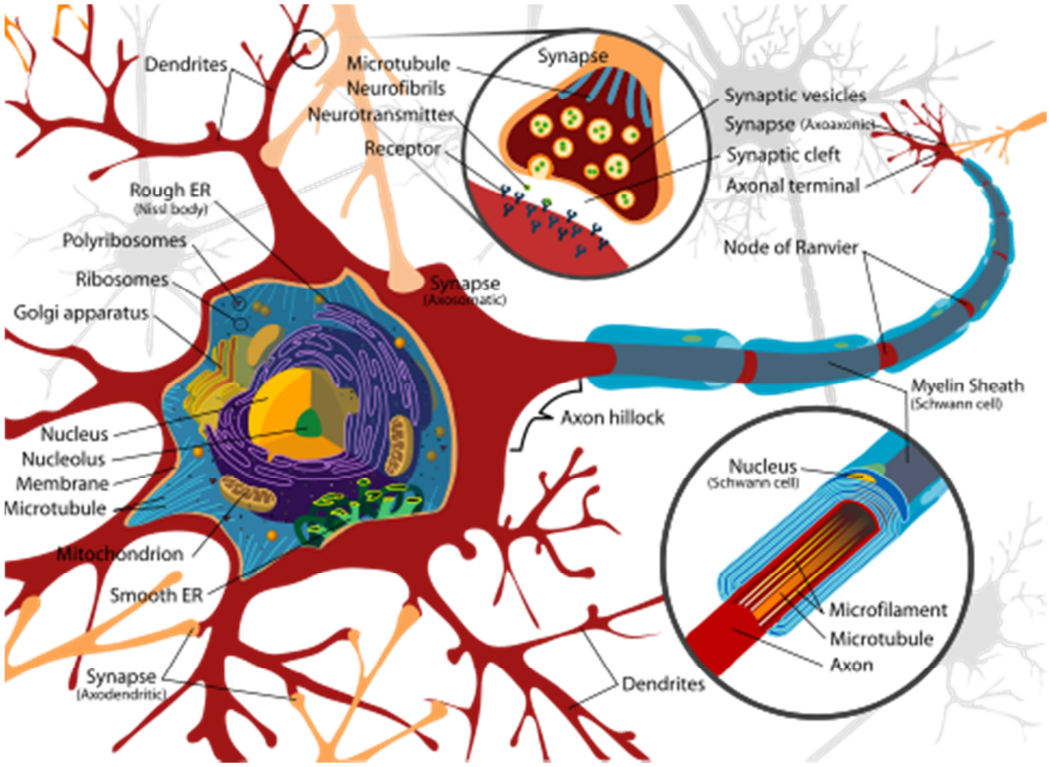

Figure 2.3: The internal membrane system of neurons (Sakshat Virtual Labs, 2010)

2.2.2 The Dendrites

The dendrites (fig. 2.1-2.2) form a tree-like structure as they branch out of the soma. They are larger at the point of attachment to the soma and get narrower as they ramify and extend away from the soma. The dendrites provide the surface for synaptic contacts from other neurons and by increasing the surface area of the neuron, they facilitate a larger number of such synaptic inputs received by the cell. The larger and more extensive the dendritic branches the greater the number and diversity of the synaptic contacts on them. Thus, the extent and variety of the synaptic connections is determined by the physical structure and arrangement of the dendrites (Kingsley, 2000; Nicholls *et. al.*, 1992).

2.2.3 The Axon

Axons are generally longer than dendrites and transmit the signals received by them. The axons usually maintain a constant radius along their entire length until they branch out at their distal end just before they terminate. The axonal branches terminate by making synaptic contacts with a small group of neighbouring cells or with a single cell. In some cases, the axons can have major branches that extend out to different groups of cells before each of them finally sprouts many subordinate branches that establish the synaptic contacts (fig. 2.4 and fig. 2.5). The axon usually can be divided into three regions: a) the initial segment, b) the axon proper and c) the synaptic bouton.

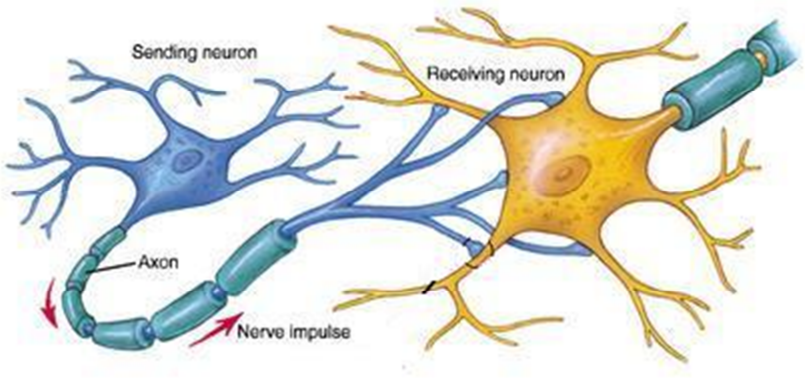

Figure 2.4: The synaptic transmission between two neurons via neurotransmitter channels (Eulo, 2008).

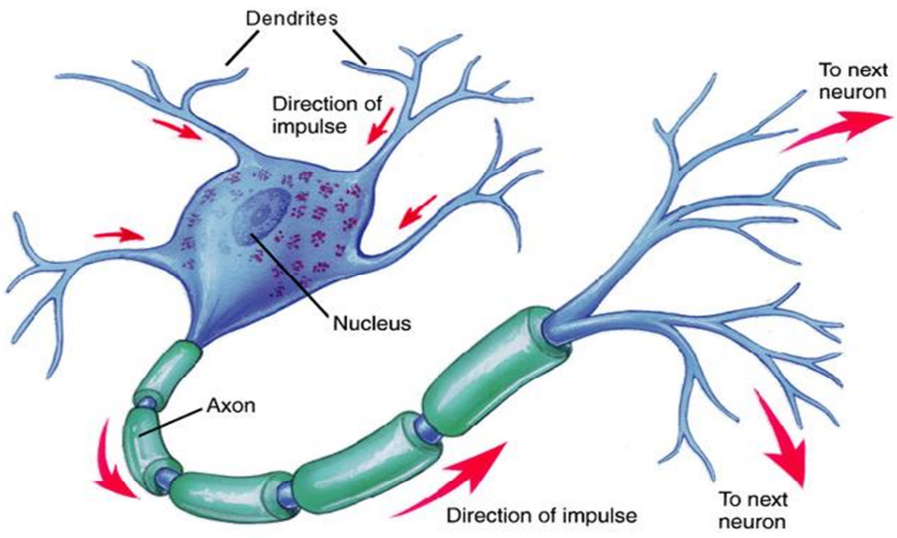

Figure 2.5: The information processing and signal flow in a typical neuron (Eulo, 2008).

2.2.3.1 The Initial Segment

In some large neurons, a conical region within the soma fails to stain with basic dyes and lacks free ribosomes and rER. This region is referred to as the *axon hillock* (fig. 2.3) and it contains long parallel bundles of neurotubules and neurofilaments. These filaments remain bundled for the first 20 to 50 μm of the axon length, a region called the initial segment. Here, one finds a layer of dense material undercoating the plasma membrane that makes the membrane in this region appear thicker under low-power electron micrographs. Voltage-sensitive sodium gates are abundantly distributed in the initial segment and the electron dense material, as seen under an electron microscope, may be due to the presence of these channels. The length of the initial segment is highly variable and is easily recognised in myelinated axons, where the distal ends of the initial segments correspond to the start of the first segment of the myelin sheath. The initial segment of the axon is the primary site of initiation and propagation of action potentials (Peters *et. al.*, 1991; Kingsley, 2000; Patestas and Gartner, 2006).

2.2.3.2 The Axon Proper

As the name suggests, the axon proper is the main body of the axon and is a long process whose diameter remains roughly constant throughout its length. Myelinated axons have

the myelin sheath beginning at the axon proper and ending at the axon terminal. In the CNS, the myelin sheath is produced by the glial cells while the Schwann cells make the myelin covering in the PNS. Discontinuous segments characterise the myelin sheath, where each myelin segment is called an internode and the discontinuities between them are referred to as nodes of Ranvier. The cytoplasm of the axon proper contains the usual cellular organelles except for free ribosomes and rER. Thus, proteins manufactured within the soma need to be continuously transported into the axoplasm (Patestas and Gartner, 2006; Nicholls *et. al.*, 1992).

2.2.3.3 The Synaptic Bouton

The synaptic bouton is a specialised structure formed by the terminal ending of an axon. It lies in close apposition to the plasma membrane of the target cell and permits the presynaptic cell to communicate with the postsynaptic or target cell. The synaptic boutons contain mitochondria, synaptic vesicles, enzymes and neurochemicals. In response to incoming electrochemical impulses, neurotransmitter molecules contained in the synaptic vesicles are released from the synaptic bouton into the synapses, specialised structures between two neurons.

Synaptic boutons usually form synapses with the dendrites or their spines of other neurons or directly onto the soma of a neighbouring neuron. These types of synapses are referred to as *axodendritic* and *axosomatic* synapses respectively, and are the most common types of synapses seen in the CNS. Less frequently, synaptic contacts are also seen between the synaptic bouton and the axon of the neighbouring neuron in which case the synapse is called an *axoaxonic* synapse (Kingsley, 2000; Patestas and Gartner, 2006).

2.3 Signal flow and Synaptic transmission

The axons and the dendrites are functionally differentiable. The synaptic boutons at the end of axon branches are used for transmitting information between neurons. The neurons are highly interconnected as their dendrites are surrounded by the synaptic

boutons of other neurons thus having about 10^4 synaptic connections between neurons (Arbib, 1995; De Wilde, 1997). Within a neuron, the dendrites initiate a flow (fig. 2.4) by taking stimulus signals from other neurons and passing them to the soma. The information is processed and the resulting output in the form of neural signals is carried by the axon to its terminals (synaptic boutons). Due to multiple synaptic connections between neurons (fig. 2.5), interneuron signal transmission (also known as synaptic transmission) occurs as signal is passed to surrounding neurons.

2.3.1 Synapses

The synapse, which derives its name from the Greek words '*syn*' meaning *together* and '*haptein*' meaning *to clasp* is responsible for the intercellular communication.

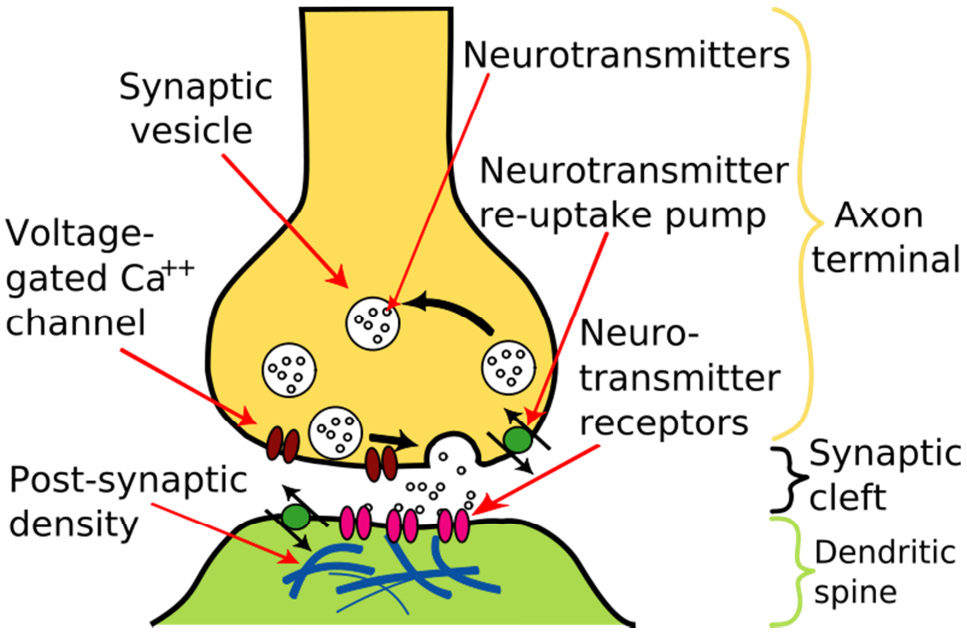

Figure 2.6: A schematic of an axodendritic chemical synapse shows how neurotransmitters bind to receptors on a dendrite after an action potential (Wong, 2009).

A chemical synapse between a presynaptic axon and a postsynaptic dendrite involves the release of neurotransmitters from the axon's synaptic bouton and their binding on dendritic receptors (fig. 2.6). In a neuron, the synaptic transmission initiates when an action potential reaches the synaptic bouton. The calcium channels open allowing the calcium ions (Ca^{++}) to rush into the bouton. The influx of these Ca^{++} ions causes the synaptic vesicles to fuse with the cell membrane and release the stored neurotransmitter

molecules in the synaptic bouton by exocytosis. The released neurotransmitter molecules diffuse across the synaptic cleft and are received by the neurotransmitter receptors on the postsynaptic dendrite.

If the neurotransmitter molecule received by the postsynaptic receptor is excitatory, the sodium (Na^+) channels open and allow Na^+ ions to rush into the cell causing a depolarization resulting in an action potential of the postsynaptic cell. If the neurotransmitter binds a different receptor and potassium (K^+) ions diffuse outward hyperpolarizing the membrane, it inhibits the action potential in the postsynaptic cell.

Each neuron in the brain and the spinal cord, may receive hundreds of excitatory and inhibitory synapses. The neuron summates the information from neurotransmitter potentials and transmits the impulse across the synapse if the summation is excitatory. In order to keep the signal duration short, enzymes in the synaptic cleft and postsynaptic membranes rapidly decompose some neurotransmitters. The remaining transmitters are reabsorbed back by the synaptic bouton via the neurotransmitter re-uptake pump.

2.3.2 Synaptic Interactions

The resting potential of the neural membrane is between -40mV and -90mV, which represents the period of no external stimulation. On external stimulation, a nerve impulse, travels along the length of the axon in the form of an action potential or a neural spike. These action potentials propagate as a wave and branch out along the axon without a change in the form the neural spikes.

Synaptic interactions occur between coupled neurons when the action potential reaches a synapse. At the synapse, the arrival of an action potential at the presynaptic cell releases neurotransmitters, which bind to the receptors and create a passage for ion-flow across the synaptic cleft into the dendrite of the postsynaptic cell (Arbib, 1995). The dendrite of the postsynaptic neuron also has a membrane potential thus an ion flow leads to an excitatory or inhibitory post-synaptic potential. If the ion channel between the synaptic

bouton and the dendrite is permeable to Na^+ and K^+ ions, it is classed as excitatory. An inhibitory postsynaptic potential prevents the membrane potential of the axon to generate a spike by releasing neurotransmitters that activate chloride (Cl^-) or K^+ ions (Eccles 1964).

There are ten thousand millions of neurons in the human brain. The axodendritic connections are of the magnitude of the number of stars in the galaxy. This shows that the human brain has a very complex underlying signalling mechanism. Each individual neuron constitutes a fundamental unit of this system making an understanding of this type of cell very important to neural information processing.

2.4 Physiology of Neural Spiking

Neural spiking or the action potential is the fundamental expression of a neural activity. This action potential is a nerve impulse, which is evoked by an external stimulation of a neuron. Physiological studies show that this electrical activity depends on the movement of charge across the plasma membrane of the neuron. The charge carriers, the *ions*, are responsible for this action potential, which is a result of transmembrane ion flow (Levitan and Kaczmarek, 1997).

The phospholipid bilayer of the plasma membrane acts as an electrical insulator and in the absence of an external stimulus, maintains equilibrium between the inside and outside of the cell. This state of rest, represented by a voltage, is known as the *equilibrium potential* or the *resting potential* of the neuron and is between -40mV and -90mV. This potential is expressed relative to the extracellular fluid, where a negative resting potential indicates that the inside of the cell membrane is more negatively charged than the outside. A cell is said to be *depolarized* if the membrane potential is less negative than the resting potential, while a cell is *hyperpolarized* if the membrane potential is more negative than the resting potential.

Highly specialised proteins that form hydrophilic pores are distributed along the plasma membrane that aid in selective transmembrane ion flow. These proteins act as regulated

ion channels and are responsible for the generation of an action potential. As the plasma membrane acts an as insulator, a strong electromotive force is required to open the ion channels for ion flow and elicit the action potential. The regulated activation and inactivation of these ion channels is gated by a voltage gradient across the membrane that allows passage of sodium (Na^+) and potassium (K^+) ions..

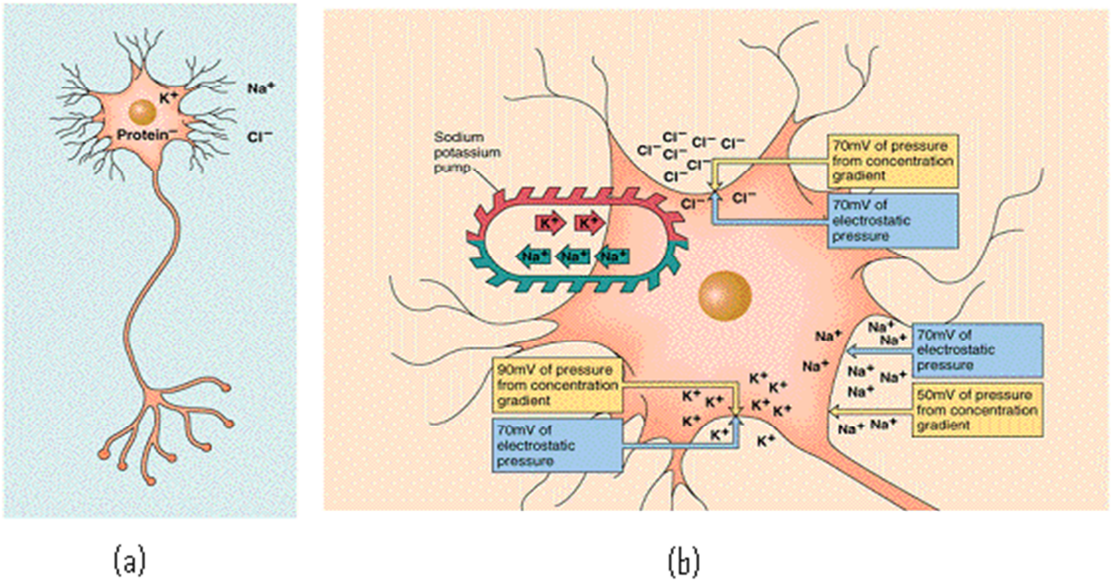

Figure 2.7: Ion exchange across ion channels. The transmembrane ion flow is fundamental for the action potential (Sakshat Virtual Labs, 2010).

At resting potential, the concentration of K^+ ions is higher inside the cell than the extracellular fluid while the concentration of Na^+ ions is higher outside compared to the inside of the cell (fig. 2.7a). The extracellular fluid also contains the chloride (Cl^-) ions. The sodium pump in the cell membrane actively exports 3 Na^+ ions out of the cell for every 2 K^+ ions that it imports into the cell (fig. 2.7b). This creates a potential difference of approximately -70 mV across the membrane. As the inside of the cell become less negative, it increases the probability that ion channels will open. With the decrease in transmembrane potential difference, a strong electromotive force causes the ion channels to open, the voltage drops further, causing more channels to open until the membrane depolarizes. The ion channels are voltage-dependent with Na^+ channels being more sensitive to voltage change than K^+ channels and so they open more rapidly. During depolarization, the Na^+ ions will rush in faster than the K^+ ions moving outwards causing

a sudden depolarization and a potential difference of approximately +30 mV. The K^+ ion channels open slowly and allow K^+ ions to flow out, which ends the action potential. The Na^+ ion channels initiate the action potential, while the K^+ ion channels terminate it. Finally, the ion channels close when the sodium pump restores the resting potential of -70 mV. These pumps transfer ions against their concentration level to restore the concentration gradient across the membrane. This restoration of ion concentration accounts for about 70% of the total metabolic consumption of a neuron (Trappenberg, 2002). Amino acids act as gates and changes in membrane potential result in conformational changes in the ion channel proteins resulting in them opening or closing.

2.4.1 The Action Potential

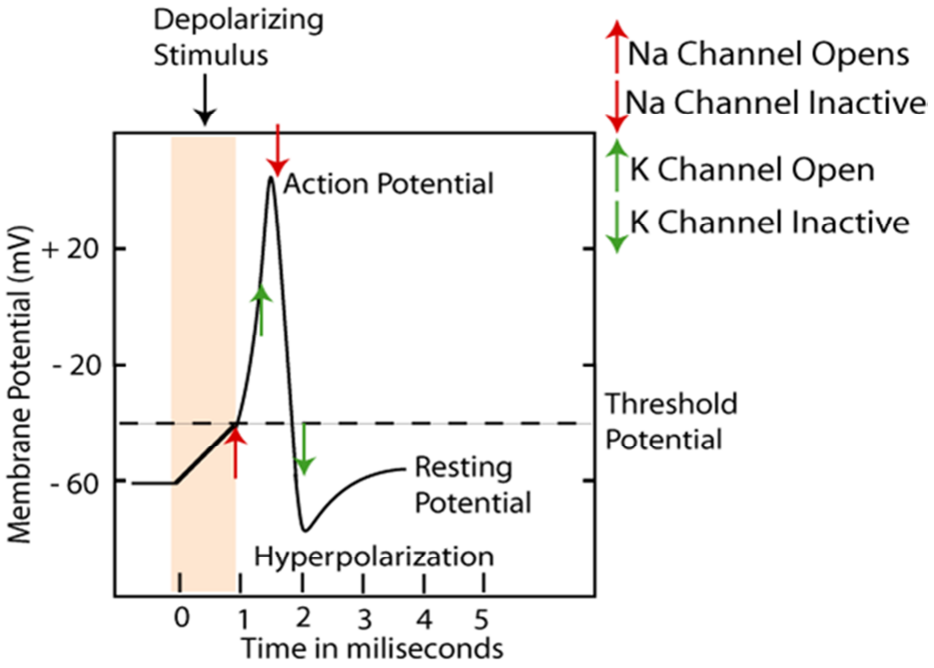

Figure 2.8: The action potential or a neural spike is the result of a transmembrane ion flow (adapted from Mann, 2008).

For instance, consider a neuron at rest (-6omV) i.e. there is no external stimulus and the plasma membrane is at equilibrium with the extracellular fluid. If an external stimulus is applied to the neuron, it disturbs the state of equilibrium by increasing the external positive charge. This depolarizing stimulus creates a strong electromotive force, which if exceeds the threshold, opens the Na^+ channels. The opening of the Na^+ channels due to a supra-threshold stimulus depolarizes the neuron and the inside of the cell becomes more

positive than the outside. The K^+ channels open slowly to balance the charge with an efflux of K^+ ions while the Na^+ channels, being more sensitive to voltage changes, close allowing the neuron to hyperpolarize. The K^+ channels close after the membrane potential drops below the threshold. The neuron then enters a *refractory period* and does not fire another action potential for a few milliseconds. Once the charges are balanced, the membrane reaches the equilibrium potential, the neuron comes back to rest and a depolarizing stimulus can re-evoke another action potential (fig. 2.8).

2.5 The Computational Model – Hodgkin Huxley Neuron

The British physiologists Alan Lloyd Hodgkin and Andrew Fielding Huxley first demonstrated through their experiments how action potentials initiate and propagate along the giant axon of a squid (Hodgkin and Huxley, 1952). They put forth these results in the form of mathematical equations that explained the role of ion channels in neural spiking. This set of nonlinear ordinary differential equations replicate the elegant biophysics and accurately simulate a real biological neuron (Abbott *et. al.*, 1990; Agüera y Arcas *et. al.,* 2003a; Hasegawa, 2000; Izhikevich, 2006; Izhikevich, 2003; Kepler *et. al.,* 1992; Kistler *et. al,.* 1997; Lundström, 1974; Maršálek, 2000; Moore and Ramon, 1974; Offner, 1974; Shriki *et. al,.* 2003; Wang and Buzsáki, 1996). Hodgkin and Huxley received the 1963 Nobel Prize in Physiology or Medicine for their work on ion channels and action potential. This model known as the Hodgkin-Huxley (HH) neuron model considers the resting potential of the neuron at 0mV for mathematical simplicity. Physiological studies later revealed the actual resting potential to be -65mV and the HH computational model uses this as the resting potential.

2.5.1 The HH Neuron Model

The HH neuron model is derived from the physiology of a neuron with each component having a biophysical analog (refer to section 2.2). The phospholipid bilayer of the plasma membrane, which acts as an electrical insulator, is represented as a capacitance C. The voltage-gated ion channels determine the ionic currents that pass through the membrane.

These ionic currents depend on the conductance of the specific ion channel. The rate of flow of ions across the plasma membrane is determined by a combination of factors a) the concentration gradient of the ions, b) the transmembrane voltage difference and c) the conductance of the ion channels. The HH model therefore can be represented as a Resistor-Capacitor (RC) circuit (fig. 2.9)

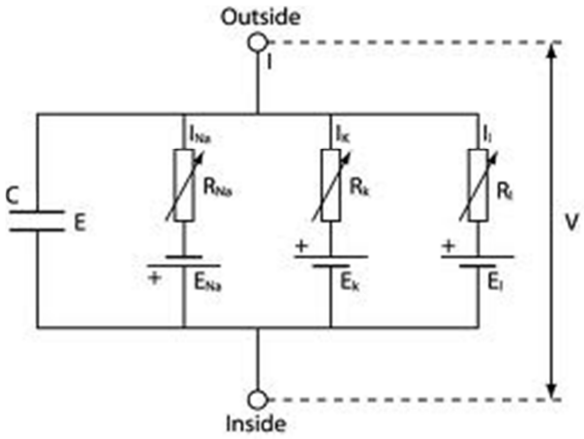

Figure 2.9: A schematic of the neural membrane represented as a RC circuit (adapted from Trappenberg, 2002).

The plasma membrane has hydrophilic pores that act as ion channels. If R_{Na}, R_K and R_L are the resistances of the sodium, potassium and the chlorine channels respectively, the number of open ion channels is proportional to electrical conductivity (inverse of resistance) and is represented by g_{Na}, g_K and g_L respectively. The conductance of an ion channel determines the amount of ions that flow across the membrane. The ionic current flowing through each channel is therefore represented by I_{Na}, I_K and I_L. The leak current consists mainly of Cl^- ions. The membrane potential V, is expressed relative to the resting potential and E_{Na}, E_K and E_L represent the equilibrium potentials for the three ion channels, which are expressed relative to the resting potential of the neuron and represented as a battery (fig. 2.9).

The equilibrium potential is the voltage required to oppose the flow of any given ion. Thus, E_{Na}, E_K and E_L are the voltages required to stop the transmembrane ion exchange and avoid a potential difference due to ionic concentration gradient. Let X^+ be an ion whose concentration is represented by $[X^+]_O$ for outside and $[X^+]_I$ for inside of the cell. The

equilibrium potential has been defined by Walther Nernst and is also known as the Nernst equilibrium potential.

$$E_X = \frac{RT}{zF} \log_e \frac{[X^+]_O}{[X^+]_I} \tag{2.1}$$

where R is the gas constant, T is the temperature in Kelvin, z is the charge on the ion and F is Faraday's constant, which is the charge in Coulombs carried by a mole of monovalent ions.

Goldman (Goldman, 1943) attempted to find the resting potential of a neuron by using the Nernst equation as a base. Hodgkin and Katz (Hodgkin and Katz, 1949) used Goldman's equation to calculate the resting potentials of cells. This equation, known as the Goldman-Hodgkin-Katz equation, gives the resting potential of a neuron (2.2).

$$V_R = \frac{RT}{zF} \log_e \frac{K_O + [p_{Na}/p_K]Na_O + [p_{Cl}/p_K]Cl_I}{K_I + [p_{Na}/p_K]Na_I + [p_{Cl}/p_K]Cl_O} \tag{2.2}$$

where p_{Na}, p_K and p_{Cl} represent the permeability of Na, K and Cl (Levitan and Kaczmarek, 1997).

2.5.2 Equations of the HH neuron

The current passing through an ion channel is given by Ohm's Law

$$I_{ion} = g_{ion}(V - E_{ion}) \tag{2.3}$$

where V is the resting potential, E_{ion} is the equilibrium potential of the ion and g_{ion} is the conductance of the ion channel. As discussed above, the generation of an action potential is governed by the voltage-dependent Na^+ and K^+ ions so Hodgkin and Huxley introduced empirically three dynamic variables, n, m and h. The variable n describes the activation of potassium channel, m describes the activation of the sodium channel and h describes the inactivation of the sodium channel. These variables, known as gating variables, give the

probability of an ion channel being open. The HH model considers that there are four potassium channels, three sodium channels and a leakage channel. The probability that all gates for an ion being open is n^4, m^3 and h respectively.

The variables m and h control the activation and inactivation of the sodium channels, hence the current passing through the sodium channel is

$$I_{Na} = m^3 h\, g_{Na}(V - E_{Na}) \tag{2.4}$$

The current passing through the potassium channel is

$$I_K = n^4\, g_K(V - E_K) \tag{2.5}$$

while the leakage current is

$$I_L = g_L(V - E_L) \tag{2.6}$$

By applying Kirchoff's Law of conservation of electric charge to fig. 2.9, we get

$$I(t) = I_C(t) + \sum_{ion} I_{ion}(t) \tag{2.7}$$

where $I(t)$ is the external current.

From the definition of capacity,

$$C = Q / v \tag{2.8}$$

where Q is a charge and v is the voltage across the capacitor. The charging current through the capacitor is

$$I_C = C\frac{dv}{dt} \tag{2.9}$$

An action potential is the rate of change of membrane potential with time. Therefore, 2.7 can be rewritten as

$$C\frac{dv}{dt} = -\sum_{ion} I_{ion}(t) + I(t) \tag{2.10}$$

Expanding 2.10, we have

$$\left.\begin{aligned} C\frac{dv}{dt} = & -g_{Na}\, m(t)^3\, h(t)(v(t) - E_{Na}) - g_K\, n(t)^4 (v(t) - E_K) \\ & - g_L (v(t) - E_L) + I(t) \end{aligned}\right\} \tag{2.11}$$

The gating variables m, n and h evolve according to the differential equations 2.12-2.14.

$$\frac{dm}{dt} = -(\alpha_m + \beta_m)m + \alpha_m \tag{2.12}$$

$$\frac{dh}{dt} = -(\alpha_h + \beta_h)h + \alpha_h \tag{2.13}$$

$$\frac{dn}{dt} = -(\alpha_n + \beta_n)n + \alpha_n \tag{2.14}$$

The functions α and β are empirical functions of v adjusted by Hodgkin and Huxley. For a better understanding, the equations 2.12-2.14 can be written in a common form

$$\frac{dx}{dt} = -\frac{1}{\tau_x(v)}[x - x_0(v)] \tag{2.15}$$

where x is either m, n or h. The gating variables approach their asymptotic values of m_0, n_0 and h_0 with a time constant $\tau_m(v)$, $\tau_n(v)$ and $\tau_h(v)$ respectively. The asymptotic values and the time constants are given by equations 2.16-2.17.

$$x_0(v) = \frac{\alpha_x(v)}{[\alpha_x(v) + \beta_x(v)]} \tag{2.16}$$

$$\tau_x(v) = \frac{1}{[\alpha_x(v) + \beta_x(v)]} \tag{2.17}$$

The physical values calculated by Hodgkin and Huxley are described in the form of equations 2.18-2.23

$$\alpha_m = 0.1(V + 40)/[1 - e^{-(V+40)/10}] \tag{2.18}$$

$$\alpha_h = 0.07e^{-(V+65)/20} \tag{2.19}$$

$$\alpha_n = 0.01(V + 55)/[1 - e^{-(V+55)/10}] \tag{2.20}$$

$$\beta_m = 4e^{-(V+65)/18} \tag{2.21}$$

$$\beta_h = 1/[1 + e^{-(V+35)/10}] \tag{2.22}$$

$$\beta_n = 0.125e^{-(V+65)/80} \tag{2.23}$$

Hodgkin wrote of Huxley's arduous task of fitting the derived biophysics to the equations by saying that it took three weeks on a desktop, hand-cranked calculator to complete the calculation of an action potential (Hodgkin, 1976; Rinzel, 1990). The work of Hodgkin and Huxley revealed the effect of ion permeability in voltage-gated ion channels and thus the initiation and propagation of an action potential. Their work established the fundamental concept behind an action potential and earned them a Nobel Prize for Physiology or Medicine in 1963.

2.5.3 Neural Dynamics of the HH Neuron

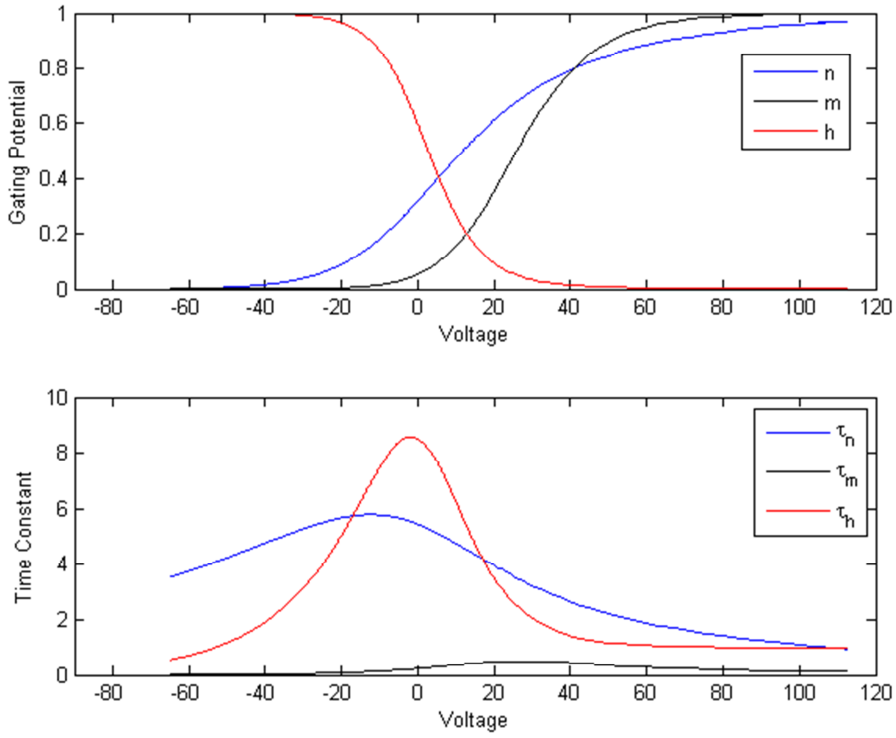

Figure 2.10: The neural dynamics of the HH neuron during an action potential very clearly describe the opening and closing of ion channels.

The open-close mechanism of the ion channels is responsible for creating an ionic concentration gradient, which initiates an action potential. The above section describes the probabilities in the form of gating variables, which effect this activation and inactivation of the ion channels. The HH model elaborately details the interplay of the gating variables, known as the neural dynamics. The neural dynamics clearly describe the time and voltage-dependence of the ion-channels during an action potential.

As observed physiologically, the time constant of the sodium channels is very small, approximately 1ms. The potassium channels, however, have a slower time constant, which in comparison with sodium channels is large (fig. 2.10). This shows that the sodium channels control the initiation of an action potential (depolarization) and the potassium channels control the termination (hyperpolarization). The dynamics traced out by the gating variables m, n and h are between 0 and 1 and outline the change in the permeability of ions in voltage-gated ion channels.

2.6 Extended Computational Models based on the HH neuron

The interplay of the gating variables that shape the formation of the action potential are defined as nonlinear ordinary differential equations. These highly nonlinear equations are of the fourth order with m, n, h and V varying with time. Since 1952, the HH neural dynamics have been the basis of numerous computational models like the Wilson model of cortical neurons (Wilson, 1999b), the Wang-Buzsaki model (Wang and Buzsaki, 1996), the Spike Response Model (Gernster and Kistler, 2002), the Izhikevich models of spiking neurons (Izhikevich, 2003; Izhikevich, 2006) to name a few. This section describes briefly two such computational models a) the Wilson model of cortical neurons and b) the Integrate and Fire neuron model that mimic physiological behaviour of neurons.

2.6.1 The Wilson Model of Human and Mammalian Neocortical Neurons

Hugh R Wilson (1999b) presented an approximation to the neocortical neurons based on ion permeability studies of Hodgkin and Huxley (Hodgkin and Huxley, 1952). The Wilson model incorporates four simulated ion currents namely the sodium current I_{Na}, the potassium current I_K, the calcium current I_T and a slow calcium mediated potassium hyperpolarizing current I_{AHP}. In addition to Na^+ and K^+, the model has Ca^{2+} equilibrium potentials due to the presence calcium channels in cortical neurons.

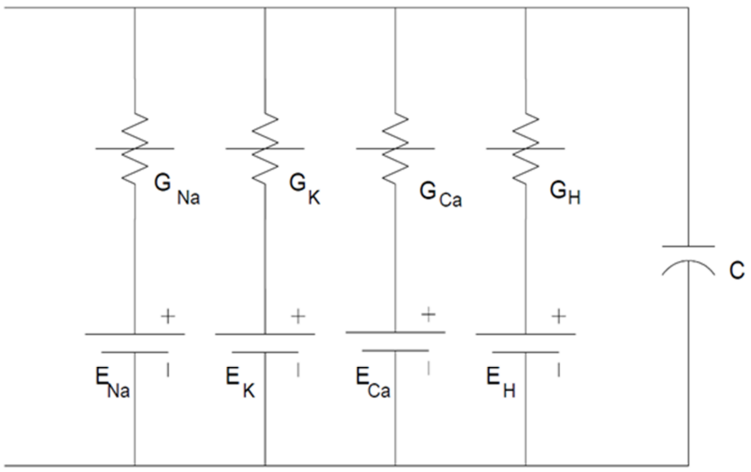

Figure 2.11: A schematic of Wilson's model of human and mammalian cortical neuron based on the HH neuron model.

Wilson noted that his model produced good approximation to spike forms, firing rates and bursting behaviour throughout the physiological range. It is observed that the fast currents (I_{Na} and I_K) are responsible for spike generation while the slower currents (I_T and I_{AHP}) produce spike frequency adaptation and bursting via firing modulation. Wilson incorporated biophysical inactivation of I_{Na} and I_T currents rather than an inactivation variable. The inactivation is done by the hyperpolarization currents I_K and I_{AHP}. The equations of the Wilson model are

$$C\frac{dV}{dt} = -m_\infty(V-0.5) - 26R(V+0.95) - g_T T(V-1.2) - g_H H(V+0.95) + I \tag{2.24}$$

$$\frac{dR}{dt} = \frac{1}{\tau_R}(-R + R_\infty(V)) \tag{2.25}$$

$$\frac{dT}{dt} = \frac{1}{14}(-T + T_\infty(V)) \tag{2.26}$$

$$\frac{dH}{dt} = \frac{1}{45}(-H + 3T) \tag{2.27}$$

where T and H are the model conductance variables for I_T and I_{AHP}. The activation of the K^+ channel is given by a time constant τ_R with equilibrium state $R_\infty(V)$. R represents that it is a recovery variable. The activation of the Na^+ channel is given by $m_\infty(V)$.

$$m_\infty(V) = 17.8 + 47.6V + 33.8V^2 \tag{2.28}$$

$$R_\infty(V) = 1.24 + 3.7V + 3.2V^2 \tag{2.29}$$

$$T_\infty(V) = 8(V+0.725)^2 \tag{2.30}$$

The Wilson model is considered more realistic in simulating neocortical spiking in comparison with FitzHugh-Nagumo (FitzHugh, 1961; Nagumo *et. al.*, 1962) or the Hindmarsh-Rose (Hindmarsh and Rose, 1984) models.

2.6.2 The Integrate and Fire Neuron Model

Since its proposition 1952, the HH neuron model has achieved the status of a classic neuron model. The relative complexity of the neural dynamics makes is mathematically difficult to study a large network of HH neurons. The Integrate and Fire (IF), which derives its name from the ability to integrate the membrane voltage until it reaches the threshold potential and subsequently firing of a spike, is a phenomenological model that replicates the behaviour of the HH neuron.

2.6.2.1 Reduction of the HH neuron

The HH neuron has four time-dependent dynamical variables V, m, n and h. For the ease of mathematical analysis, Abbott and Kepler (Abbott and Kepler, 1990) show a reduction of the HH neuron to an IF neuron. From physiological observation and the dynamics of the HH neuron, the time constant τ_m of Na^+ activation, m, is smaller than h and n. Thus, m reaches its asymptotic value $\bar{m}(V)$ faster than other changes in the model. Replacing m by its asymptotic value $\bar{m}(V)$ reduces the number of HH dynamic variables from four to three.

$$m \approx \bar{m}(V) \tag{2.31}$$

$$F(V,m,h,n) \approx F(V,\bar{m}(V),h,n) \equiv F \tag{2.32}$$

The variables h and n have longer time constants, therefore replacing them with their asymptotic values at an auxiliary voltage variable U rather than V causes the dynamics to lag behind V but approach it asymptotically.

$$h \approx \bar{h}(U) \quad n \approx \bar{n}(U) \tag{2.33}$$

so that

$$F(V,m,h,n) \approx F(V,\bar{m}(V),\bar{h}(U),\bar{n}(U)) \equiv f(V,U) \tag{2.34}$$

After evaluating, Abbott and Kepler derived a reduced two-dimensional version of the HH model

$$C\frac{dV}{dt} = -f(V,U) + I \tag{2.35}$$

$$\frac{dU}{dt} = g(V,U) \tag{2.36}$$

where

$$g(V,U) = \frac{A}{B} \tag{2.37}$$

with

$$A = \frac{\partial F}{\partial h}\left(\frac{\bar{h}(V) - \bar{h}(U)}{\tau_h(V)}\right) + \frac{\partial F}{\partial n}\left(\frac{\bar{n}(V) - \bar{n}(U)}{\tau_n(V)}\right) \tag{2.38}$$

and

$$B = \frac{\partial f}{\partial \bar{h}}\frac{d\bar{h}(U)}{dU} + \frac{\partial f}{\partial \bar{n}}\frac{d\bar{n}(U)}{dU} \tag{2.39}$$

where $\frac{\partial F}{\partial h}$ and $\frac{\partial F}{\partial n}$ are to be evaluated at $h = \bar{h}(U)$ and $n = \bar{n}(U)$. U approaches V asymptotically when $U = V$ as $g(V,U) = 0$.

2.6.2.2 Formulation of the IF Neuron

The differential equation for V represents the capacitive properties of the cell while the differential equation in U reproduces the time dependence of the membrane conductance. V represents the integrative behaviour of the capacitive cell membrane while U represents the refractory period. IF neuron models drop the U variable, hence they do not approximate the refractory behaviour of a cell. The IF neuron can be derived from section 2.6.2.1 by eliminating the dynamics of the U variable.

Abbott and Kepler (Abbott and Kepler, 1990) treat $U = -65$ (based on the resting potential of a neuron). The approximation of the capacitive cell is

$$C\frac{dV}{dt} = -f(V,-65) + I \tag{2.40}$$

Abbott and Kepler found $f(V,-65)$ to be roughly nonlinear and the higher the value of V for which $f = 0$, defines the threshold potential. They used curve fitting to derive the nonlinear IF model

$$C\frac{dv}{dt} = -0.250v + 0.083v^2 + 0.008v^3 + I \tag{2.41}$$

with $v_{threshold} = 2.5$. The parameters for the IF neuron model are derived from the HH model and curve fitting (Kepler *et. al.*, 1992). Refer to Chapter 5 for the computational implementation of an IF neuron.

2.7 Chapter Summary

The neuron constitutes a fundamental unit of the nervous system therefore; its understanding is significant to neural processing. A neuron processes external stimulation in the form of spikes that represent the basis of a neural activity and it is believed that these spikes are involved in neural processing. The physiology of the neuron can be broadly classified into three parts a) the soma or the central body, b) the axon and c) the dendrites. The axon and dendrites are the protrusions of the soma and remain functionally differentiable. Together, they branch out to form an inter-neuronal network by forming either axo-axonic, axo-dendritic or dendro-dendritic synapses. This synaptic transmission occurs due to the release and binding of neurotransmitters between the pre-synaptic and post-synaptic neurons and causes the neuron to spike.

The study of the physiology of neural spiking revealed that this electrical activity occurred because of the movement of charge across the plasma membrane of a neuron. This

transmembrane flow is due to the ions, which act as carriers of charge. Hodgkin and Huxley (Hodgkin and Huxley, 1952) studied the giant axon of a squid and explained in the form of mathematical equations, the role of ion channels in neural spiking. This set of nonlinear ordinary differential equations, which replicate the elegant biophysics and accurately simulate a real biological neuron, also explain the dynamics of the ion channels. Computational studies reveal the voltage-dependent temporal changes in the Na^+ and K^+ channels, which explain the depolarizing and hyperpolarizing phase of a neuron. As the HH neuron has a biophysical analog, the model has been extended to more complex neurons such as the cortical neuron. Wilson (1999b), introduced a model of a neocortical neuron based on the ion permeability studies of Hodgkin and Huxley. The Wilson model incorporates four simulated ion currents namely the sodium current I_{Na}, the potassium current I_K, the calcium current I_T and a slow calcium mediated potassium hyperpolarizing current I_{AHP}. In addition to Na^+ and K^+ channels, as observed in the HH neuron model, the Wilson model has Ca^{2+} equilibrium potentials due to the presence calcium channels in cortical neurons.

The ease of mathematical analysis is inversely proportional to the complexity of neurons. It is mathematically difficult to study a large network of HH neurons due to the relative complexity of their neural dynamics. The Integrate and Fire (IF), which derives its name from the ability to integrate the membrane voltage until it reaches the threshold potential and subsequently firing of a spike, is a phenomenological model that replicates the behaviour of the HH neuron. The IF neuron, which is a reduced-order model, loses its plasticity (refractoriness) due to the reduction of the Na^+ activation variable, m, to its asymptotic value. In brief, this chapter covers the evolution of computational neuroscience through literature and more specifically, the development of a computational neural model from physiological observations.

The next chapter focuses on the effect of synaptic stimuli on the neural responses and dynamics of HH neurons.

3 Chaotic Oscillations in a Hodgkin-Huxley neuron: Similarity Estimation of Neural Responses

3.1 Introduction

The intrinsically inseparable relationship of a neural stimulus and its response is fundamental for any neural activity. Each neural activity constitutes a neuron, an external stimulus and a corresponding response. This biologically important relationship is a subject of intensive research (Lundström 1974; Abbott and Kepler 1990; Davies *et. al.*, 2006; Diba *et. al.*, 2006; Izhikevich 2006) and several computational neuron models like the Hodgkin-Huxley (Hodgkin and Huxley, 1952), Integrate and Fire (Abbott and Kepler 1990), Wilson (Wilson, 1999b) and Izhikevich (Izhikevich 2003; Izhikevich, 2006) embody this fundamental relationship, which governs the basis of any neural activity. These models can be used to predict the neural response for a pre-defined stimulus. This chapter describes the effect of temporal variation in stimulation on neural responses and investigates whether similarity between stimuli can be predicted from neural responses. This objective aims to be physiologically relevant in situations where the neural responses are known but information regarding their stimuli is unknown. This chapter approaches this objective with a well-known computational model of a bipolar neuron, the Hodgkin-Huxley (HH) neuron (see Chapter 2, section 2.5).

The steady state response of the HH neuron to a constant-current stimulus is a series of action potentials that are approximately the same amplitude with precise Inter-Spike Intervals (ISI). However, on injection of a periodic or sinusoidal stimulus this steady state response is no longer preserved (Guttman *et. al.*, 1980; Matsumoto *et. al.*, 1980; Aihara *et.*

al., 1984; Matsumoto *et. al.*, 1984; Hayashi *et. al.*, 1985; Holden 1987; Hasegawa 2008; Kaplan and Glass 1995; Wilson 1999). The self-excited oscillations of a HH neuron may become chaotic i.e. the neural responses have irregular ISI and varying amplitudes, when a sinusoidal stimulus is applied with proper choices of magnitude and frequency (Aihara *et. al.*, 1984; Matsumoto *et. al.*, 1984; Kaplan and Glass 1995; Wilson 1999). Physiological experiments on squid giant axons (Guttman *et. al.*, 1980; Matsumoto *et. al.*, 1980) and Onchidium neurons (Hayashi *et. al.*, 1985) have confirmed the occurrence of chaotic oscillations. The nature of a periodic stimulus is responsible for inducing these chaotic oscillations in a biological neuron resulting in neural responses displaying irregular ISI and fluctuating amplitudes, which are the characteristics of chaotic oscillations and are absent in steady state neural responses generated by constant-current stimuli. The simulations carried out in this chapter are explained in the form of an algorithm in Appendix A, section A.5.1.

3.2 Neural Stimuli

A stimulus acts as a trigger for any neural activity that results in a neural response characterised by the temporal nature of the stimulus (Wilson and Cowan, 1973; Hasegawa, 2000; Gernster and Kistler, 2002). This stimulus can be a step-current, a constant-current, a time-varying stimulus or a periodical pulse current based on biological synapses. The following section presents examples of constant-current and periodic stimuli that trigger a neural response.

3.2.1 Constant-Current Stimuli

A constant-current stimulus is a static offset applied externally to the neuron. It is required that the selected static offset needs to be supra-threshold (substantial enough to evoke an action potential, see Chapter 2, section 2.4). The HH neuron responds to an external supra-threshold external stimulus, $I_i = 25\mu A$, with a typical display of precise firing times and constant amplitudes (fig. 3.1). Similar responses have been studied by researchers and are important as an indicator of a computational neuron model's ability to

reproduce a firing pattern similar to that of a biological neuron (Davies *et. al.* 2006; Fourcaud-Trocmé *et. al.* 2003; Kaske and Maass 2006; Kepecs and Lisman 2006; Klien *et. al.* 2006; Li and Ascoli 2006). Previous research suggests that either the firing rate or firing time of individual spikes carries specific information of the neuronal response (Rinzel 1985, Gabbiani *et. al.*, 1999, Panzeri *et. al.*, 1999, Bialek *et.al.*, 1991). This applies to all steady state responses of a neuron when a constant-current stimulus is applied.

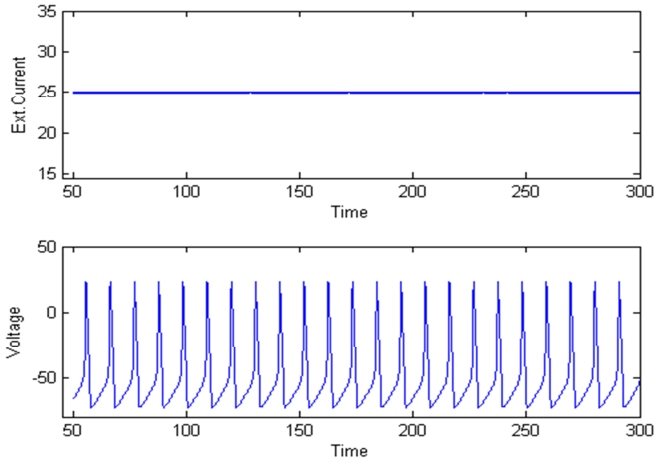

Figure 3.1: Response of the HH neuron to a constant-current stimulus. Top: A constant-current stimulus (with stochastic variations) of 25μA injected into the neuron. Bottom: Neural response to a constant-current stimulus.

3.2.2 Periodical Synaptic Stimuli

Biological synapses form an integral part of the interneuron communication channels and signal transmission and their computational representations of neuron coupling are very accurate (Nicholls *et.al.*, 1992; Gernster and Kistler, 2002). The stimulation of a HH neuron by a periodical stimulus based on synaptic modelling (Hasegawa 2000, Park and Kim 1996) is described below.

A periodical stimulus is a composite of a static offset and a periodical pulse. A presynaptic spike train injected through a synapse generates a periodical pulse train; a static offset added to this pulse train represents the synaptic periodical stimulus.

$$U_i(t) = V_a \sum_n \delta(t - t_f) \tag{3.1}$$

where V_a is the membrane resting potential, $\delta(t)$ is the delta-function which defines presynaptic spikes and t_f is the firing time defined as

$$t_{fnext} = t_f + T \tag{3.2}$$

$$t_f(1) = 0 \tag{3.3}$$

T represents the ISI of the input spike train and can be varied to generate a different pulse current. This spike train is injected through a synapse to give the pulse current I_P.

$$I_P = g_{syn} \sum_n \alpha(t - t_f)(V_a - V_{syn}) \tag{3.4}$$

g_{syn} and V_{syn} represent the conductance and reversal potential of the synapse respectively, V_a is the membrane resting potential. The $\alpha - function$ is defined as

$$\alpha(t) = (t/\tau)e^{-t/\tau}\Theta(t), \quad \Theta(t) = \begin{cases} 0, t < 0, \\ 1, t \geq 0, \end{cases} \tag{3.5}$$

where, τ is the time constant of the synapse and $\Theta(t)$ is the Heaviside step function (Park and Kim 1996). $V_a = 30mV, \tau_{syn} = 2ms, g_{syn} = 0.5mS/cm^2$ and $V_{syn} = -50mV$.

The total external stimulus (I_{ext}) applied to the neuron is a composite of the pulse current (3.4) and a static offset.

$$I_{ext} = I_S + I_P + \varepsilon \tag{3.6}$$

where, I_S is the static offset and I_P is the pulse current. ε is the random Gaussian noise with mean $\mu = 0$ and standard deviation $\sigma = 0.025$.

3.2.2.1 Biological relevance of the periodical stimulus

The transmitter-activated ion channels involved in synaptic transmission release neurotransmitters into the synaptic cleft following the activation of a presynaptic neuron. These transmitter molecules diffuse to the other side of the cleft and activate receptors

that are located in the postsynaptic membrane (Nicholls *et.al.*, 1992; Hille, 1992; see Chapter 2, section 2.3). Thus, activation of the postsynaptic receptor results in the opening of certain ion channels and results in an postsynaptic current. For more detail on synaptic transmission, refer to Chapter 2, section 2.3.

The time-dependent conductivity $g_{syn}(t)$ of the transmitter-activated ion channel opens the ion channels at the arrival of a presynaptic spike. Using Ohm's Law, the current passing through these channels depends on the difference of its reversal potential E_{syn} and the actual value of the membrane potential (Gernster and Kistler, 2002).

$$I_{syn}(t) = g_{syn}(t)(u - E_{syn}) \tag{3.7}$$

E_{syn} and $g_{syn}(t)$ characterise different type of synapses and u is the membrane resting potential.

3.2.2.1.1 GABA

GABA (γ-aminobutyric acid), a neurotransmitter associated with the fast inhibitory neurons in the central nervous system of higher vertebrates, can be mathematically modelled as

$$g_{syn}(t) = \sum_{f} \bar{g}_{syn} e^{-(t-t^{(f)})/\tau} \Theta(t - t^{(f)}) \tag{3.8}$$

$\bar{g}_{syn}(t)$ represents the conductance of the inhibitory synapses described by a simple exponential decay with a time constant τ (Gernster and Kistler, 2002).

3.2.2.1.2 AMPA

A single excitatory synapse in the central nervous system has more than one type of glutamate receptors, usually NMDA (N-methyl-D-aspartate) and non-NMDA, which are classified by certain amino acids.. The most prominent non-NMDA receptor, AMPA (α-

amino-3-hydroxyl-5-methyl-4-isoxazole-propionate), can be modelled by the time course of its postsynaptic conductivity as

$$g_{AMPA}(t) = \overline{g}_{AMPA} \cdot \mathrm{N} \cdot [e^{-(t-t^{(f)}/\tau_{decay})} - e^{-(t-t^{(f)}/\tau_{rise})}]\Theta(t-t^{(f)}) \tag{3.9}$$

where $N = 1.273$ is a constant.

Ion channels controlled by AMPA-receptors are characterised by a fast response to presynaptic spikes and a quickly decaying postsynaptic current (Gernster and Kistler, 2002).

3.2.2.2 Response of the HH neuron to periodic stimulus

A sinusoidal stimulus with proper choices of magnitude and frequency induces self-excited oscillations in the HH neuron, which may become chaotic (Matsumoto *et. al.*, 1984, Aihara *et. al.*, 1984, Kaplan and Glass 1995, Wilson 1999). Physiological experiments on squid giant axons (Guttman *et. al.*, 1980, Matsumoto *et. al.*, 1980), Onchidium neurons (Hayashi *et. al.*, 1985) and epileptic seizures (Milton and Jung, 2003) have confirmed the occurrence of chaotic oscillations due to sinusoidal or periodic stimulation.

The injection of a periodic or sinusoidal stimulus does not preserve the steady state dynamics therefore the corresponding neural response exhibits varying amplitudes and irregular firing times. Both these features are exclusive to periodic and sinusoidal stimulation and are absent in steady state responses generated by constant current stimuli. It is clear that there is significant temporal difference between neural responses generated by constant current (fig. 3.1) and periodic or sinusoidal stimuli (fig. 3.2d).

The static current of the periodic stimulus, $I_S = 25\mu A$, is based on experiments carried out by Hasegawa (Hasegawa 2000). The results below (fig. 3.2) are consistent with Hasegawa and conform to physiological observations (Guttman *et. al.*, 1980, Matsumoto *et. al.*, 1980, Matsumoto *et. al.*, 1984, Aihara *et. al.*, 1984, Hayashi *et. al.*, 1985, Holden 1987, Hasegawa 2008).

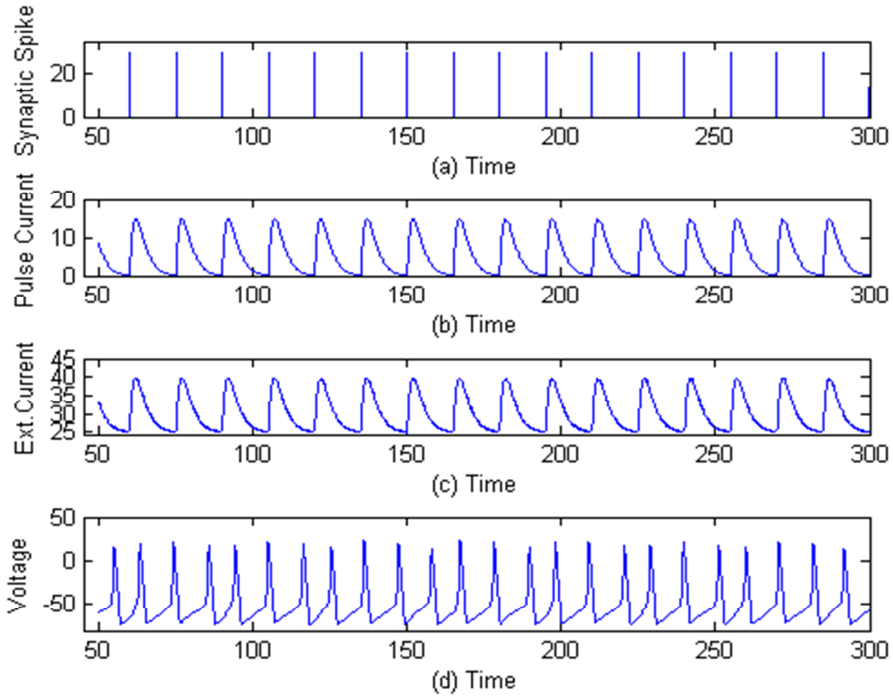

Figure 3.2: Response of a HH neuron to a synaptic input a) The pre-synaptic spike train generated by (3.1), b) The post-synaptic pulse current, c) The total external periodic stimulus (with static component and stochastic fluctuations) d) The response of the neuron to synaptic input in c.

3.3 Chaotic Oscillations and their effect on Neural Dynamics

Periodic and non-periodic neural responses of the membrane of squid giant axon to sinusoidal stimulation have elucidated the dynamical structure of the axon. The state of repetitive firing of action potentials corresponds to that of a dissipative structure with a stable limit-cycle (Matsumoto *et.al.*, 1984; Kaplan and Glass, 1995; Guckenheimer and Labouriau, 1993).

The complex non-periodic oscillations of membrane potentials found in squid giant axons under repetitive firing on injection of sinusoidal current with certain frequency and amplitude are also observed in the HH neuron (Hasegawa, 2000) (fig. 3.3). Studies show that these oscillations might be due to chaotic responses of the membrane potentials to the sinusoidal current stimulation (Matsumoto *et. al.*, 1980).

Matsumoto studied the exact nonlinear properties of the complex oscillations using stroboscopic and Lorenz plots which show that there is a complicated attractor, given as a ω-limiting set by the stroboscopic plot (Matsumoto *et. al.*, 1984). This *strange* attractor

evidently differs from other ordinary attractors consisting of a point, N points and a closed curve.

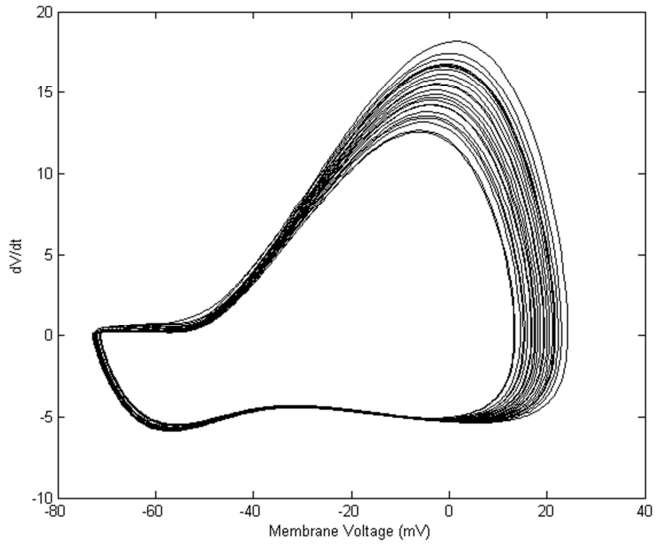

Figure 3.3: The stroboscopic plot of the HH neural dynamics shows the occurrence of chaotic oscillations in the membrane for periodic or sinusoidal stimulation. The effect of these oscillations is evident on the neural dynamics with the neural responses exhibiting fluctuating amplitudes and irregular firing times (fig. 3.2d).

In the Lorenz plot (see Matsumoto *et. al.*, 1980; Hasegawa, 2000), two curves with upward peaks are superposed and appear asymptotically. The power spectrum analysis conducted by Matsumoto (Matsumoto *et. al.*, 1980) reveals that there are two main components, each of which is a band indicating that spectral broadening occurs. The characteristics in the stroboscopic plots, the Lorenz plot and the power spectrum analysis, show that the complex oscillations of the membrane potentials exhibited due to sinusoidal stimulation are chaotic.

3.3.1 Neural Dynamics and their effect on Neural Response Similarity Estimation

As discussed above, the response of a HH neuron is dependent on the temporal nature of the stimulus, which defines its underlying dynamics. These neural dynamics represent the regulated activation and inactivation of the ion channels, which results in the depolarization or hyperpolarization of the neural membrane on application of an external stimulus. This physiological relevance requires consideration for all neural responses

generating from sinusoidal or periodic stimuli. Estimating similarity between neural responses therefore requires an implicit understanding of the neural dynamics.

The existing similarity estimation technique of neural responses is based on firing times of neural spikes, which holds for all steady state responses of a neuron when a constant-current stimulus is applied (Joeken and Schwegler, 1995). In addition, there exist other types of stimuli, which are temporally distinct from constant-current stimuli and the effect of these stimuli on the neural dynamics differs from constant-current stimulation. A constant-current stimulus causes regulated depolarization and hyperpolarization of the neural membrane due to constant strength of the stimulation. On the other hand, periodic stimuli have a varying temporal nature causing irregular alternating cycle of activation-inactivation of the ion channels, which results in irregular ISI and fluctuating amplitudes in the neural responses. In view of these stimulus-dependent dynamics, it is necessary to consider if amplitudes are required for similarity estimation (Sarangdhar and Kambhampati 2008a,b, Sarangdhar and Kambhampati 2009).

To understand the requirement of amplitude fluctuations for similarity estimation, similarity between neural responses exhibiting chaotic oscillations is first estimated using only the firing times of neural spikes. This similarity estimation is based on the principle of relative coincidences without coincidences by chance also known as 'coincidence factor' and is denoted by Γ (Joeken and Schwegler, 1995; Kistler *et. al.*, 1997).

3.4 Similarity Measure based on Neural Firing Times

Coincidence factor (Γ) is a similarity measure that estimates similarity based on firing time precision of individual neural spikes.

Consider two HH neurons HH_1 and HH_2 with neural responses R_1 and R_2 and corresponding number of spikes N_1 and N_2 respectively. In the event that the firing times of all spikes in R_1 coincide with the corresponding firing times of spikes in R_2 with a

precision of Δms, Γ returns a similarity estimate of 1. If $\Gamma = 0$, it indicates that R_1 and R_2 are highly dissimilar. The coincidence factor is defined as

$$\Gamma = \frac{N_{coinc} - \langle N_{coinc} \rangle}{1/2(N_1 + N_2)} \frac{1}{N} \tag{3.10}$$

where, N_1 and N_2 are the number of spikes in the two neural responses R_1 and R_2. N_{coinc} is the number of coincidences with a precision $\Delta = 2$ms between R_1 and R_2. $\langle N_{coinc} \rangle = 2\nu\Delta N_1$ is the number of expected coincidences generated by a homogeneous Poisson process with the same rate (ν) as the spike train to be compared. $N = 1 - 2\nu\Delta$ is the normalising factor.

Coincidence factor defines the similarity of the firing precision of a computational neuron compared to a biological neuron (Joeken and Schwegler 1995, Kistler *et. al.*, 1997).

3.4.1 Estimating Similarity using Neural Firing Times

For a bipolar neuron, distinct periodic stimuli generated by varying the ISI (T) in (3.2) invoke neural responses that are unique to the stimulus (Davies *et. al.*, 2006; Chechik *et. al.*, 2006). This unique stimulus-responses relationship, which arises from the independent neural dynamics due to the chaotic oscillations in membrane of the HH neurons (fig. 3.5), is observed by injecting HH_1 with a periodic stimulus of $T = 14ms$ and comparing the response with that of HH_2 which is stimulated by periodic stimulus of $T = 15ms$ (fig 3.4).

The results agree with physiological observations (Davies *et. al.*, 2006; Chechik *et. al.*, 2006; Hasegawa, 2000) and this unique stimulus-response relationship is also observed in other pair of neural responses generated by periodic stimuli with $T = 15ms$ and $T = 16ms$ (fig. 3.6). The chaotic oscillations induced by these two synaptic stimuli have a distinct influence on the neural dynamics and therefore the neural responses display non-identical firing patterns and amplitudes. This 1ms difference in the ISI is sufficient for a

change in the neural dynamics, which could possibly affect the information content of a neural response (fig. 3.7) (Wilson, 1999a).

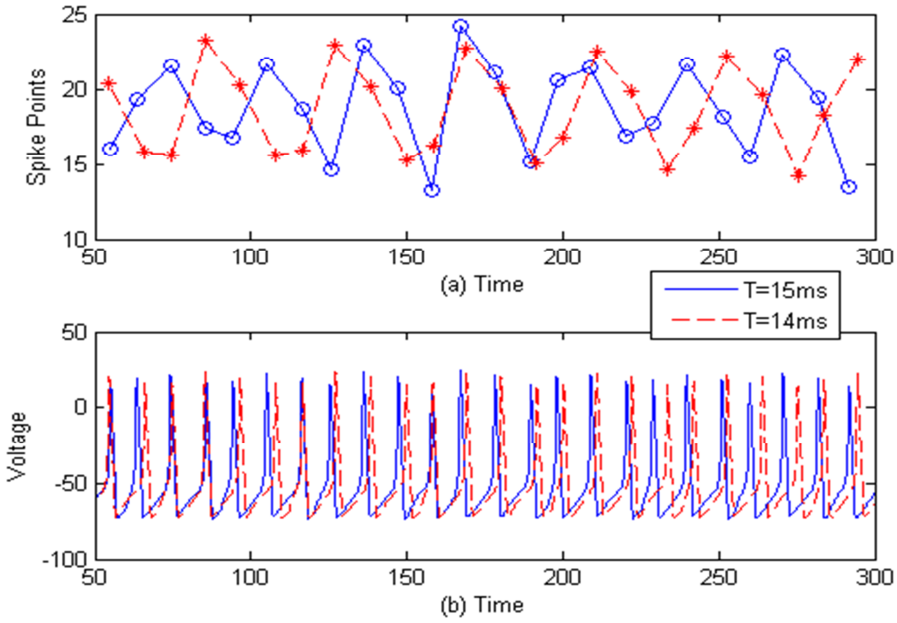

Figure 3.4: Comparison of neural responses of HH_1 and HH_2. (a) The corresponding magnitude of spikes for the responses at T=14ms and T=15ms. (b) A difference of 1ms in the ISI is sufficient to invoke characteristically different neural dynamics.

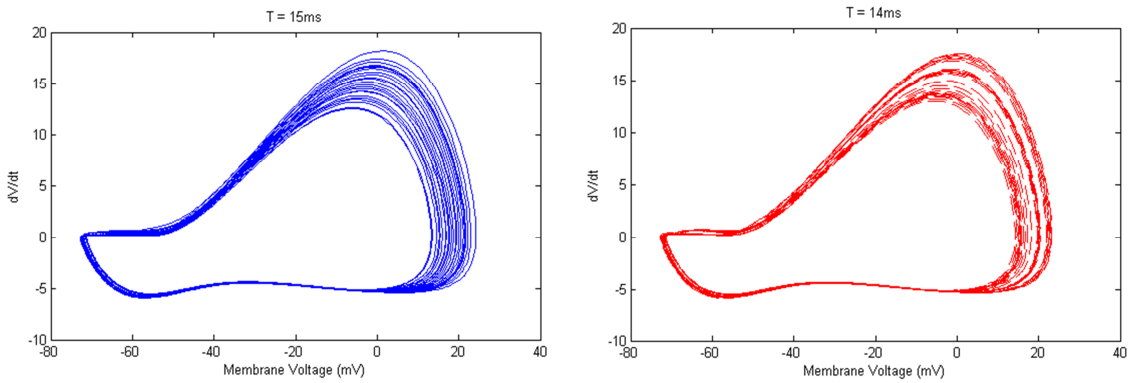

Figure 3.5: The chaotic oscillations in HH_1 and HH_2 are distinct. The effect of dissimilar periodic stimulation is clearly observed in the neural dynamics.

Unlike constant-current stimuli, this small change in the strength (static offset) or ISI of periodic stimuli effects a corresponding change in the neural dynamics, which results in stimulus-dependent neural responses.

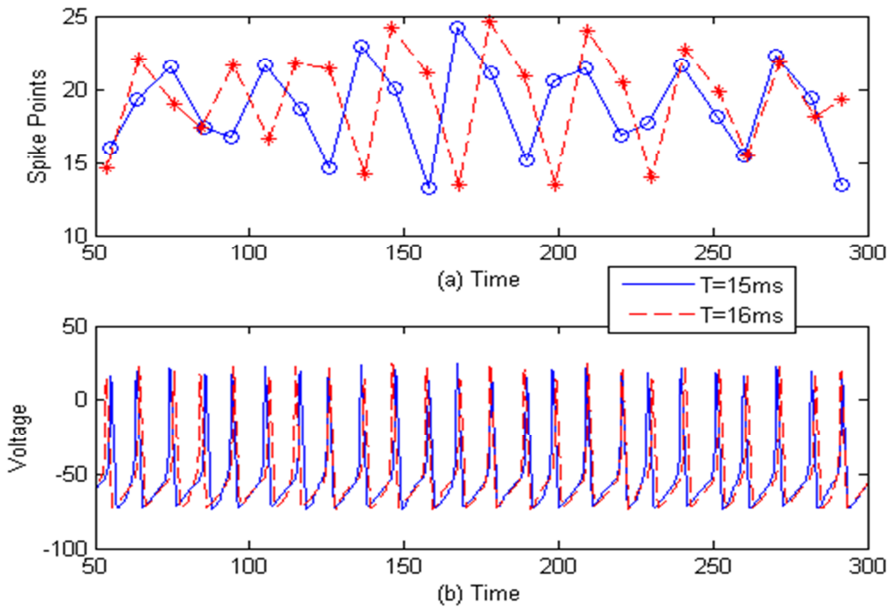

Figure 3.6: Comparison of neural responses of HH_1 *and* HH_2. (a) The corresponding magnitude of spikes for the responses at T=15ms and T=16ms. (b) A difference of 1ms in the ISI is sufficient to invoke characteristically different neural dynamics.

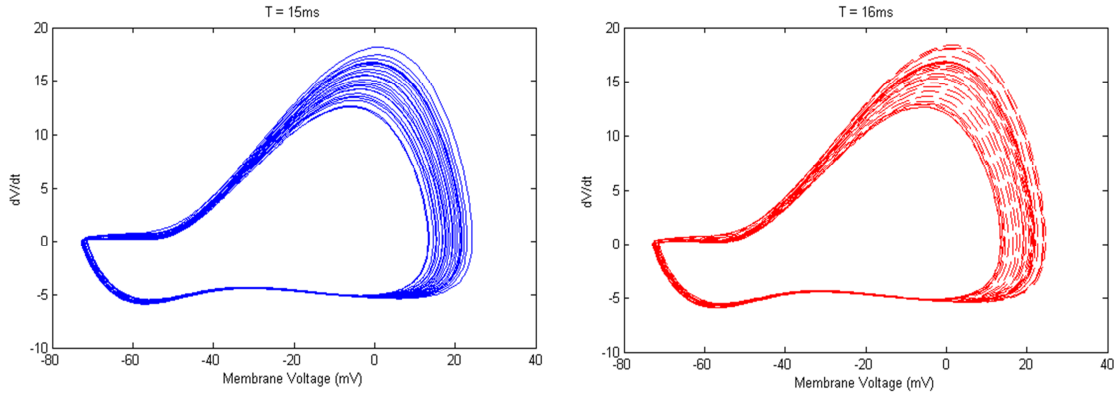

Figure 3.7: The underlying chaotic oscillations in HH_1 *and* HH_2 are dissimilar, indicating that the effect of the periodic stimulation is distinct and the neural responses evoked as a result are non-identical. The attractor traced by HH_1 is denser than HH_2.

Computational neuroscientists accept 2ms as a biologically relevant neural firing precision time based on the refractory nature of an action potential. As discussed in Chapter 2, an action potential is initiated by the opening of sodium channels. The sodium channels have a very small time-constant and they shut within 1ms. This sudden depolarization, which causes the neuron to spike will stop after the sodium channels close. The subsequent opening of the potassium channels, which have a higher time-constant than sodium, eventually bring the neuron to its resting potential via hyperpolarization. The time for a neuron to fire and return to its resting potential is approximately 2ms.

It is seen that a tiny change in the ISI (T) of stimulation leads to dissimilar neural dynamics, so to determine similarity between stimulus-dependent neural responses, two HH neurons (HH_1 and HH_{ref}) are stimulated using periodic stimuli by minimally varying T. HH_1 is stimulated by varying T between 14ms-16ms (set I), 13ms-15ms (set II) and 15ms-17ms (set III) and similarity is estimated by comparing its responses with the response R_{ref} of HH_{ref} for each set. HH_{ref} is stimulated by a periodic stimulus with a fixed ISI(T_{ref}) which is 15ms for set I, 14ms for set II and 16ms for set III.

3.4.1.1 Set I: Similarity Estimation, 14ms-16ms

$T_{ref} = 15ms$ represents the ISI of the periodic stimulus which stimulates HH_{ref}. The corresponding R_{ref15} is considered as a reference neural response for set I. As the neural dynamics are sensitive to change in stimulation, T is varied in small increments between 14ms and 16ms to stimulate HH_1. Each response of HH_1 is compared against R_{ref15} and similarity is estimated by coincidence factor Γ. As discussed above, Γ estimates similarity based on firing time precision of individual neural spikes.

If N_1 and N_2 are the number of spikes in R_{ref15} and any HH_1 response respectively, N_{coinc} represents the number of firing time coincidences with a precision $\Delta = 2$ms. $\langle N_{coinc} \rangle = 2\nu\Delta N_1$ gives the number of expected coincidences generated by a homogeneous Poisson process with the same rate ν as the neural response to be compared (i.e. HH_1). $N = 1 - 2\nu\Delta$ is the normalising factor that bounds the similarity estimate between 0 and 1.

Let β be the difference between the corresponding ISIs of the stimuli such that

$$\beta = T - T_{ref} \tag{3.11}$$

where T and T_{ref} represent the ISI of periodic stimuli stimulating HH_1 and HH_{ref} respectively.

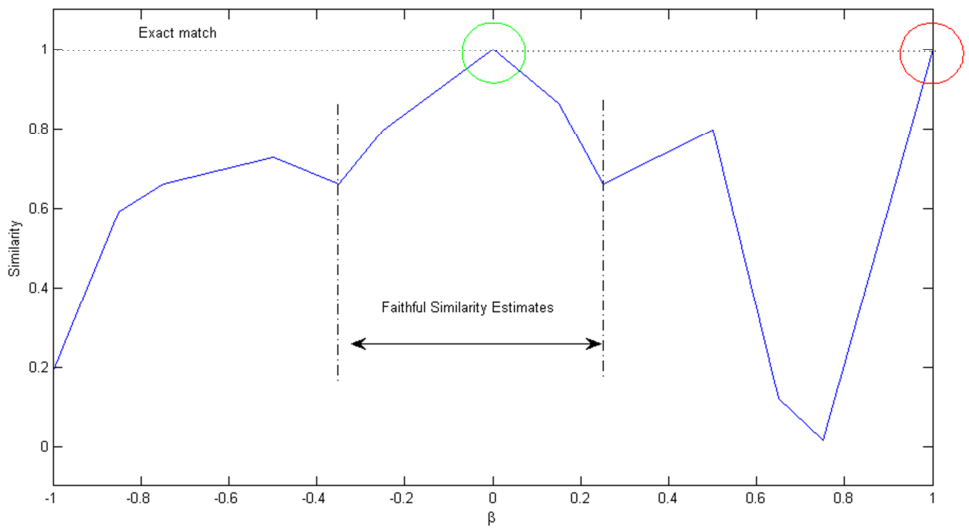

Figure 3.8: Similarity estimates based on firing times for $14ms \leq T \leq 16ms$ and $T_{ref} = 15ms$. It is expected that similarity between neural responses generated by identical stimuli will be high. This is highlighted by the green circle. It indicates that the two neural responses are an exact match. Interestingly, when $\beta = +1$, the resulting similarity between responses is high. This is seen as a false positive in view of temporal dependency, which defines a neuron's underlying dynamics.

At $\beta = -1$, $T = 14ms$ and $T_{ref} = 15ms$, the pre-synaptic spike trains and their resulting postsynaptic periodic stimuli generated by T and T_{ref} are 1ms apart therefore having distinct temporal effect on the neural dynamics of HH_1 and HH_{ref} respectively. This is reflected by the different firing times and amplitudes of the neural responses (fig. 3.9). Γ estimates the similarity between the neural responses as 0.1987 (fig. 3.8). This low coincidence factor indicates the responses are very dissimilar to each other, possibly due to irregular firing of spikes and the fluctuation in the amplitudes.

At $\beta = 0$, $T = 15ms$ and $T_{ref} = 15ms$, both stimuli are identical and the estimated similarity $\Gamma = 1$ indicates that corresponding neural responses are an exact match (fig. 3.10). This result is expected from a mathematical and signal transmission standpoint and conforms to physiological observations (Davies *et. al.*, 2006, Chechik *et. al.*, 2006; Hasegawa, 2000). Hence, $\beta = 0$, also indicates that the periodic stimuli are identical as they have equal ISI. $\beta = +1$ represents $T = 16ms$ and $T_{ref} = 15ms$ and it is seen for these ISI values of stimulation (fig. 3.11), the neural responses show a similarity $\Gamma = 1$ (fig. 3.8). This high coincidence factor is unexpected and it is important to note that as both stimuli are non-identical they have distinct effect on the neural dynamics and an exact match

between neural responses is unlikely. This result therefore, is a *false positive* and it incorrectly indicates that the two neurons HH_1 and HH_{ref} have identical stimulation.

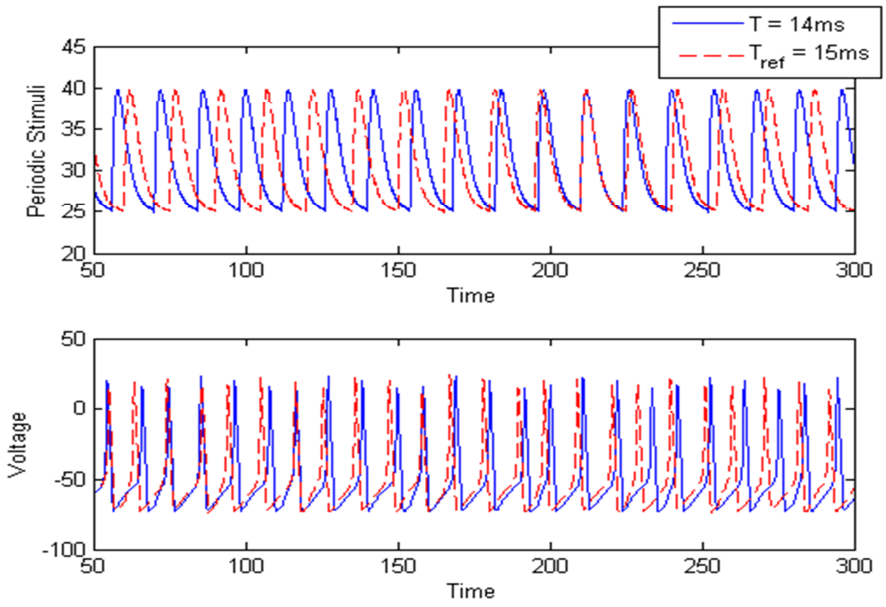

Figure 3.9: Effect of temporal variation of periodic stimuli on neural dynamics is seen in the dissimilarity between responses of HH_1 and HH_{ref}. Stimuli are generated with $T = 14ms$ and $T_{ref} = 15ms$ and correspond to $\beta = -1$.

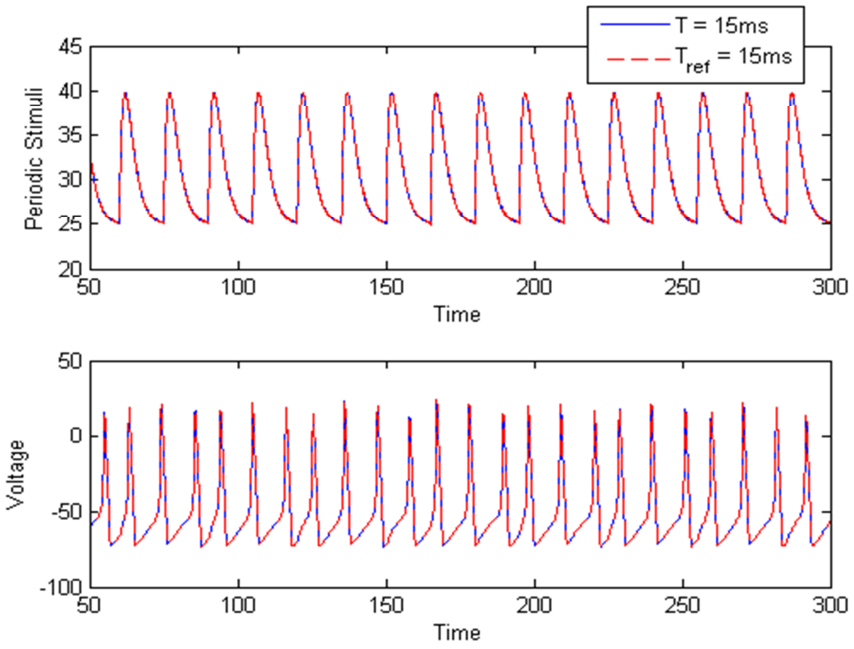

Figure 3.10: Identical stimuli have similar effect on the neural dynamics therefore resulting in exactly matching neural responses. Periodic stimuli generated with $T = 15ms$ and $T_{ref} = 15ms$ correspond to $\beta = 0$.

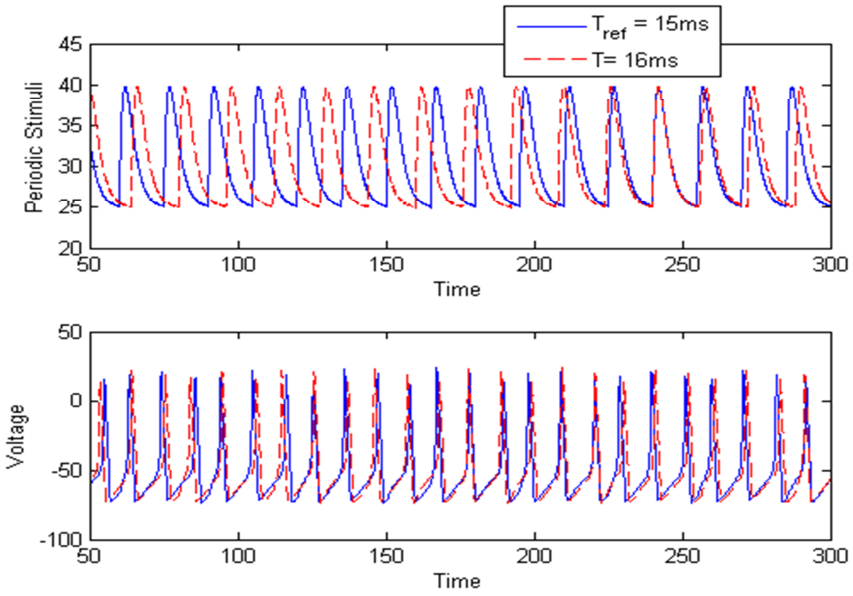

Figure 3.11: The periodic stimuli are generated with $T = 16ms$ and $T_{ref} = 15ms$ and correspond to $\beta = +1$. The distinct pulse widths of the stimuli are responsible for dissimilar chaotic oscillations in the membrane. The resulting neural responses differ in corresponding firing times and amplitudes.

Across the range of stimulation for set I, the estimated similarity increases with an increase in β from -1 to -0.5. For values of β between -0.5 to -0.35, the similarity decreases with increase in β while similarity for $-0.35 \leq \beta \leq 0.25$ decreases with the increase in β. An inconsistent trend of similarity estimates is observed for $0.25 < \beta \leq 1$, which can be attributed to the underlying chaotic oscillations in the neural membrane caused by periodic stimulation resulting in irregular firing times and fluctuating amplitudes. In summary, the existence of false positive in set I is the result of coincidence factor estimating similarity using only firing times coincidences.

3.4.1.2 Set II: Similarity Estimation, 13ms-15ms

In set II, the ISI is varied between 13ms-15ms to further study the effect of ISI variation on neural responses. HH_{ref} stimulated by periodic stimulus with ISI, $T_{ref} = 14ms$, generates the reference response R_{ref14} while T is varied between 13ms-15ms to stimulate HH_1. Each response of HH_1 is compared against R_{ref14}.

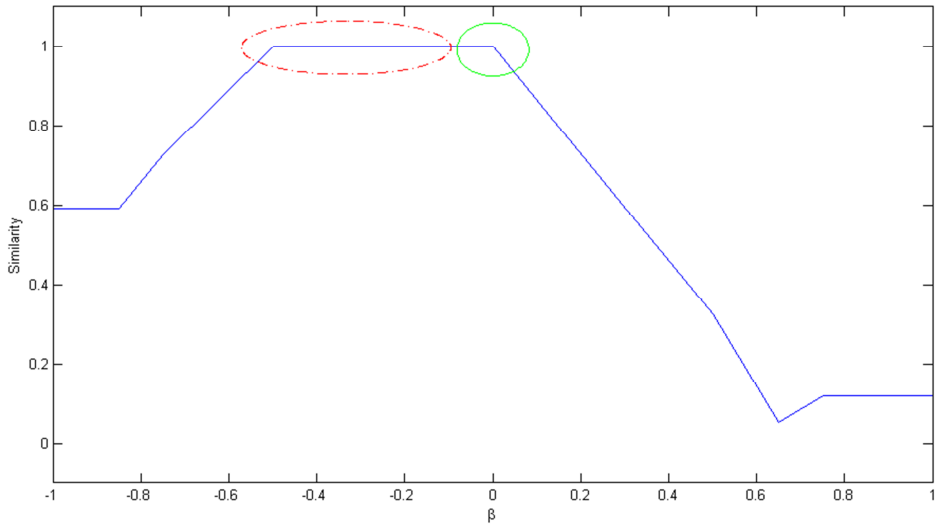

Figure 3.12: Similarity estimates based on firing times for $13ms \leq T \leq 15ms$ and $T_{ref} = 14ms$. Identical stimuli ($\beta = 0$) generate exactly matching neural responses. This is highlighted by the green circle. For $-0.5 \leq \beta < 0$, neural responses exhibit very high similarities. These represent false positives in view of temporal dependency which defines a neuron's underlying dynamics (red dashed circle).

For $\beta < 0$, approximately 40% of dissimilar neural response pairs are incorrectly shown to be identical as $\Gamma = 1$ for $-0.5 \leq \beta < 0$ (fig. 3.12). These false positives are a result of coincidence factor considering only firing times of neural spikes to estimate similarity. These neural responses have spikes that fire within a precision of 2ms, however, there exist amplitude fluctuations and if the neural responses were identical, their neural dynamics (opening/closing of ion channels) would be regulated at similar time intervals. The observed fluctuations in the amplitudes indicate ion channels do not follow identical activation-inactivation cycles. Hence, these high similarity estimates are termed as false positives. As discussed in the above section, unless $\beta = 0$, each pair of stimuli have distinct effect on the neural dynamics and an exact match of neural responses is unlikely.

3.4.1.3 Set III: Similarity Estimation, 15ms-17ms

The ISI of the periodic stimulus is varied between 15ms-17ms while $T_{ref} = 16ms$ is used to stimulate HH_{ref}, the reference response R_{ref16} acts as a reference for estimating similarity in set III. T is varied between 15ms and 17ms to stimulate HH_1 and each response of HH_1 is compared against R_{ref16}.

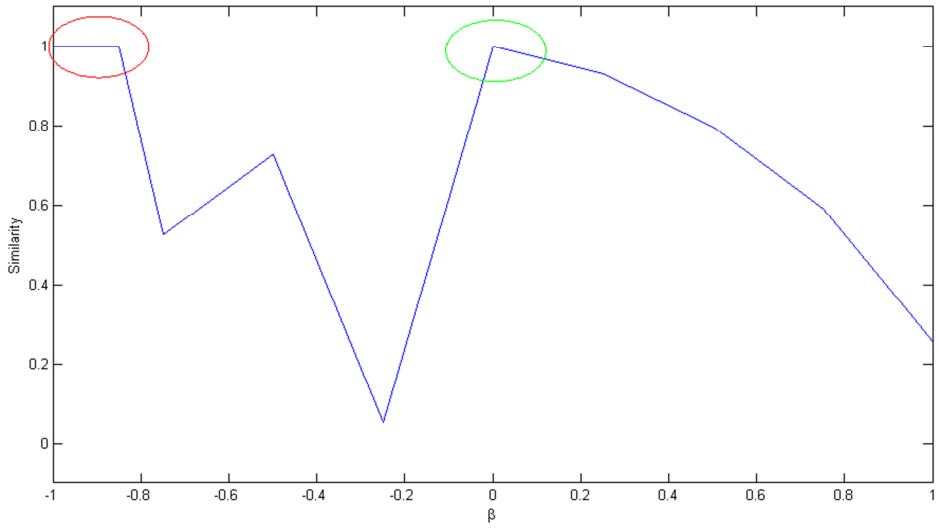

Figure 3.13: Similarity estimates based on firing times for $15ms \leq T \leq 17ms$ and $T_{ref} = 16ms$. Identical stimuli ($\beta = 0$) generate exactly matching neural responses. This is highlighted by the green circle. For $-1 \leq \beta \leq -0.85$, neural responses exhibit very high similarities. The false positives are represented by red dashed circle. For $0 \leq \beta \leq +1$, the similarity estimated by Γ decreases with an increase in β.

The results (fig. 3.13) show that *false positives* also exist in set III. The similarity estimated by Γ decreases between $-0.85 \leq \beta \leq -0.75$ and $-0.5 < \beta \leq -0.25$ while Γ increases between $-0.75 < \beta \leq -0.50$ and $-0.25 < \beta \leq 0$. When $T = 15ms$ and $T_{ref} = 16ms$, $\beta = -1$, the two periodic stimuli have non-identical pulse widths. This temporal variation in the stimuli has a significant role in shaping the neural dynamics (see section 3.3), which results in dissimilar corresponding firing times and amplitudes due to non-identical oscillations (fig. 3.7). The similarity estimated for this pair of neural responses is 1 and classifies the two neural responses as identical. As discussed earlier, this too is a false positive.

The similarity for $\beta = -1$ in set III is exactly similar to $\beta = +1$ in set I as they both correspond to ISIs $15ms$ and $16ms$. This establishes that similarity estimated by Γ is consistent for the same pair of neural responses across different sets, however, as seen in the three sets, the approach based on firing time coincidences cannot be scaled to neural responses exhibiting chaotic oscillations especially in view of the false positives. These false positives incorrectly identify two neural responses as identical and for a bipolar neuron, it leads to inaccurate classification of stimuli being similar.

These results show that in cases where significant fluctuations in membrane voltages exist, this one-dimensional approach of firing times coincidences is not sufficient to establish similarity between neural responses. Two key observations derived from sections 3.4.1.1-3.4.1.3 are a) coincidence factor generates false positives for some pairs of neural responses and b) for a single neuron, a false positive incorrectly indicates that the underlying neural stimuli are identical. The false positives show that formulation of coincidence factor did not consider temporal variations, which are dependent on the neural dynamics. It is therefore concluded that coincidence factor is insufficient to estimate similarity between neural responses exhibiting chaotic oscillations and was first outlined by Sarangdhar and Kambhampati (2008a,b; 2009).

3.5 Analysis of Neural Responses

The results in the previous sections show that the temporal nature of periodic stimuli influences the neural dynamics which are responsible for irregular firing times and fluctuating magnitudes of spikes. This section aims to identify the existence of any relationships between the intrinsic parameters of the neural responses, such as the rate of fire, variations in amplitudes, the mean and standard deviation of neural responses, the relationship between ISI of the stimulus and corresponding neural response and their effect on similarity estimation.

3.5.1 Set I: Analysis, 14ms-16ms

Unlike constant-current stimuli, neural responses generated by periodic stimuli exhibit fluctuating amplitudes that are due to underlying chaotic oscillations in the neural membrane. It is seen (fig. 3.14) that mean amplitudes vary between 18.60mV for R_{14} (response with $T_{in} = 14ms$) to 19.26mV for R_{16} with corresponding standard deviation $\sigma_{Amp_{14}} = 3.03$ for R_{14} and $\sigma_{Amp_{16}} = 3.58$ for R_{16}. The maximum mean amplitude μ_{AmpMax} is 19.68mV for $R_{15.65}$ and maximum mean standard deviation σ_{AmpMax} is 4.75 for $R_{15.75}$. These results suggest that the mean amplitudes, μ_{Amp}, tend to increase with the ISI, possibly suggesting that the increase in the ISI causes more depolarization. However, it is

observed that a few neural responses show a decrease in μ_{Amp} with an increase in the ISI. The alternating activation-inactivation of ion channels is not regulated at specific time intervals as seen in steady state neural responses, this decrease in μ_{Amp} is due to the hyperpolarization induced by the opening of the potassium channels and the refractory nature of a neuron. The standard deviation, σ_{Amp}, increases with μ_{Amp} and vice-versa. The increase in μ_{Amp} can be attributed to the increase in the period (ISI) of the stimuli which acts as a sustained supra-threshold current.

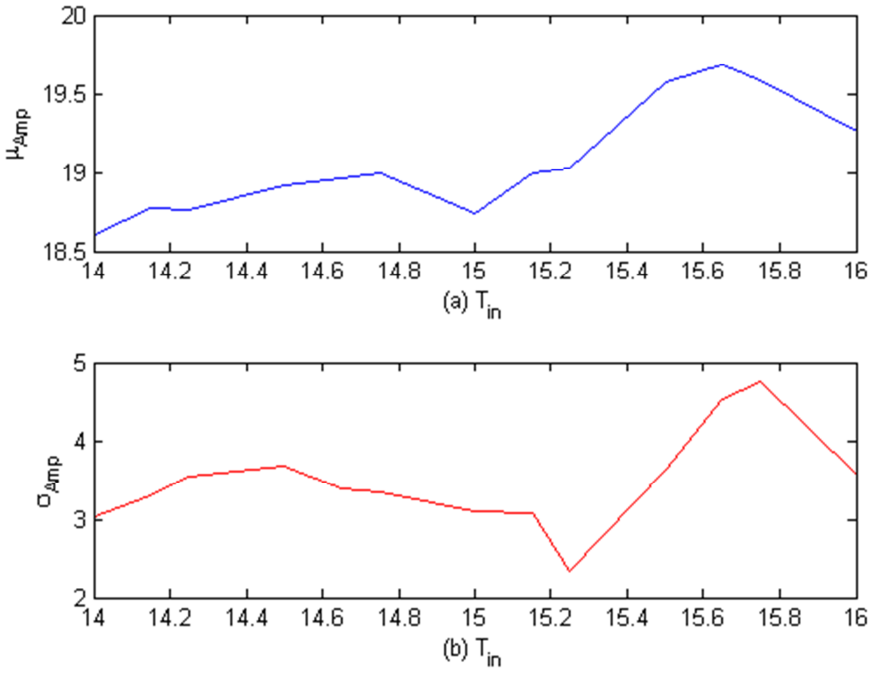

Figure 3.14: The effect of periodic stimulus on the amplitude of neural spikes of HH_1 and HH_{ref}. a) The mean amplitudes, μ_{Amp}, of neural responses for various ISIs (T_{in}) of stimuli. b) The standard deviation in the amplitudes for each neural response corresponding to T_{in}. The neural responses exhibit fluctuating amplitudes across the entire set with standard deviation $2.34 < \sigma_{Amp} < 4.75$.

The mean ISI of the neural responses ($\mu_{T_{Out}}$) is recorded across the set shows that a change in the period T_{in} of the stimuli has little or no effect on the output ISI, T_{Out}, of the neural responses. This is confirmed by the minimal variation in $\mu_{T_{Out}}$ and corresponding $\sigma_{T_{Out}}$ and is consistent with the observations of Hasegawa (Hasegawa 2000). The ratio, $= \mu_{T_{Out}}/T_{in}$, gives the relative change of response ISI to the stimulus ISI. As T_{in} increases, T_{Out} remains almost unchanged therefore the value of k decreases along the set. Similarity

estimate of 1 for $\beta = 0$ is observed for $k = 0.6577$ (fig. 3.15) indicating that T_{Out} is lower than T_{in}.

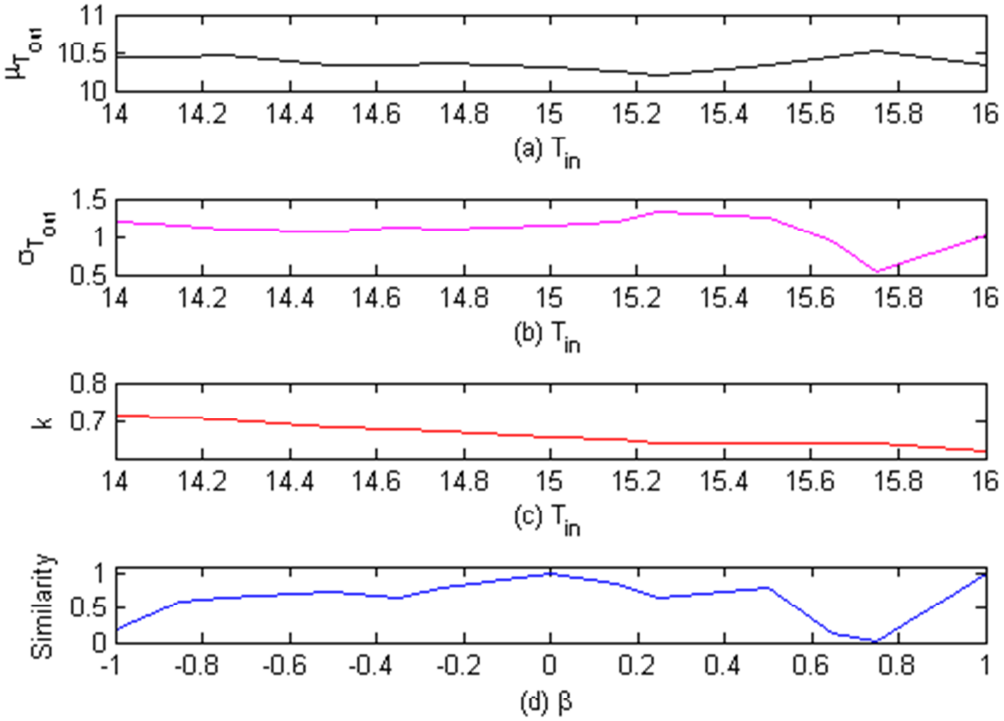

Figure 3.15: The effect of periodic stimulus on the firing times of a HH neuron. a) The variation in the mean ISI ($\mu_{T_{Out}}$) of neural responses is minimal, $10.20 < \mu_{T_{Out}} < 10.51$. b) The corresponding standard deviation in ISI for each neural response is low, $0.55 < \sigma_{T_{Out}} < 1.32$. c) The ratio (k) of $\mu_{T_{Out}}$ to T_{in} confirms that the output ISI, T_{Out}, is almost constant and marginally relies on T_{in}. d) Similarity estimates based on firing times.

3.5.2 Set II: Analysis, 13ms-15ms

The mean amplitudes, μ_{Amp}, show variation with increase in the period of stimuli. It is seen (fig. 3.16) that mean amplitudes vary between 18.70mV for R_{13} to 18.74mV for R_{15} with standard deviation $\sigma_{Amp_{13}} = 3.69$ for R_{13} and $\sigma_{Amp_{15}} = 3.10$ for R_{15}. The maximum mean amplitude μ_{AmpMax} is 18.99mV for $R_{14.75}$ and maximum mean standard deviation σ_{AmpMax} is 3.74 for $R_{13.15}$. The effect of underlying chaotic oscillations is evident in set II as an increase or decrease in μ_{Amp} is not directly attributed to a change in T_{in}.

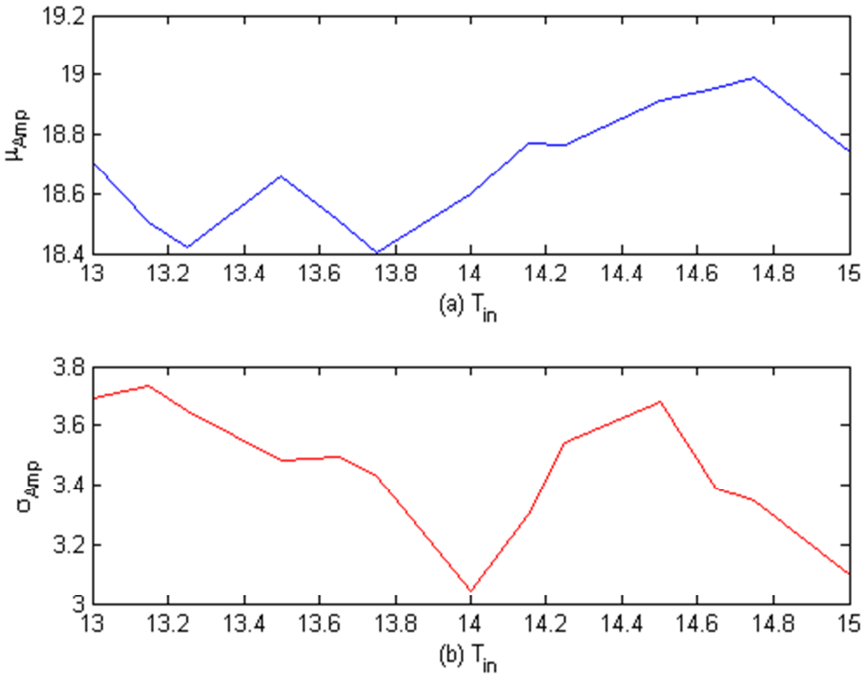

Figure 3.16: Effect of periodic stimuli on the amplitude of neural spikes of HH_1 and HH_{ref}. a) The mean amplitudes, μ_{Amp}, of neural responses for various ISIs (T_{in}) of stimuli. b) The standard deviation in the amplitudes for each neural response corresponding to T_{in}. The neural responses exhibit fluctuating amplitudes across the entire set with standard deviation $3.04 < \sigma_{Amp} < 3.73$.

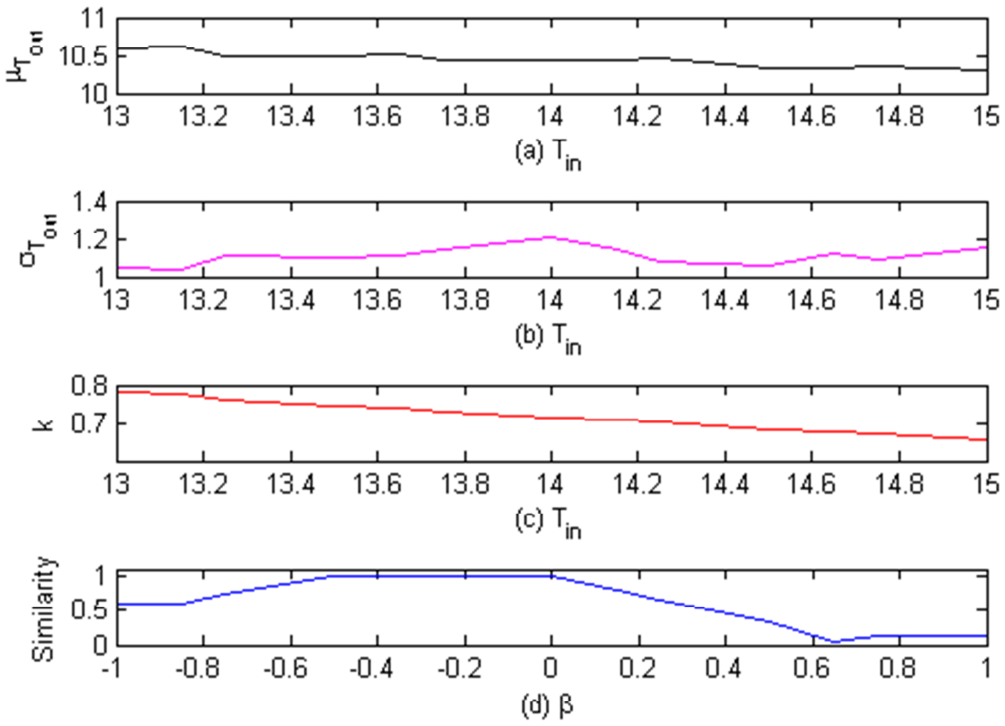

Figure 3.17: a) Increase in the period (T_{in}) of the synaptic stimuli has minimal effect on $\mu_{T_{Out}}$, $10.30 < \mu_{T_{Out}} < 10.63$ b) Corresponding minimal variation in the T_{Out}, $1.03 < \sigma_{T_{Out}} < 1.20$. c) The ratio (k) confirms that the T_{Out} is always lower than T_{in}. d) Similarity estimates based on firing times.

The change in T_{in} cannot force the HH neuron to respond with significantly distant spikes and as seen in fig. 3.17, the rate of fire varies between 10.30ms and 10.63ms across the set. In addition, the standard deviation in the firing rate, $\sigma_{T_{Out}}$, is within 1.03ms and 1.20ms. Biological precision is limited to 2ms, therefore, this change in firing rate is considered as minimal and the rate of fire of the neuron can be regarded as constant. These results suggest that the false positives of high similarity, which exist in set II, are due to this small variation in T_{Out} not considered by coincidence factor while estimating similarity. A correct estimate of high similarity for $\beta = 0$ is observed for $k = 0.7141$ (fig. 3.17) indicating that T_{Out} is lower than T_{in}.

3.5.3 Set III: Analysis, 15ms-17ms

In general for set III (fig 3.18), an increase in T_{in} along the set increases μ_{Amp}. It is observed that the mean amplitudes vary between 18.74mV for R_{15} to 19.81mV for R_{17} with standard deviation $\sigma_{Amp_{15}} = 3.10$ for R_{15} and $\sigma_{Amp_{17}} = 3.41$ for R_{17}. The maximum mean amplitude μ_{AmpMax} is 19.81mV for R_{17} and maximum mean standard deviation σ_{AmpMax} is 4.75 for $R_{15.85}$.

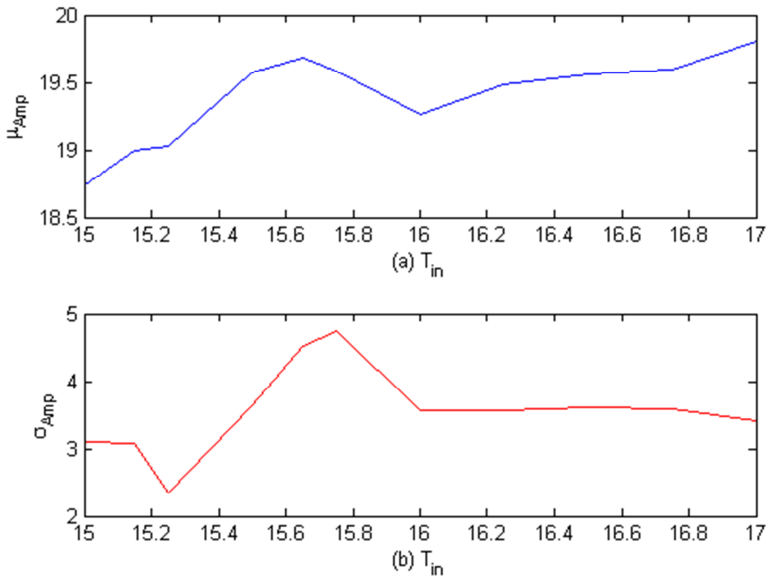

Figure 3.18: a) The mean amplitudes, μ_{Amp}, of neural responses for show a general increase along with T_{in}. μ_{Amp} decreases between $15.65 < T_{in} < 16$. b) The standard deviation in the amplitudes for each neural response corresponding to T_{in}. σ_{Amp} is pronounced between $15.15 < T_{in} < 16$ but almost constant for $16 < T_{in} < 17$. The standard deviation across the entire set is $2.34 < \sigma_{Amp} < 4.74$.

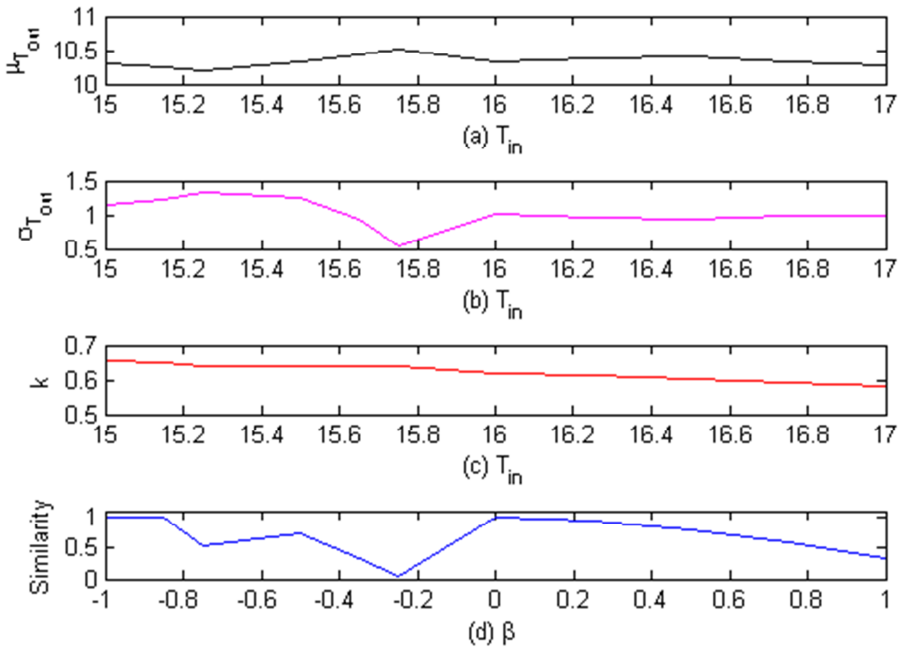

Figure 3.19: a) Increase in the period (T_{in}) of the synaptic stimuli has minimal effect on $\mu_{T_{Out}}$, $10.20 < \mu_{T_{out}} < 10.51$ b) Corresponding minimal variation in the T_{Out}, $0.55 < \sigma_{T_{out}} < 1.33$. c) The ratio (k) confirms that the T_{Out} is always lower than T_{in}. d) Similarity estimates based on firing times.

The increase in the period (T_{in}) of the stimuli has limited effect on firing rate as $\mu_{T_{Out}}$ remains almost constant and the rate of fire of the neuron varies between 10.20ms and 10.51ms across the set. In addition, the standard deviation in the firing rate, $\sigma_{T_{Out}}$, is within 0.55ms and 1.33ms. A correct estimate of high similarity for $\beta = 0$ is observed for $k = 0.6193$ (fig. 3.19) indicating that T_{Out} is lower than T_{in}.

Sections 3.4.1-3.4.3 indicate that exactly matching neural responses occur with $k_{set\ I} = 0.6577$ for $T_{in} = 15ms$, $k_{set\ II} = 0.7141$ for $T_{in} = 14ms$ and $k_{set\ III} = 0.6193$ for $T_{in} = 16ms$. It is observed that the increase in T_{in} has little or no effect on the rate of fire of the neuron. This observation contrasts with a neuron stimulated by a constant-current stimulus. Sections 3.3 and 3.4 show evidence that periodic stimuli causing chaotic oscillations shape the neural dynamics and resultant neural responses display temporal patterns uncommon to steady state neural responses. In addition, based on these results estimating similarity by neural firing time coincidences is insufficient in view of a) false positives and b) incorrect inference about neural stimuli. It is therefore suggested that as

both irregular firing times and fluctuating amplitudes reflect the true dynamics of the neuron, similarity estimates should be based on a composite measure of firing time and amplitude coincidences in view of periodic or sinusoidal stimulation (Sarangdhar and Kambhampati, 2008a,b, Sarangdhar and Kambhampati, 2009).

3.6 Binary Clustering – Identifying dissimilarity

The similarity estimates of coincidence factor are accurate for neural responses with constant amplitudes but these estimates of similarity do not extend to neural responses with underlying chaotic oscillations. The results in the above sections show that two visually and temporally distinct (amplitude fluctuations) neural responses would generate a high coincidence factor if similarity is estimated using only firing time coincidences of neural spikes. Therefore, from the results in sections 3.4 and 3.5, eliminating false positives for such neural responses requires both firing time and amplitude information.

This section further demonstrates this requirement by using a binary clustering algorithm to show that the clustering solution is unique to each neural response, therefore aiding distinguishability. An example of false positive is considered for which a pair of neural responses are incorrectly classified as identical by coincidence factor. Refer section 3.4.1.1 and fig. 3.11.

3.6.1 Binary Clustering - False Positive

The peak of each spike in a neural response is considered an object (Obj) and is defined as point in 2D space with a firing time and corresponding amplitude. Therefore, the number of objects for each neural response is equal to the number of spikes. The X co-ordinate of Obj is the firing time and Y co-ordinate is the amplitude or magnitude of the action potential.

$$Obj = [Firingtime, Amplitude] \tag{3.12}$$

The Euclidean distances between each pair of objects are calculated using (3.13) where N_r , N_S are the objects in the spike train. Once the distance between each pair of objects is determined, the objects are clustered based on the *nearest neighbour* approach using (3.14) where n_r, n_s are the number of objects in the respective clusters. The binary clusters are plotted to form a hierarchical tree whose vertical links indicate the distance between two objects (spikes) linked to form a cluster.

A number is assigned to each cluster as soon as it is formed. Clusters are numbered from $(m+1)$, until no more clusters can be formed; where $m = number\ of\ an\ object$. (See Appendix B for a sample test case cluster formation)

$$d_{rs}^2 = (N_r - N_s)(N_r - N_s)' \tag{3.13}$$

$$\left.\begin{aligned} d(r,s) &= \min(dist(N_{ri} - N_{sj})) \\ i &\in (1,\ldots,n_r), j \in (1,\ldots,n_s) \end{aligned}\right\} \tag{3.14}$$

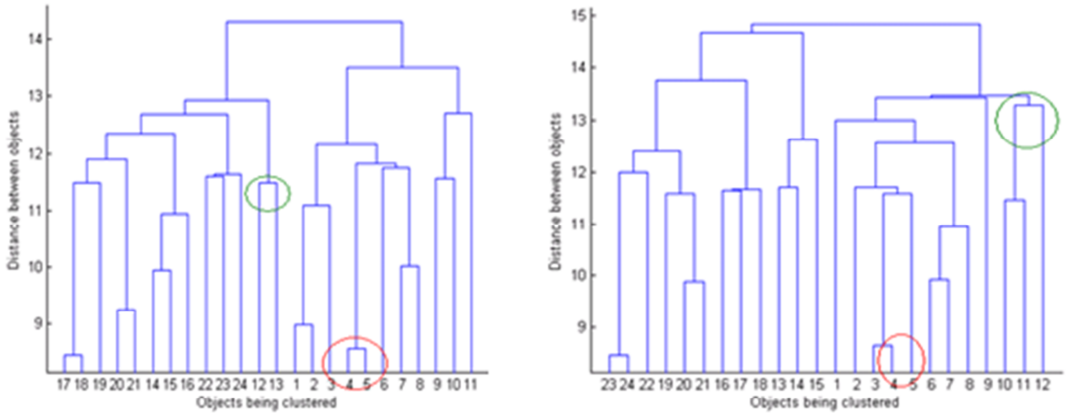

(a) ISI = 15ms (b) ISI= 16ms

Figure 3.20: a) Clustering solution for $T_{in} = 15ms$ and $T_{in} = 16ms$ indicating objects being clustered are different from each other. b) The distance between the objects being clustered (y-axis) are unequal. This demonstrates that the two neural responses are intrinsically dissimilar and the estimate of similarity given by coincidence factor is a false positive.

The false positive ($\Gamma = 1$) observed in section 3.4.1.1 for this pair of neural responses indicates that they are identical. The clustering trees (fig. 3.20) show that these responses are intrinsically dissimilar from each other by a margin not captured by the coincidence

factor. The corresponding green and red circles show that a) the objects clustered together are different for each response and b) the distances between these objects differ for each neural response. It is also observed from the clustering solutions that the shape, form, heights as well as linkages are dissimilar for the two neural responses.

These results indicate that the two neural responses are inherently distinct and there is additional information besides the firing times which is not considered by Γ. This explains the existence of *false positives* in similarity estimation of neural responses evoked by periodic stimuli. Hence, it is suggested that though determining firing time coincidences is crucial, additional consideration of the varying amplitudes is necessary for estimating similarity between neural responses with fluctuating membrane voltages (Sarangdhar and Kambhampati, 2008a,b; Sarangdhar and Kambhampati, 2009).

3.7 Chapter Summary

A synaptic sinusoidal or periodic stimulus induces oscillations in the membrane voltage of the HH neuron (Matsumoto et. al., 1980; Hasegawa, 2000). These oscillations are absent in steady state neural responses which are stimulated by a constant-current stimulus. Due to the presence of oscillations, the temporal nature of the neural responses stimulated by sinusoidal or periodic stimuli differs significantly from those generated by constant-current stimulus. Studies show that these oscillations are chaotic and also physiologically observed (Guttman *et. al.*, 1980; Aihara *et. al.*, 1984; Hayashi *et. al.*, 1985; Holden 1987; Kaplan and Glass 1995; Matsumoto *et.al.*, 1980; Matsumoto *et.al.*, 1984).

The effect of these chaotic oscillations is very prominent on the neural dynamics and result in neural spikes having irregular firing times and fluctuating amplitudes. It observed that due to the underlying oscillations the steady state of the neural response is not preserved, hence these responses differ from steady state responses. The results show that the similarity estimated using only the firing times of neural spikes leads to a) false positives and b) incorrect inference about neural stimuli similarity. These similarity

estimates based on firing time coincidences of neural spikes classify non-identical neural responses as identical (false positives) which indicate that they are generated by similar stimuli. It is already known that identical stimuli evoke similar neural dynamics therefore corresponding neural responses exhibit high similarity (Davies *et. al.*, 2006, Chechik *et. al.*, 2006; Hasegawa, 2000). Analysis of these neural responses has revealed that the ISI (T_{in}) of the stimulus has little or no effect on the ISI (T_{out}) of the neural response. This relation between T_{in} and T_{out} has also been observed by Hasegawa (Hasegawa, 2000). Further analysis carried out in this chapter indicates that T_{in} has an effect on the amplitude fluctuations of the neural responses. The results show that the mean amplitude μ_{Amp} increases with T_{in} for most neural responses, however, μ_{Amp} shows a decrease with an increase in T_{in} for a few cases, this is attributed to the refractory nature of the neuron and longer hyperpolarization caused by the underlying chaotic oscillations.

Hence, in these cases, the similarity between neural responses cannot be estimated exclusively by the firing times of neural spikes as due to the effect of the chaotic oscillations, the firing times and amplitudes together reflect the true dynamics of the neuron. This is supported by a clustering algorithm, which identifies the requirement of amplitude fluctuations, in addition to irregular firing times in order to estimate neural response similarity. Therefore, similarity estimation of neural responses exhibiting chaotic oscillations should consider both these features (Sarangdhar and Kambhampati, 2008a,b; Sarangdhar and Kambhampati, 2009).

The next chapter presents a framework to establish similarity between neural responses exhibiting chaotic oscillations.

4 Similarity Estimation based on Neural Dynamics: Formulation of $\Gamma_{chaotic}$

4.1 Introduction

The temporal nature of a periodic stimulus responsible for inducing chaotic oscillations in a biological neuron causes irregular ISI and fluctuating amplitudes, which are absent in steady state responses generated by constant current stimuli. The results in Chapter 3 show that estimating similarity between neural responses based only on firing times (coincidence factor) is insufficient in view of a) false positives and b) as stimuli similarity can be derived from neural response comparison, coincidence factor gives incorrect inference about neural stimuli similarity. It is observed that the firing times of neural spikes are adequate to estimate similarity of steady state responses. However, in the presence of chaotic oscillations or when the amplitudes of a neural response fluctuate, amplitude and firing time collectively reflect the true dynamics of a neuron and therefore both should feature in similarity estimation (Sarangdhar and Kambhampati, 2008a,b; Sarangdhar and Kambhampati, 2009).

As identified by the false positives in Chapter 3, estimating similarity between neural responses exhibiting chaotic oscillations requires a new similarity measure. Therefore, this chapter presents a mathematical framework to determine similarity between neural responses generated by periodic, excitatory and inhibitory stimuli by considering the effect of neural dynamics. This similarity measure estimates similarity between neural response pairs by considering the amplitude distribution and the firing times of neural responses when chaotic oscillations occur. To eliminate the false positives, it is suggested that estimate of similarity based on both firing time and amplitude coincidences will be

more realistic than similarity based on either firing time or amplitude coincidences alone and the similarity between two neural responses thus obtained will relate to respective stimuli. Identical stimuli have very similar effect on the neural dynamics and therefore, as the temporal inputs to the neuron are identical, the occurrence of identical dynamics result in a high estimate of similarity for the neural responses exhibiting chaotic oscillations (Sarangdhar and Kambhampati, 2010a, b).

The amplitudes of a neural response exhibiting chaotic oscillations are considered to fit a Normal distribution and using the properties of Normal distribution, it is possible to determine amplitude coincidences. Similarity between these responses is estimated by a composite similarity measure based on amplitude and firing time coincidences. The effect of distinct periodic stimuli is evident in the dissimilar chaotic patterns displayed in the neural responses (see Chapter 3, section 3.3). It indicates that neural responses with high similarity originate from very similar periodic stimuli. This agrees with the physiological observations that initial representation of a neural response is unique to the stimulus (Davies *et. al.*, 2006, Chechik *et. al.*, 2006, Sarangdhar and Kambhampati, 2008a,b; Sarangdhar and Kambhampati, 2009). The simulations carried out in this chapter are explained in the form of an algorithm in Appendix A, section A.5.2.

4.2 Definitions

Let $sp_n(f_N, a_N)$ be a neural response generated by a Hodgkin-Huxley (HH) neuron in response to a periodic stimulus S_n. Each spike sp_{n_i} of a neural response is represented by its firing time (f_i) and corresponding amplitude (a_i). The total number of spikes in a spike train is given by N and $1 \leq i \leq N$ represents the i^{th} incident of firing of an action potential. The firing times of the spikes occur either at regular or irregular intervals of time i.e. they can have fixed or variable Inter-Spike Interval (ISI) depending on the stimulation. The amplitudes in sp_n, generated by a periodic stimulus S_n have a Normal distribution $\aleph$.

Definition 1:

A Firing Time Set (FTS) is a set of successive firing times for a given neural response such that $FTS = \{f_i / f_i \in \Re^+\}$ where f_i is the firing time of a neural spike. If a neural response sp_n has N firing times, then the FTS for sp_n is given by

$$FTS = \{f_1, f_2, ...f_i, ...f_N\} \tag{4.1}$$

Definition 2:

An amplitude set (AS) is a set of successive non-negative peaks for a given neural response such that $AS = \{a_i / a_i \geq 0;\ a_i \in \Re\ \}$ where a_i represents the amplitude. If a neural response sp_n has N amplitudes, then the AS for sp_n is given by

$$AS = \{a_1, a_2, ...a_i, ...a_N\} \tag{4.2}$$

Definition 3:

A neural response is represented by a tuple (f_i, a_i) where $i = 1,2,3...N$. Thus, the Spike Train Set (STS) is given by

$$STS = \{(f_1, a_1), (f_2, a_2), ...(f_i, a_i), ...(f_N, a_N)\} \tag{4.3}$$

where amplitudes $\{a_1, a_2, ...a_i, ...a_N\}$ occur at corresponding firing times $\{f_1, f_2, ...f_i, ...f_N\}$

Definition 4:

${}_nC_r$ is the total number of combinations of 'r' objects selected from 'n' where

$$\binom{n}{r} = {}_nC_r = \frac{n!}{r!(n-r)!} \tag{4.4}$$

Definition 5: Conditional Expectation or Conditional Mean

If X and Y have joint density function $f(x,y)$, then the conditional density function of Y given X is $f(y \mid x) = f(x,y)/f_1(x)$ where $f_1(x)$ is the marginal density function of X. The conditional expectation or conditional mean of Y given X can be defined by

$$E(Y \mid X = x) = \int_{-\infty}^{\infty} y\, f(y \mid x)\, dy \tag{4.5}$$

Definition 6: Similarity of Spikes

Let $sp_1(f_i^1, a_i^1)$ and $sp_2(f_i^2, a_i^2)$ be any two neural responses represented by their spike train sets 'STS_1'and 'STS_2'. The i^{th} spike in sp_1 is said to be similar to the i^{th} spike in sp_2 if $\left|f_i^1 - f_i^2\right| \le \Delta$ and $\left|a_i^1 - a_i^2\right| \le \delta$ (4.6)

where Δ is the precision of firing time coincidence and δ is the precision of amplitude coincidence.

If $\forall\, i$, (4.6) holds then sp_1 is said to be similar to sp_2.

Definition 7: Similarity of Stimuli

Let the neural responses $sp_1(f_i^1, a_i^1)$ and $sp_2(f_i^2, a_i^2)$ be generated by periodic stimuli 'S_1' and 'S_2' respectively. If 'sp_1' and 'sp_2' are similar, it implies that the periodic stimuli 'S_1' and 'S_2' are identical.

For a single bipolar neuron such as the HH, similar periodic stimuli influence the neural dynamics in identical patterns and therefore the underlying oscillations in 'sp_1' and 'sp_2' are within precision of similarity (Sarangdhar and Kambhampati, 2008a,b; Sarangdhar and Kambhampati, 2009).

Definition 8:

Let $\Gamma_{chaotic}$ be a similarity measure that estimates similarity between neural responses exhibiting chaotic oscillations.

sp_1 is said to be completely similar to sp_2 if $\Gamma_{chaotic}$ = 1. If $\Gamma_{chaotic}$ = 0, then the two spike trains sp_1 and sp_2 are said to be dissimilar. When $0<\Gamma_{chaotic}<1$, sp_1 and sp_2 are partially similar.

4.3 Formulating $\Gamma_{chaotic}$

Let sp_1 and sp_2 be two neural responses with underlying chaotic oscillations generated by periodic stimuli S_1 and S_2 where $S_1 \neq S_2$. Studies have focused on firing times of neural spikes because it is thought that the information in a spike train can be encoded either in the firing times or the firing rate; this is possible for all steady state responses where the stimulus is non-periodic (Rinzel, 1985; Gabbiani *et. al.*, 1999; Panzeri *et. al.*, 1999; Bialek *et. al.*, 1991). If the stimulus is periodic or sinusoidal, chaotic oscillations occur, which do not exhibit a fixed pattern and estimating similarity between responses using only the firing times of neural spikes eliminates one aspect of chaotic dynamics (i.e. amplitude fluctuations) by treating the neural responses as steady state with varying or irregular ISI. In order to establish similarity between such responses similarity estimation requires considering the variance of both firing times and amplitudes.

The neural spikes are the result of a stimulus-dependent open-close mechanism of the ion channels that regulate the membrane voltage (see Chapter 2, section 2.4). To understand this stimulus-dependent nature of the membrane voltage it is necessary to consider the amplitude variations caused by chaotic oscillations. Determining similarity requires that a) firing times coincide, b) given that firing times coincide, corresponding amplitudes coincide. This similarity is based on relative number of coincidences without coincidences by chance. Coincidence by chance is a probability concept also known as '*mathematical*

expectation' or '*expected number of coincidences'*. The following sections describe the derivation of the expected number of amplitude and firing time coincidences. The mathematical expectation is an absolute number, which remains constant for a pair of neural responses.

4.3.1 Determining amplitude coincidences by chance

Let N_1 and N_2 be the total number of spikes in the neural responses sp_1 and sp_2 respectively. Hence, there are f_{N_1} and f_{N_2} firing times with corresponding amplitudes a_{N_1} and a_{N_2} represented by their Spike Train Sets STS_1 and STS_2. The amplitudes of these neural responses are *Normally Distributed* and for a large number of samples, the amplitude distribution would fit a normal curve with mean μ and standard deviation σ. Therefore, let $\aleph_1$ and $\aleph_2$ be the Normal distributions for the amplitudes of sp_1 and sp_2 with means, μ_1 , μ_2 and respective standard deviations σ_1 and σ_2.

Consider the Normal distribution $\aleph_1$, applying the Empirical rule for a Normal distribution, 68.27% of amplitudes lie within $\mu_1 \pm 1\sigma_1$. In addition, almost all i.e. 99.73% of the amplitudes of the spikes will lie within three standard deviations i.e. $\mu_1 \pm 3\sigma_1$. The probability that an amplitude lies within a given Normal distribution is calculated using the Z-scores and a Z-table (Normal table).

Let a_i be any amplitude from AS_1 ; the probability that a_i lies in $\aleph_1$ is given by the Z-score for a_i

$$z_i = \frac{a_i - \mu_1}{\sigma_1} \tag{4.7}$$

where $\sigma_1 > 0$;

The probability that a_i will lie in $\aleph_1$ can be found from the Z-score of a_i in the Z-table.

$$p(z_i) = z_i\big|_{from\ Z-table} \tag{4.8}$$

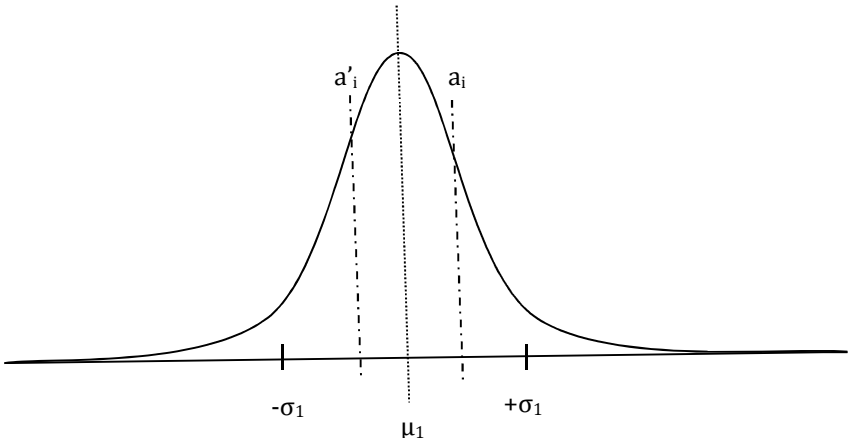

Figure 4.1: The Normal distribution $\aleph_1$ with mean μ_1 and standard deviation σ_1. The probability of an amplitude a_i to lie within $\aleph_1$ can be found using the Z-table.

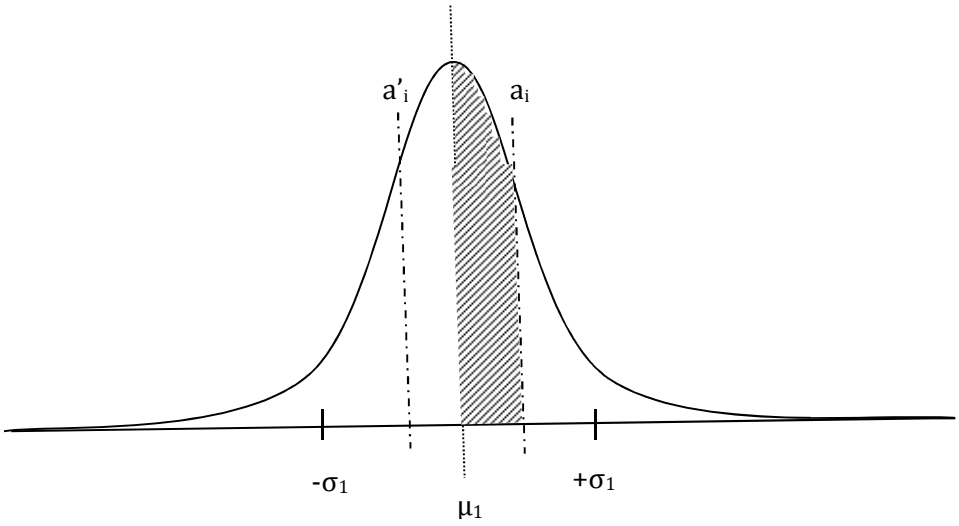

Figure 4.2: The probability of an amplitude that lies within a_i and μ_1 is shown by the shaded area. The area between a'_i and μ_1 is exactly the same due to symmetry of the Normal distribution.

The Normal distribution in fig. 4.1 shows the likelihood of an amplitude a_i from AS_1 lying in $\aleph_1$. As the Normal distribution is symmetrical about the mean, the probability that another amplitude a'_i lying in the negative half of $\aleph_1$ is identical to the probability of a_i (4.8).

The probability of any amplitude a_{any} lying between a_i and μ_1, is given by

$$p(a_{any}) = p(a_i) - p(\mu_1) \tag{4.9}$$

where, $p(\mu_1)$ is the probability of μ_1 and is represented by the shaded area (fig. 4.2).

Using equations (4.7-4.9), the probability that an amplitude from AS_2 lying within $\aleph_1$ can also be calculated. This indicates that the probability of coincidence of two amplitudes from $\aleph_1$ and $\aleph_2$ can be found from the shaded area in fig. 4.2. In order to find that an amplitude from $\aleph_2$ coincides with an amplitude from $\aleph_1$, the corresponding Z-scores are calculated

$$z_x = \frac{a_x - \mu_1}{\sigma_1} \tag{4.10}$$

where, a_x is any amplitude from the distribution $\aleph_2$ and z_x is the corresponding Z-score for a_x. The probability that a_x will coincide with an amplitude from $\aleph_1$ is obtained from (4.10) and (4.11)

$$p(z_x) = z_x\big|_{from\ Z-table} - p(\mu_1)\big|_{from\ Z-table} \tag{4.11}$$

The mean probability of coincidence of any amplitude from $\aleph_2$ with an amplitude from $\aleph_1$ can be approximated using the mean of $\aleph_2$.

$$z_{mean} = \frac{\mu_2 - \mu_1}{\sigma_1} \tag{4.12}$$

$$\overline{z_{mean}} = p(z_{mean}) = z_{mean}\big|_{from\ Z-table} - p(\mu_1)\big|_{from\ Z-table} \tag{4.13}$$

where $\overline{z_{mean}}$ is the mean probability of coincidence. (4.12) and (4.13) give the mean probability than an amplitude from $\aleph_2$ will lie within $\aleph_1$ and coincide with an amplitude

from $\aleph_1$ (fig. 4.3). The expected number of amplitude coincidences for any two neural responses generated by periodic stimuli is therefore $\overline{z_{mean}}N_1$, where N_1 is the number of spikes in sp_1.

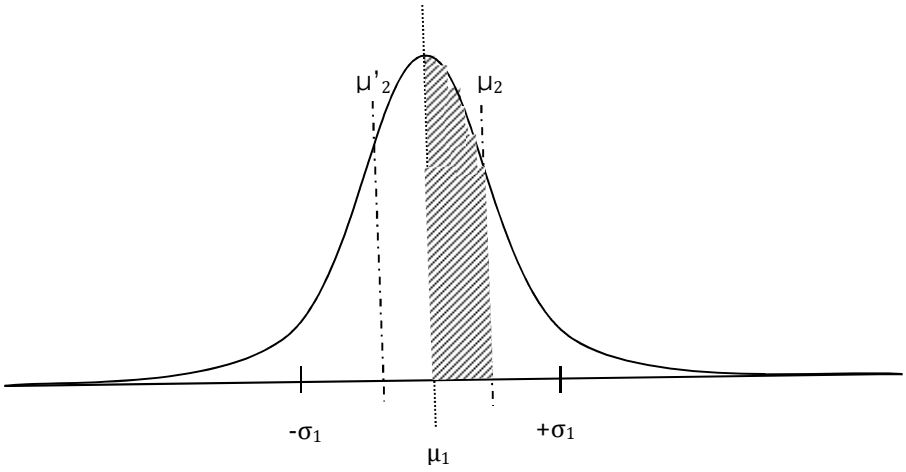

Figure 4.3: The mean probability that any amplitude from $\aleph_2$ that will coincide with an amplitude from $\aleph_1$ is shown by the shaded area.

Thus for any two neural responses, the mean probability that amplitudes from each distribution will coincide can be determined using (4.13) and is represented by the shaded area (fig. 4.3) bounded by the means of either distribution.

4.3.2 Determining firing time coincidences by chance

As discussed above, there are f_{N_1} and f_{N_2} firing times represented by their firing time sets FTS_1 and FTS_2 and corresponding amplitudes a_{N_1} and a_{N_2}. The firing time coincidences generated for neural responses exhibiting steady state or chaotic oscillations using this approach are consistent with Kistler (Kistler *et. al.*, 1997) on steady state neural responses.

Let the total simulation time (T_{tot}) be divided into *'K'* bins of 4ms each. A time window of 4ms guarantees that a bin can have at most one firing time from the HH neuron (due to refractoriness). If the f_{N_1} firing times are spread within these K bins, the number of bins filled is f_{N_1} while the number of empty bins is $K - f_{N_1}$. If the f_{N_2} firing times are

sequentially allocated to the $K - f_{N_1}$ bins such that each bin receives at most one firing time – a firing time coincidence is generated if a bin has one f_{N_1} and one f_{N_2} firing time. The coincidence generation is governed by a hyper-geometric distribution and the probability of encountering $N_{ftcoinc}$ firing time coincidences is therefore given by

$$p(N_{ftcoinc}) = \frac{\begin{pmatrix} f_{N_1} \\ N_{ftcoinc} \end{pmatrix}\begin{pmatrix} K - f_{N_1} \\ f_{N_2} - N_{ftcoinc} \end{pmatrix}}{\begin{pmatrix} K \\ f_{N_2} \end{pmatrix}} \tag{4.14}$$

Using definition 4, the probability of $N_{ftcoinc}$ firing time coincidences can be calculated. The mean of this hyper-geometric distribution is given by

$$\overline{N_{ftcoinc}} = \frac{f_{N_1} f_{N_2}}{K} \tag{4.15}$$

The mean gives the expected number of firing time coincidences for any two neural responses sp_1 and sp_2.

4.3.3 Similarity based on amplitude and firing time coincidences

The similarity between neural responses exhibiting chaotic dynamics can be estimated using both firing time and amplitude coincidences. The probability of encountering firing time coincidences is given by (4.14) while a mathematical relation between two normal distributions to determine amplitude coincidences is described by (4.10) and (4.11). A mathematical framework to estimate similarity between neural responses exhibiting chaotic oscillations can be derived from related work by Kistler (Kistler *et. al.*, 1997) on steady state neural responses.

This similarity can be determined by the difference between the actual coincidences and the coincidences by chance relative to the average number of spikes in the two neural

responses. This similarity normalised by a normalising factor gives an estimate between 0 (total dissimilarity) and 1 (exact match).

The number of spikes in sp_1 and sp_2 is N_1 and N_2, therefore the number of firing times are f_{N_1} and f_{N_2}. As $N_1 = f_{N_1}$ and $N_2 = f_{N_2}$; let N_{pcoinc} be the number of conditional coincidences (amplitude coincidence given firing time coincidence) between the two spike trains, $\overline{N_{pcoinc}}$ be the conditional mean or expected coincidences (average number of amplitude coincidences given firing time coincidences) and $N_{chaotic}$ be the normalising factor for the similarity measure.

The mean of the hyper-geometric distribution in (4.15) can be written as

$$\overline{N_{ftcoinc}} = \frac{N_1 N_2}{K} \tag{4.16}$$

where, K is the total number of bins each of 4ms and $\Delta = 2ms$ is the firing time precision, then

$$\overline{N_{ftcoinc}} = \frac{N_1 N_2}{\frac{T_{tot}}{4}} \tag{4.17}$$

$$\overline{N_{ftcoinc}} = 4\, N_2\, \nu \tag{4.18}$$

where, $\nu = \frac{N_1}{T_{tot}}$ is the rate of fire of the neural response sp_1.

$$\overline{N_{ftcoinc}} = 2\nu\Delta N_2 \tag{4.19}$$

This expected number of firing time coincidences $\overline{N_{ftcoinc}}$ is consistent with (Jolivet *et. al.*, 2004). Using definition 5, the conditional mean $\overline{N_{pcoinc}}$ or the expected coincidences by chance is given by

$$\overline{N_{pcoinc}} = \overline{N_{ftcoinc}}\ \overline{z_{mean}} \tag{4.20}$$

$$\overline{N_{pcoinc}} = 2\nu\,\Delta\,N_2\ \overline{z_{mean}} \tag{4.21}$$

The normalising factor $\mathrm{N}_{chaotic}$ normalises the estimate of similarity to a value between 0 (dissimilarity) and 1(exact match)

$$\mathrm{N}_{chaotic} = 1 - 2\nu\,\Delta\,\overline{z_{mean}} \tag{4.22}$$

The similarity between neural responses exhibiting chaotic oscillations can be determined using $\Gamma_{chaotic}$

$$\Gamma_{chaotic} = \frac{N_{pcoinc} - \overline{N_{pcoinc}}}{\frac{1}{2}(N_1 + N_2)}\ \frac{1}{\mathrm{N}_{chaotic}} \tag{4.23}$$

This formulation is based on the concept of *'coincidence'* (Joeken and Schwegler, 1995) where similarity based on firing times was estimated through relative number of coincidences without coincidences by chance. Similarity based only on firing times can be determined from (4.23) by omitting the amplitude considerations in N_{pcoinc}, (4.21) and (4.22). The similarity estimates of firing times are consistent with Jolivet's work on similarity estimation (Jolivet *et. al.*, 2004).

$\Gamma_{chaotic}$ estimates similarity through difference between the actual coincidences N_{pcoinc} and the expected number of coincidences $\overline{N_{pcoinc}}$ relative to the average number of spikes in

the two spike trains. This similarity is normalised between 0 and 1 by a normalising factor $\mathrm{N}_{chaotic}$.

From definition 8, two neural responses are partially similar if $\Gamma_{chaotic} \neq 0$ and $\Gamma_{chaotic} \neq 1$. If $0.5 < \Gamma_{chaotic} < 1$, there is a higher degree of similarity while low degree of similarity exists for $0 < \Gamma_{chaotic} \leq 0.5$. If two neural responses sp_1 and sp_2 are completely similar, all the corresponding firing times coincide i.e. $N_1 = N_2 = N_{pcoinc} = N$ and the amplitude distributions of sp_1 and sp_2 have identical means. Hence, $\overline{N_{pcoinc}}$ reduces to zero, indicating that there are no coincidences by chance and due to identical means of amplitude distributions, $\mathrm{N}_{chaotic}$ is maximised to unity. Hence, the value of $\Gamma_{chaotic}$ in (4.23) is unity if the neural responses are similar.

4.4 Computational Results - I

Chaotic oscillations occur in the neuronal membrane in response to a periodic stimulus. Periodic stimuli with variable ISI (T) are injected into the HH neurons (HH_1 and HH_{ref}) to induce chaotic oscillations in the neurons. Let T_{ref} be a reference ISI that stimulates HH_{ref} to generate a chaotic neural response R_{ref}. T is varied to generate a range of potential periodic stimuli that stimulate HH_1 and each response of HH_1 is compared with R_{ref} to determine similarity. Similarity is estimated for three cases where T_{ref} is equal to, greater than and less than T used for stimulating HH_1. Let β be the difference between the corresponding ISIs of the stimuli such that

$$\beta = T - T_{ref} \tag{4.24}$$

4.4.1 Case I: $T_{ref} = T, \beta = 0$

$T_{ref} = T = 15ms$

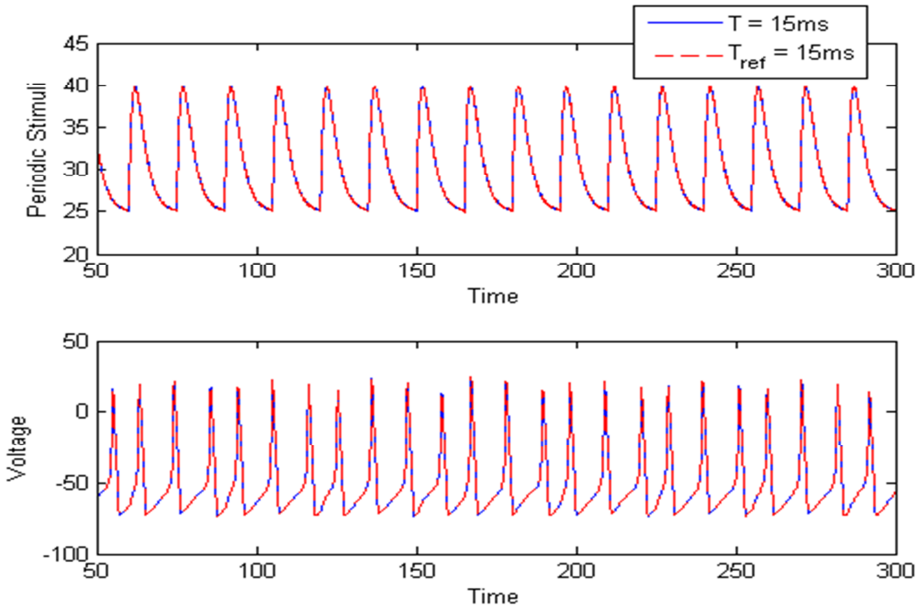

Figure 4.4: The periodic stimuli (top) with both T and T_{ref} = 15ms generate neural responses exhibiting chaotic oscillations (below). The neural dynamics have the same temporal input from the periodic stimuli. The resulting neural dynamics are identical and this is reflected in the temporal pattern of the neural responses.

It is observed that chaotic neural responses generated by identical periodic stimuli have similar firing times and amplitudes (fig. 4.4) and the similarity estimated by firing time coincidences of coincidence factor is 1. This indicates that these two neural responses are an exact match as all firing times coincide. This approach, however, does not consider one aspect of chaotic dynamics – fluctuating amplitudes; the similarity between these neural responses is very high, as the degree of overlap is maximum. The similarity between the two responses using both amplitudes and firing time coincidences gives a similarity estimate $\Gamma_{chaotic} = 1$. This result indicates that the underlying oscillations are identical and hence corresponding firing times and amplitudes of HH_1 and HH_{ref} are an exact match. This result indicates that the two neurons HH_1 and HH_{ref} are stimulated by identical stimuli. As the temporal input to the neuron is similar, the occurrence of identical chaotic patterns justifies the estimate of similarity $\Gamma_{chaotic} = 1$, hence this result is a *true positive*.

4.4.2 Case II: $T_{ref} > T, \beta < 0$

$T_{ref} = 15ms,\ T = 14ms$

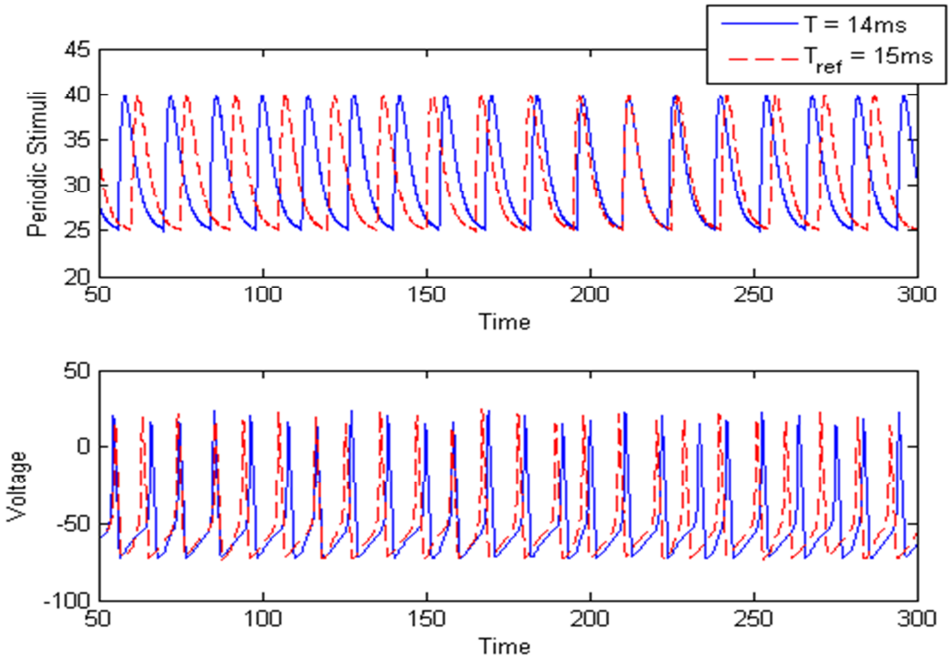

Figure 4.5: The periodic stimuli (top) with $T = 14ms$ and $T_{ref} = 15ms$ generate neural responses exhibiting chaotic oscillations (below). The stimuli are distinct and influence the neuronal dynamics differently. The resulting chaotic dynamics are temporally distinct and this is reflected in both firing times and amplitudes of HH_1 and HH_{ref}.

The distinct periodic stimuli $T_{ref} = 15ms$ and $T = 14ms$ induce chaotic oscillations in HH_1 and HH_{ref} (fig. 4.5) (for the chaotic oscillations, refer to Chapter 3, section 3.4.1, fig. 3.5). Coincidence factor estimates similarity between the two responses based on firing times is 0.120671. A low similarity is due to distinct temporal influence on the neural dynamics by the periodic stimuli. The similarity using both firing times and amplitude coincidences is determined by a conditional probability as in (4.23) which gives $\Gamma_{chaotic}$= 0.119016. The similarity based on both firing times and amplitudes is expectedly lower than similarity based on firing time coincidences alone.

4.4.3 Case III: $T_{ref} < T, \beta > 0$

$T_{ref} = 15ms,\ T = 16ms$

The firing time similarity estimated by coincidence factor for this pair of neural responses is very high, $\Gamma = 1$ indicating that the responses are an exact match and therefore generated by identical stimuli (false positive, see Chapter 3, section 3.4.1.1). However, $\Gamma_{chaotic}$ = 0.272938 indicates that a high firing time similarity does not essentially affect

amplitude coincidences. There is a sharp contrast in estimated similarity by $\Gamma = 1$ (based on firing times alone) and $\Gamma_{chaotic} = 0.272938$ (a realistic estimate considering the neural dynamics) as a result of amplitude variation. In the event of steady state responses, firing time comparison is sufficient, however, in the cases outlined in this section, the responses are chaotic and as the steady state is not preserved, both firing times and amplitudes of neural spikes reflect the dynamics and are required to estimate similarity.

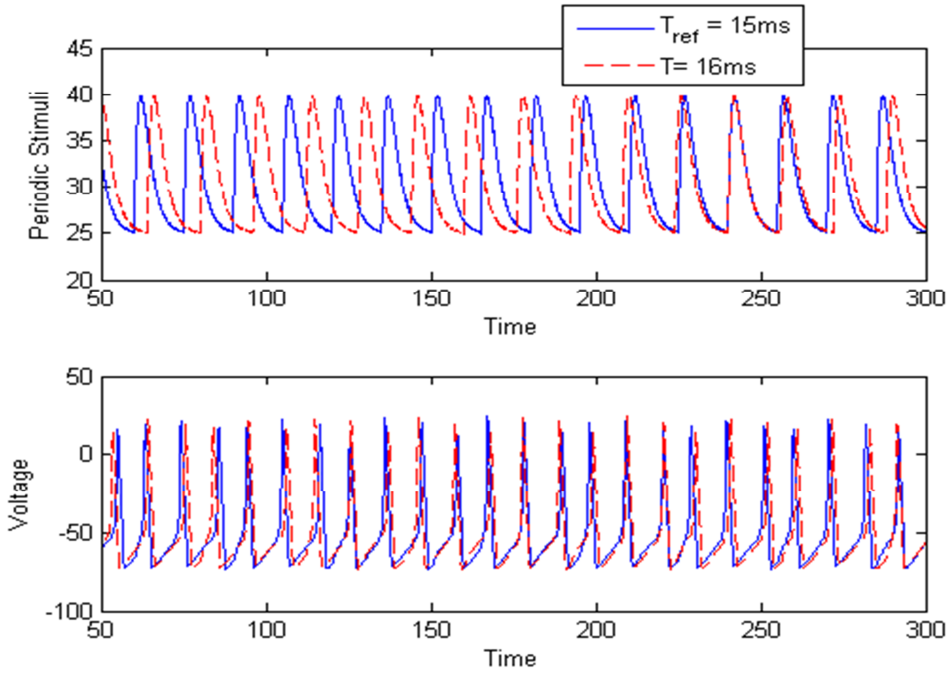

Figure 4.6: The periodic stimuli (top) with $T_{ref} = 15ms$ and $T = 16ms$ generate neural responses exhibiting chaotic oscillations (below). The stimuli are distinct and influence the neuronal dynamics differently. The resulting chaotic dynamics are temporally distinct and this is reflected in both firing times and amplitudes of HH_1 and HH_{ref}. The pulse width of each stimulus is different and has an important role in effecting the neural dynamics.

4.4.4 Discussion

To understand the effect of amplitude fluctuations on similarity estimation, it is required to find the amplitude coincidences, which is carried out using (4.23) and omitting the firing time considerations. Irregular ISI and varying amplitudes represent underlying chaotic oscillations therefore similarity estimation considering both these characteristics becomes necessary. The aim is to understand the similarity between two neural responses in view of periodic stimulation. The results tabulated (table 4.1) show the similarity based on firing time coincidences, amplitude coincidences and similarity estimated using $\Gamma_{chaotic}$

(4.23). It is observed that for case I that $\Gamma_{chaotic}$ is 1 indicating that the neural responses are an exact match. This result is justified by the high similarity of firing time coincidences and amplitude coincidences. In case II, $\Gamma_{chaotic}$ is 0.119016, which indicates low partial similarity. The corresponding firing time and amplitude similarity is low which expectedly lowers the estimate of similarity for case II. Case III is of special interest and is one of the objectives behind the formulation of $\Gamma_{chaotic}$. If the similarity is estimated considering only the firing time coincidences of neural spikes, the two responses are an exact match. However, as the neural responses exhibit chaotic oscillations, the chaotic dynamics are reflected in the amplitude fluctuations. The number of amplitude coincidences specifically answers how similar the responses are in the presence of chaotic oscillations. It is observed that though all firing times coincide for case III, the amplitude similarity is low i.e. 0.240947. This justifies a low similarity estimate $\Gamma_{chaotic}$ = 0.272938. As $\Gamma_{chaotic}$ is based on conditional coincidence (i.e. amplitude coincidence given firing time coincidence), it is neither commutative nor additive of amplitude coincidences and firing time coincidences.

Similarity estimated by Firing-time coincidences	Similarity estimated by Amplitude coincidences	Similarity estimated by $\Gamma_{chaotic}$	Similarity estimated by Γ
$T_{ref} = T$			
1.0000	1.0000	1.0000	1.0000
$T_{ref} > T$			
0.120671	0.193823	0.119016	0.120671
$T_{ref} < T$			
1.0000	0.240947	0.272938	1.0000

Table 4.1: Comparison of similarity estimates using a) firing time coincidences, b) amplitude coincidences, c) a composite similarity estimate $\Gamma_{chaotic}$ based on amplitude coincidences given firing time coincidences.

4.5 Computational Results – II

As established in Chapter 3, due to the nature of periodic stimuli and the presence of chaotic oscillations, estimating similarity between neural responses based on firing times is inaccurate in view of a) false positives and b) incorrect inference about stimuli similarity. To understand the effect of a broad range ISI on neural response similarity, two HH neurons (HH_1 and HH_{ref}) are stimulated using periodic stimuli. HH_1 is stimulated by varying the stimulus ISI (T) within a limit of 2ms and HH_{ref} is stimulated by a periodic stimulus with fixed ISI (T_{ref}). HH_1 is stimulated by varying T between 14ms-16ms (set I), 13ms-15ms (set II) and 15ms-17ms (set III) and similarity is estimated by comparing these responses with the response of HH_{ref} for each set. T_{ref} for the each set is 15ms for set I, 14ms for set II and 16ms for set III. A comparison of the similarity estimates of coincidence factor (Γ) and $\Gamma_{chaotic}$ is described in the following sections.

4.5.1 Set I: Evaluating Similarity Estimates of Γ and $\Gamma_{chaotic}$, 14ms-16ms

β represents the difference between T and T_{ref} as defined in (4.24). If $\beta \neq 0$, it indicates that the neural stimuli have dissimilar ISI and their respective influence on neural dynamics is distinct. As discussed above, neural responses with underlying chaotic oscillations display amplitude fluctuations and irregular firing times, which are not considered by coincidence factor for similarity estimation. It is observed that the false positive obtained by coincidence factor at $\beta = +1$ is eliminated using both amplitude and firing time coincidences (fig. 4.7). The similarity between pairs of neural responses estimated by $\Gamma_{chaotic}$ is lesser in comparison with Γ due to a composite consideration of amplitude fluctuations and firing times.

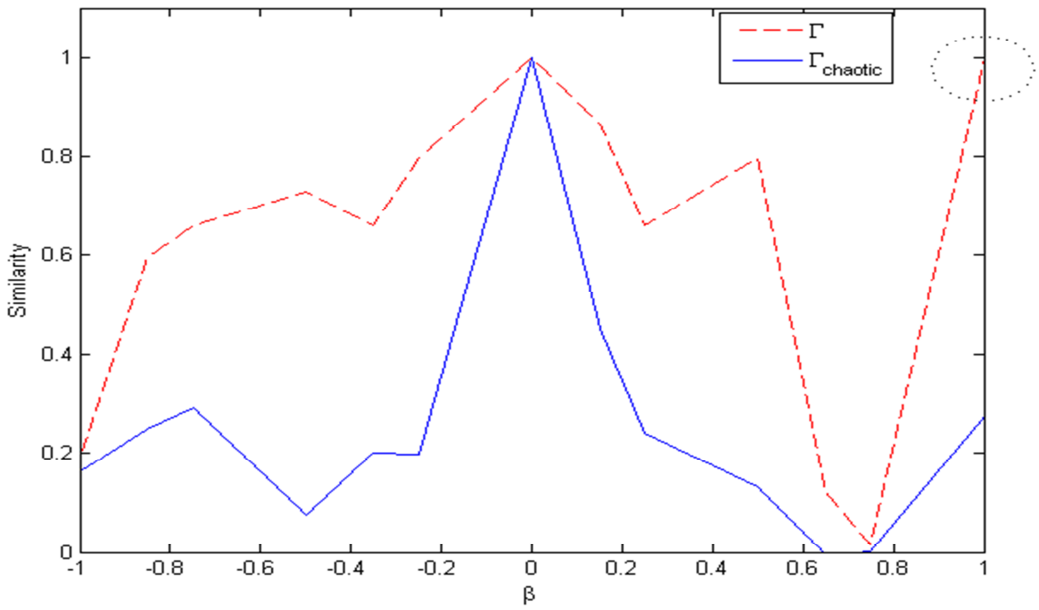

Figure 4.7: Similarity between neural responses generated by periodic stimuli with $14ms \leq T \leq 16ms$ and $T_{ref} = 15ms$. Γ represents the similarity estimated by coincidence factor and $\Gamma_{chaotic}$ is the similarity based on firing times and amplitudes coincidences. The use of amplitude fluctuations to estimate similarity eliminates false positive (circled) at $\beta = +1$.

If T is the ISI of the periodic stimulus to HH_1 and $T_{ref} = 15ms$ is the ISI of the periodic stimulus to HH_{ref}, then their responses are denoted as R_T and R_{ref15} respectively. Table (4.2) gives a clear comparison of firing time and amplitude coincidences for the pairs of neural responses in Set I. At $\beta = -1$, half of the neural spikes from R_{14} and R_{ref15} coincide with a precision of $\Delta = 2ms$. However, only 20.83% of the amplitudes coincide with a precision of $\delta = 2mV$. This is characteristic of neural responses exhibiting chaotic oscillations – a small change in the stimulus reflects on the neural dynamics. *Absolute coincidences* are conditional coincidences i.e. number of amplitude coincidences given that corresponding firing times coincide. The number of absolute coincidences obtained is 16.67%, which implies that in R_{14} and R_{ref15}, only 16.67% pairs of neural responses exhibit amplitude and firing time coincidences. The similarity estimated by $\Gamma_{chaotic}$ is 0.161 and it accurately reflects the absolute coincidences. In addition, $\Gamma_{chaotic}$ considers coincidences by chance or the expected coincidences, which renders the similarity estimated by $\Gamma_{chaotic}$ unique to a pair of neural responses.

β	Firing time Coincidences (%)	Amplitude Coincidences (%)	Absolute Coincidences (%)	$\Gamma_{chaotic}$
-1	50	20.83333	16.6667	0.161
↓	75	29.1677	25	0.2489
	79.1667	37.5	29.1667	0.2908
	83.3333	12.5	8.3333	0.0753
	79.1667	25	20.8333	0.1997
	87.5	29.1667	20.8333	0.1984
$\beta = 0$	100	100	100	1
↓	91.6667	50	45.8333	0.4513
	79.1667	33.3333	25	0.2392
	87.5	16.6667	16.6667	0.1312
	37.5	12.5	4.1667	0.0003
+1	100	29.1667	29.1667	0.2729

Table 4.2: Firing time, amplitude and absolute coincidences for various values of β in set I. $\Gamma_{chaotic}$ represents the similarity between pairs of neural responses. Firing time coincidence precision is $\Delta = 2ms$, amplitude coincidence precision is $\delta = 2mV$ and absolute coincidence is a conditional coincidence of amplitudes given that corresponding firing times coincide. $\Gamma_{chaotic}$ accurately estimates similarity and this is correlated with the percentage of absolute coincidences.

At $\beta = 0$, both stimuli have the same ISI ($T = 15ms, T_{ref} = 15ms$). It is observed from Table 4.2, that all neural spikes coincide in firing times and amplitudes. The absolute coincidences confirm that the neural responses are an exact match, hence, the similarity estimated by $\Gamma_{chaotic} = 1$. At $\beta = +1$, as all neural spikes show firing time coincidences, coincidence factor classifies these neural responses, R_{16} and R_{ref15}, as identical. This result is a '*false positive*' as indicated by the number of amplitude fluctuations. Though all neural spikes coincide in firing times, only 29.17% of amplitudes coincide, hence the absolute coincidences are 29.17%. The corresponding estimate of similarity by $\Gamma_{chaotic} = 0.2729$ is substantially lower than 1 (estimated by coincidence factor Γ) and also confirms it as a false positive. The consideration of amplitude fluctuations in addition

to firing time information successfully eliminates this false positive (Sarangdhar and Kambhampati, 2010a,b).

4.5.2 Set II: Evaluating Similarity Estimates of Γ and $\Gamma_{chaotic}$, 13ms-15ms

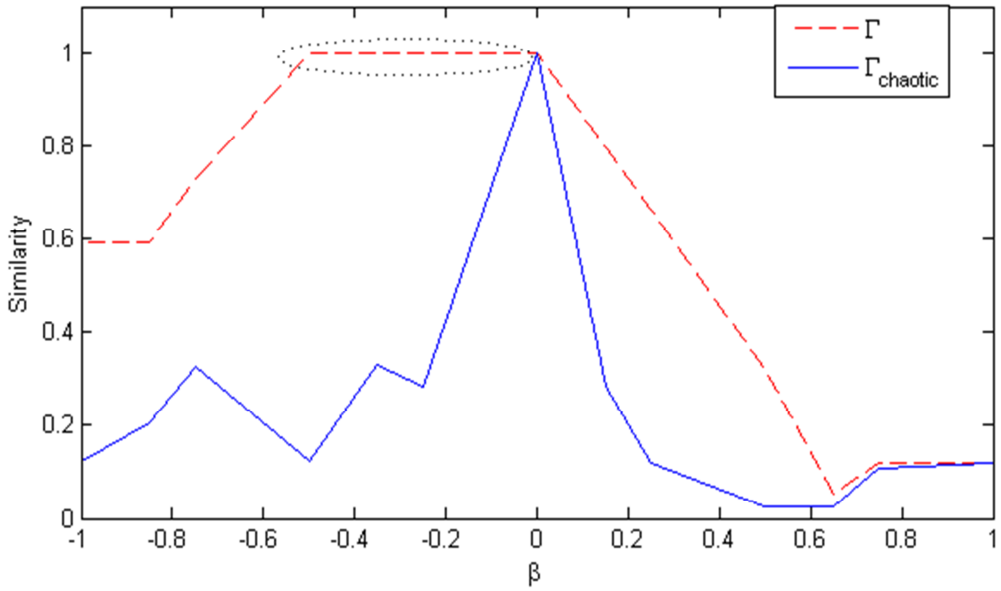

Figure 4.8: Similarity between neural responses generated by periodic stimuli with $13ms \leq T \leq 15ms$ and $T_{ref} = 14ms$. Γ represents the similarity estimated by coincidence factor and $\Gamma_{chaotic}$ is the similarity based on firing times and amplitudes coincidences. $\Gamma_{chaotic}$ eliminates false positives (circled) between $-0.5 \leq \beta < 0$.

The false positives estimated by coincidence factor Γ (see Chapter 3, section 3.4.1.2), shown in fig. 4.8., occur between $-0.5 \leq \beta < 0$. Table 4.3 shows that firing time coincidences are 100% between $-0.5 \leq \beta < 0$. Naturally, based on firing times, these pairs of neural responses are classified as identical by Γ. However, the corresponding amplitude coincidences are 12.5%, 33.33% and 29.17% which indicate that though all firing times coincide, the corresponding amplitude fluctuations are not identical, hence these coincidences are termed as *false positives*. These non-identical amplitude fluctuations are due to dissimilar ISI of periodic stimuli and underlying oscillations. The corresponding absolute coincidences for the false positives are 12.5%, 33.33% and 29.17%. The similarity estimated by $\Gamma_{chaotic}$ is 0.1224, 0.3302 and 0.2846 respectively, which correlates with the observed absolute coincidences. The composite consideration of the irregular firing times and varying amplitudes helps differentiate these neural responses and relate this obtained dissimilarity to corresponding stimuli.

β	Firing time Coincidences (%)	Amplitude Coincidences (%)	Absolute Coincidences (%)	$\Gamma_{chaotic}$
-1	75	16.6667	12.5	0.1204
↓	75	25	20.8333	0.2044
	83.3333	37.5	33.3333	0.3272
	100	12.5	12.5	0.1224
	100	33.3333	33.3333	0.3302
	100	29.1667	29.1667	0.2846
$\beta = 0$	100	100	100	1
↓	87.5	37.5	29.1667	0.2857
	79.1667	16.6667	12.5	0.1178
	58.3333	8.3333	4.1667	0.0263
	41.6667	33.3333	4.1667	0.0243
	45.8333	45.8333	12.5	0.1075
+1	45.8333	20.8333	12.5	0.1188

Table 4.3: Firing time, amplitude and absolute coincidences for various values of β in set II. $\Gamma_{chaotic}$ eliminates the false positives occurring between $-0.5 \leq \beta < 0$. The similarity estimated by $\Gamma_{chaotic}$ correlates with the percentage of absolute coincidences.

At $\beta = 0$, the neural responses are generated by identical stimuli ($T = 14ms$ and $T_{ref} = 14ms$). These identical stimuli cause similar oscillations in the neural dynamics resulting in neural responses, which are an exact match. This is seen in table 4.3 and fig. 4.8, at $\beta = 0$, the firing time coincidences, amplitude coincidences and the absolute coincidences are 100%. This justifies that the neural responses are an exact match and are generated by identical stimuli, hence $\Gamma_{chaotic} = 1$. The similarity determined by $\Gamma_{chaotic}$ for other neural response pairs is also consistent in correlation with the observed absolute coincidences.

4.5.3 Set III: Evaluating Similarity Estimates of Γ and $\Gamma_{chaotic}$, 15ms-17ms

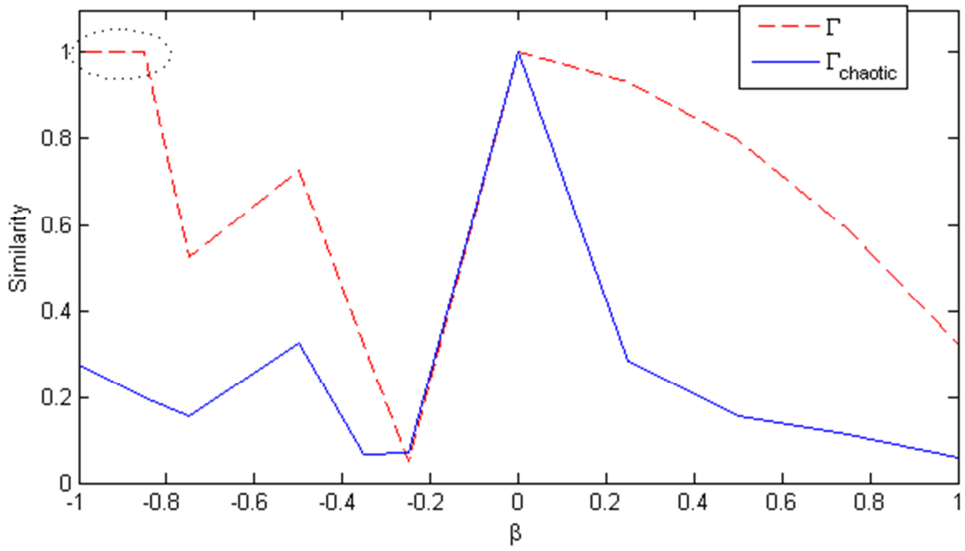

Figure 4.9: Similarity between neural responses generated by periodic stimuli with $15ms \leq T \leq 17ms$ and $T_{ref} = 16ms$. Γ represents the similarity estimated by coincidence factor and $\Gamma_{chaotic}$ is the similarity based on firing times and amplitudes. The incorporation of amplitude fluctuations to estimate similarity helps $\Gamma_{chaotic}$ eliminate false positives (circled) for $-1 \leq \beta \leq -0.75$.

Set III exhibits *false positives* between $-1 \leq \beta \leq -0.75$ (fig. 4.9, see Chapter 3, section 3.4.1.3). Table 4.4 shows that the corresponding firing time coincidences are 100%, which results in coincidence factor Γ classifying the pairs of neural responses as identical. However, the amplitude coincidences are 29.17% and 20.83% indicating that the underlying oscillations are non-identical. The corresponding similarity determined by $\Gamma_{chaotic}$ is 0.2754 and 0.1992. As $\Gamma_{chaotic} \neq 1$, it can be concluded that the neural responses do not match and they are generated by dissimilar stimuli.

At $\beta = 0$, the neural responses are generated by identical stimuli ($T = 16ms$ and $T_{ref} = 16ms$) and $\Gamma_{chaotic}$ identifies the highly similar neural responses ($\Gamma_{chaotic} = 1$). Dissimilar periodic stimuli ($\beta \neq 0$) causing non-identical chaotic oscillations are correctly identified and similarity estimates correlate with the observed absolute coincidences. For $\beta > 0$, $\Gamma_{chaotic}$ decreases with an increase in β indicating that similarity between the neural responses decreases with an increase in the difference in the ISI of two stimuli. Any change in the ISI of a stimulus causes a temporal variation and effects on neural dynamics which is evident in the dissimilarity (*1-similarity*) estimated by $\Gamma_{chaotic}$.

β	Firing time Coincidences (%)	Amplitude Coincidences (%)	Absolute Coincidences (%)	$\Gamma_{chaotic}$
-1	100	29.1667	29.1667	0.2754
↓	100	20.8333	20.8333	0.1992
	70.8333	25	16.6667	0.1581
	83.3333	33.3333	33.3333	0.3243
	58.3333	12.5	8.3333	0.0666
	41.6667	12.5	8.3333	0.0704
$\beta = 0$	100	100	100	1
↓	95.8333	33.3333	29.1667	0.2851
	87.5	20.8333	16.6667	0.1558
	75	16.6667	12.5	0.1124
+1	58.3333	37.5	8.3333	0.0617

Table 4.4: Firing time, amplitude and absolute coincidences for various values of β in set III. The false positives determined by coincidence factor between $-1 \leq \beta \leq -0.75$ are eliminated. Similarity between neural response pairs estimated by $\Gamma_{chaotic}$ correlates with the percentage of absolute coincidences.

4.6 Computational Results – III

In the previous sections, neural responses generated by characteristic periodic stimuli were compared to estimate similarity. New distinct stimuli were generated by varying the ISI (T) of the pre-synaptic spike train. In addition, there are other physiologically relevant types of stimuli that trigger a neural activity. This section estimates similarity between neural responses generated by excitatory and inhibitory stimuli. The temporal nature of an excitatory stimulus is dissimilar from an inhibitory stimulus (Luk and Aihara, 2000), therefore corresponding neural dynamics induced are distinct and an exact match between neural responses is not possible. More specifically, a cortical neuron has more than one dendritic input and it summates the total inhibitory and excitatory synapses, firing only if the summation in excitatory. This physiological relevance explains that the neural stimuli vary temporally and have distinct effects on neural dynamics (see Chapter 2, section 2.3).

Excitatory and inhibitory stimuli are generated by varying T of their pre-synaptic spike trains (see Chapter 3, section 3.2.2). Two HH neurons, HH_{Exc} and HH_{Inh} are stimulated using excitatory and inhibitory stimuli respectively with identical ISI ($\beta = 0$). T is varied between 14ms-16ms and corresponding neural responses are compared to estimate similarity.

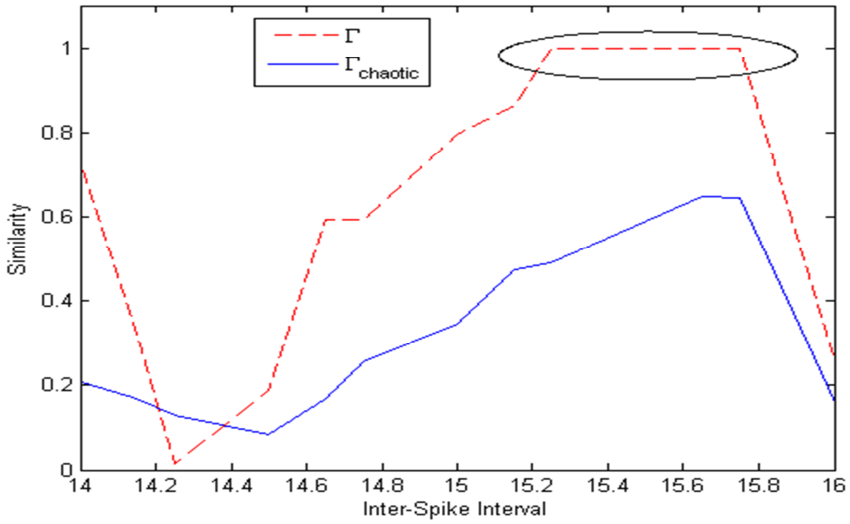

Figure 4.10: Comparison of similarity between excitatory (HH_{Exc}) and inhibitory (HH_{Inh}) neural responses estimated by Γ and $\Gamma_{chaotic}$. Coincidence factor generates false positives (circled) for neural responses with ISI between 15.25ms-15.75ms. The corresponding similarity estimated by $\Gamma_{chaotic}$ is lower indicating that the neural responses classified as identical are false positives. The temporal nature of an excitatory stimulus is distinct from an inhibitory stimulus and neural dynamics evoked by each stimulus is different, hence, an identical match is not possible.

It is observed (fig. 4.10) that coincidence factor (Γ) yields false positives between $15.25 \leq T \leq 15.75$. These false positives indicate that each neural response pair is an exact match even though the neural responses are generated by different type of stimuli. As $\Gamma = 1$ for all false positives, it indicates that excitatory and inhibitory stimuli are identical between 15.25ms and 15.75ms. These estimates of similarity are incorrect and disagree with biological and medical studies, e.g. stretch-reflex actions of muscles (MND References). It is known that inhibitory and excitatory stimuli are distinct temporally and functionally (Hille, 1992; Gernster and Kistler, 2002)and the false positives indicated by Γ contradict physiological evidence.

These incorrect estimates of similarity generated by Γ are eliminated by Γ_{chaotic} as estimates of similarity based on firing time and amplitude coincidences help identify dissimilar neural responses effectively and provide a feedback about corresponding stimuli.

4.7 Chapter Summary

The nonlinear neural dynamics can exhibit both steady state and chaotic responses depending on the nature of the stimulus. A neuron exhibits a steady state response on injection of a constant current stimulus. On the other hand, a chaotic behaviour is observed in response to a periodic stimulus. A neural response with underlying chaotic oscillations is characterised by irregular ISI and amplitude fluctuations; a phenomenon not exhibited by steady state responses.

To understand the chaotic dynamics and derive inference about corresponding stimuli, relative study of response dynamics is required. Chaos can be determined by the amplitude fluctuations and can be represented theoretically using return-maps. The amplitudes of these neural responses are considered to fit a Normal distribution and using the Empirical Rule of Normal distribution, 68.27% of the amplitudes lie within $\mu \pm \sigma$, where μ is the mean and σ is the standard deviation. Using the principle of Z-score, the probability of an amplitude coincidence can be calculated. A mean value of amplitude coincidence is given by the area under the curve bounded by means of either distribution.

A mathematically realisable composite similarity measure considering firing time coincidences and amplitude coincidences is demonstrated through various cases of neural response comparison. The ISI of the periodic stimuli is varied so that three relations between ISI arise – $ISI_1 = ISI_2$, $ISI_1 > ISI_2$ and $ISI_1 < ISI_2$. In addition, neural responses from excitatory and inhibitory stimuli are also compared to estimate similarity. Determining the similarity between chaotic responses is based on conditional coincidences, which is the number of amplitude coincidences given firing time coincidences. The resulting similarity

measure gives a value between 0 (total dissimilarity) and 1 (exact match). The results show that this estimate of similarity is realistic and unbiased. In the absence of chaotic oscillations, $\overline{z_{mean}} = 1$ and $\overline{N_{pcoinc}}$ equals $\overline{N_{ftcoinc}}$ while $N_{chaotic} = N$ therefore reducing $\Gamma_{chaotic}$ to Γ, which is consistent with the observations of Kistler (Kistler *et. al.*, 1997).

Estimating similarity for neural responses exhibiting chaotic oscillations requires that the means of two distributions be close to each other. The periodic stimuli used to induce chaotic behaviour in the neuron are similar in nature and hence means of their responses are within close proximity. A further limiting condition requires $|\mu_1 - \mu_2| < \Delta < \sigma_1$; this guarantees that the amplitude coincidences are bounded by a magnitude lesser than the standard deviation. According to the Empirical rule of Normal distribution, the sample size used for comparison is only 68.27%, however, the farther we go from the mean, the higher the amplitude deviates, so limiting the means within one standard deviation guarantees that amplitudes coincide with a precision that is biologically acceptable.

The results show that the similarity estimated using both firing times and amplitudes can be quantified by analyzing the number of absolute coincidences. Absolute coincidences are the number of spikes that coincide with respect to both firing times and amplitudes with a pre-defined precision δ. It is observed that similarity estimated by $\Gamma_{chaotic}$ correlates with the number of absolute coincidences. If the number of absolute coincidences are 25%, then the similarity estimated by $\Gamma_{chaotic}$ is approximately 0.25. This quantification ensures that the estimated similarity is realistic and mathematically realizable (Sarangdhar and Kambhampati, 2010a,b). The results show that $\Gamma_{chaotic}$ correctly identifies excitatory from inhibitory neural responses and eliminates all false positives obtained using coincidence factor (Γ).

5 $\Gamma_{chaotic}$: Model Validation, Energy Content and Energy Difference

5.1 Introduction

In the previous chapters, it is shown that due to the periodic nature of the synaptic stimuli, estimating the similarity between corresponding HH neural responses requires both amplitude and firing time information. Thus, a new similarity measure was developed to distinguish HH neural responses with underlying chaotic oscillations caused by periodic or sinusoidal stimuli. In the absence of chaotic oscillations, coincidence factor – which estimates similarity based only on firing times, is sufficient to compare neural responses. Hence, coincidence factor is adequate for model validation of reduced-order neuron models against biological neurons in the absence of chaotic oscillations. Firstly, this chapter discusses the application of $\Gamma_{chaotic}$ for validating reduced order models. It is also observed that $\Gamma_{chaotic}$ reduces to coincidence factor in the absence of amplitude fluctuations in the neural responses. This chapter also investigates the possibility of considering the energy content of neural responses as a unique method of estimating similarity by application of Slepian's principle (Slepian 1976).

The complex non-linear dynamics of the HH neuron have been studied both theoretically and physiologically in recent years to extend the understanding of its underlying neural dynamics (Lundström 1974; Abbott and Kepler 1990; Hasegawa 2000; Agüera *et. al.*, 2003a, b; Fourcaud-Trocmé 2003; Kepecs and Lisman 2003; Bokil *et. al.*, 2006; Davies *et. al.*, 2006; Diba *et. al.*, 2006; Dimitrov and Gedeon, 2006; Izhikevich 2006; Li and Ascoli 2006). Spikes or action potentials are evoked when a supra-threshold external stimulus is applied to the neuron. This complexity in the neural dynamics arises from the

probabilities associated with the open-close mechanism of the gating channels - *m*, *n* and *h*. The *m* and *h* are Na^+ activated while *n* is K^+ activated. As the HH neuron has three *m*, one *h* and four *n* channels, the equations of the HH neuron are highly nonlinear and therefore limit the mathematical analysis. In order to simplify the analysis, reduced-order neuron models such as the Integrate and Fire (IF) neuron, have been proposed and adopted (Abbott and Kepler, 1990, Izhikevich 2003). The aim of reduced neuron models is to approximate the neural response of a biological neuron in view of such reductions.

It has been shown that for the HH neuron, in the presence of chaotic oscillations or when the amplitudes of a neural response fluctuate, amplitude and firing time collectively reflect the true dynamics of a neuron and therefore both should feature in similarity estimation (Sarangdhar and Kambhampati 2008a,b; Sarangdhar and Kambhampati 2009). Similarity estimation is based on the principle of relative coincidences without coincidences by chance (Joeken and Schwegler, 1995), using a composite similarity measure based on amplitude and firing time coincidences (Sarangdhar and Kambhampati 2010a, b).

This chapter investigates the use of $\Gamma_{chaotic}$ to determine the similarity between the HH and IF neural responses for periodic and time-varying stimuli. The IF is a reduced order neuron model (see Chapter 2, section 2.6.2 for reduction) and it can fire spikes comparable to HH neural response. The aim of this comparison is to ascertain the efficacy of $\Gamma_{chaotic}$ for reduced order neuron's responses. This similarity estimation is based on conditional coincidences, which are amplitude coincidences given firing time coincidences. It is observed that the IF and HH neurons can fire at similar times for certain strength of stimuli but due to different neural dynamics, their amplitudes do not coincide. The initial representation of a neural response is unique to its stimulus (Diba *et. al.*, 2006; Chechik *et. al.*, 2006) thus, this chapter investigates if $\Gamma_{chaotic}$ can distinguish neural responses from different types of neurons. In addition, this chapter describes whether the similarity estimated by $\Gamma_{chaotic}$ for steady state neural responses is comparable and consistent with coincidence factor.

The absolute difference between neural responses can be defined by a fundamental concept known as '*energy content of a wave'*. This principle states that two neural responses are distinguishable if the difference of their energies is greater than a certain energy-difference minimum, ε_{min} (Slepian 1976). This ε_{min} can provide a benchmark to compare similarity estimates for neural responses against absolute difference. This principle is applied to neural response similarity estimation to compare $\Gamma_{chaotic}$ and Γ to see if absolute difference is estimated by either similarity measure. This chapter also determines if $\Gamma_{chaotic}$ compares effectively against ε_{min}, by correctly identifying dissimilar neural responses and showing a realistic and mathematically realisable estimate of similarity. The simulations carried out in this chapter are explained in the form of an algorithm in Appendix A, section A.5.3. Section A.5.3.1 describes the approach to model validation, section A.5.3.2 explains the use of $\Gamma_{chaotic}$ as a similarity measure for neural responses generated by constant current stimuli and section A.5.3.3 describes the application of Slepian's principle for estimating neural response similarity.

5.2 The Integrate and Fire (IF) Neuron

Hodgkin and Huxley first entailed the complexity of a biological neuron in the form of mathematical equations (Hodgkin and Huxley, 1952). However, this mathematical complexity limited the analysis of the neuronal dynamics, which prompted computational neuroscientists to consider simpler reduced-order neuron models. To assess the accuracy of the reduced-order models, their responses are compared with the responses of a sophisticated neuron model. Model validation has gained significant importance over the years as increasing effort is laboured to understand and decode the neuronal dynamics (Abbott and Kepler, 1990; Rinzel 1985; Joeken and Schwegler, 1995; Kistler *et. al.*, 1997; Izhikevich, 2003; Izhikevich, 2006).

The reduced-order model - an Integrate and Fire (IF) neuron (see Chapter 2, section 2.6.2 for reduction) generates neural responses that are comparable to a sophisticated neuron model like the HH. The HH neuron is based on physiological evidence of the complex

open-close mechanism of the ion channels. This makes the mathematical analysis of HH equations complex and limits the understanding of its neural dynamics. In order to analyse the dynamics, the HH equations are reduced to create lower order neuron models such as the IF model. The reduction is carried out by treating the Na^+-activating variable as instantaneous and replacing it with its asymptotic value; defining a linear relation between Na^+-deactivating and K^+-activating variables and therefore represented by a function of one variable alone. Reduced order models use this as a basis for reduction. The IF neuron treats the Na^+-activating as a constant therefore loses the physiological refractoriness of a biological neuron (Abbott and Kepler, 1990). However, the IF neuron can still be comparable to a HH neuron as the IF neuron offers the advantage of a fixed reset and a variable threshold.

5.2.1 Computational Model of the IF Neuron

The IF neuron is a basic representation of a biological neuron that can generate comparable neural responses (Abbott and Kepler, 1990; Gernster and Kistler, 2002). As the name suggests, the IF neuron is based on integrating the neural voltage until the firing threshold is reached. This represents physiological relevance such that only supra-threshold stimuli can generate a neural response. The basic differential equation of the IF neuron is given by

$$\tau \frac{du}{dt} = E + R \cdot I - u \tag{5.1}$$

where, τ is the time constant, E is the resting potential, R is the membrane resistance, I is the external current and u is the initial membrane voltage. Expressing the derivative $\frac{du}{dt}$ by a difference, we get

$$\frac{du}{dt} \approx \frac{u(t) - u(t - \Delta t)}{\Delta t} \tag{5.2}$$

Using indices for convenience and calculating the derivative $\frac{du_{i+1}}{dt}$ at time t_{i+1} from values at time t_i

$$u_i := u(t_i) \tag{5.3}$$

$$t_{i+1} := t_i + \Delta t \tag{5.4}$$

$$\dot{u}_{i+1} = \frac{(E + R \cdot I_i - u_i)}{\tau} \tag{5.5}$$

For each integration step, calculate u_{i+1} from the known value of u_i and the derivative.

$$\dot{u}_{i+1} = \left(\frac{du}{dt}\right)_{i+1} \approx \frac{u_{i+1} - u_i}{\Delta t} \tag{5.6}$$

$$u_{i+1} = u_i + \dot{u}_{i+1} \cdot \Delta t \tag{5.7}$$

Selecting $\Delta t << \tau$ gives good convergence. The parameters used for the simulation are E = -70mV, R=10MOhm, V_{reset} = -80mV, $V_{threshold}$ = -54mV and τ = 20ms.

5.2.2 Stimulus for the IF Neuron

The supra-threshold stimulus applied to the IF neuron is given by

$$I\_ext_{IF} = a_{static} + a_1 \sin(\omega_1 . t) + a_2 \sin(\omega_2 . t) \tag{5.8}$$

where, a_{static} is a static offset. The value of a_0 is provides the supra-threshold strength to the pre-synaptic spike train. The values of variables are a_0 = 3.95, a_1 = 0.25, a_2=0.25, ω_1 = 0.05 and ω_2 = 0.125. The values of the variables in (5.8) are chosen such that the IF neural responses are comparable for model validation.

5.2.3 Stimulus for the HH neuron

The synaptic stimulus applied to the HH neuron is based on (5.8) and is given by

$$I\_ext_{HH} = a_{dynamic} + a_1 \sin(\omega_1 t) + a_2 \sin(\omega_2 t) \tag{5.9}$$

where, $a_{dynamic}$ is a dynamically updated variable. The value of a_0 is dependent on the ISI of the pre-synaptic spike train. The values of variables are a_0 = ISI/1.5, a_1 = 0.75, a_2=0.75, ω_1 = 0.05 and ω_2 = 0.125.

Due to the reduction from the HH nonlinearity, the IF neuron has different neural dynamics hence it cannot mimic the exact behaviour of the HH neuron. (5.8) and (5.9) represent external stimuli that evoke an IF and HH neural spike at approximately similar times. The irregular ISI and fluctuating amplitudes observed in the HH neural responses are a result of the Na^+ gating channel (m) largely contributing to refractoriness. As the IF neuron approximates the instantaneous value of m to its asymptotic value, there is a loss in physiological refractoriness. This is modelled in the IF neuron using a variable threshold and a fixed reset.

5.3 Similarity estimates for the IF and HH Neuron

The IF and HH neuron are stimulated by a periodic and a time-varying stimulus with variable noise respectively. This ensures temporal similarity for both responses which are compared using a) coincidence factor (Γ) and b) $\Gamma_{chaotic}$. The aim of using this comparison of similarity estimates is to understand and determine if $\Gamma_{chaotic}$ can distinguish neural responses generated by different types of neurons.

As already discussed, a small change in neural stimulus is sufficient to induce distinct dynamics in a neuron, the noise in the external stimulus (5.8) and (5.9) is minimally varied between 0.05 and 0.50 to generate new stimuli for the IF and HH neurons. This synaptic stimulation causes fluctuations in the membrane voltage of the HH neuron and forces it to oscillate. These self-sustained oscillations in the neuronal dynamics result in varying

amplitudes and irregular ISI. The time-varying stimulus applied to the IF neuron evokes a series of action potentials that are compared with the responses of the HH neuron. The responses of the neurons plotted along with their corresponding stimuli with noise show that a small change in the temporal nature of the stimulus affects the neural dynamics that are responsible for the neural responses (fig. 5.1a-d). Table 5.1 below shows the similarity estimated for each pair of neural responses for each simulation.

$\Gamma_{chaotic}$ estimates the similarity by comparing amplitude variations along with individual firing times. This approach implicitly considers the neural dynamics (chaos and resultant varying amplitudes) therefore, it has a two-dimensional approach to comparison. However, Γ estimates similarity using firing time information alone; firing time information is sufficient when the neural dynamics are non-chaotic or the responses of the neuron are steady state.

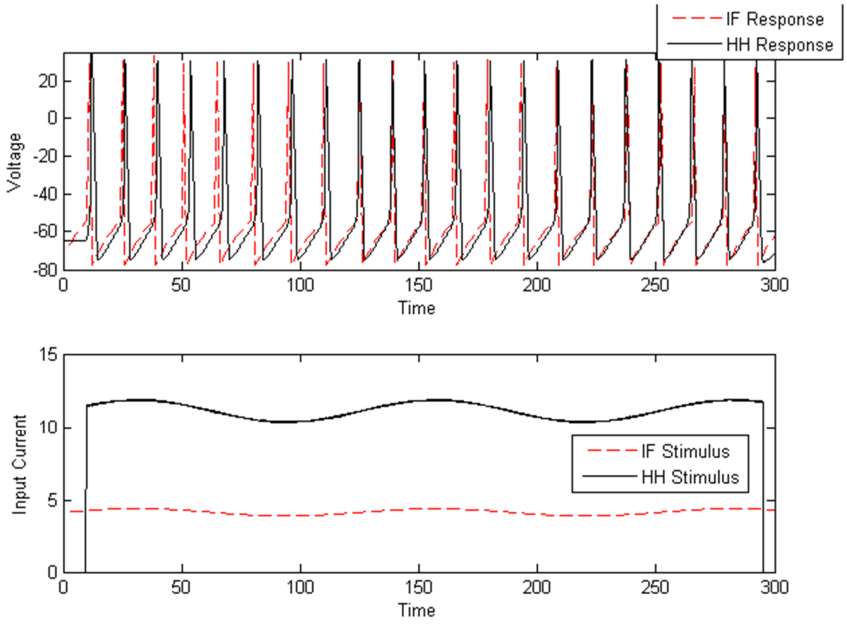

Fig. 5.1(a)

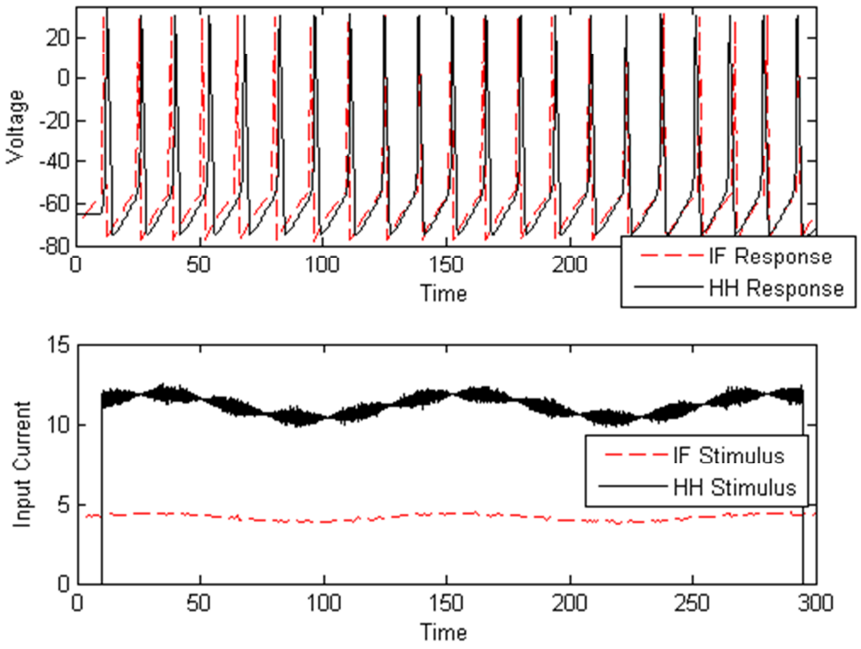

Fig. 5.1(b)

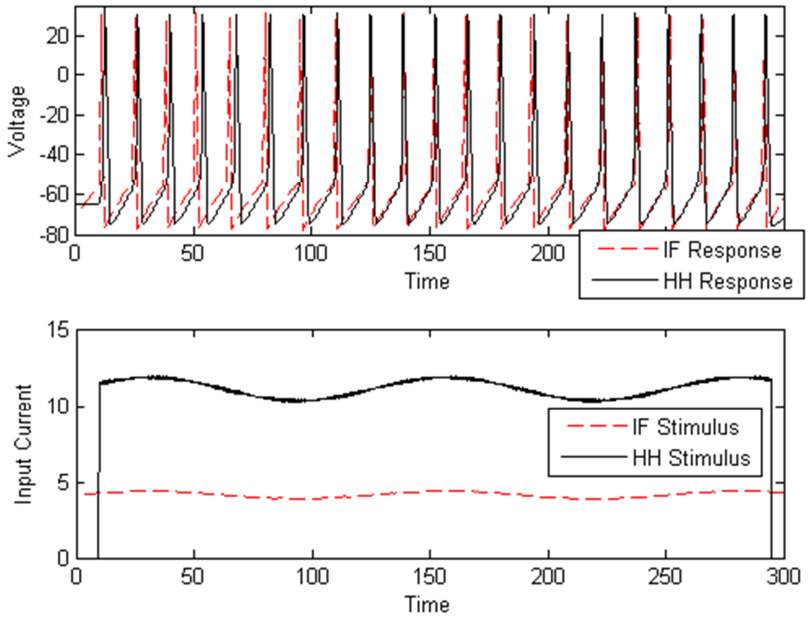

Fig. 5.1(c)

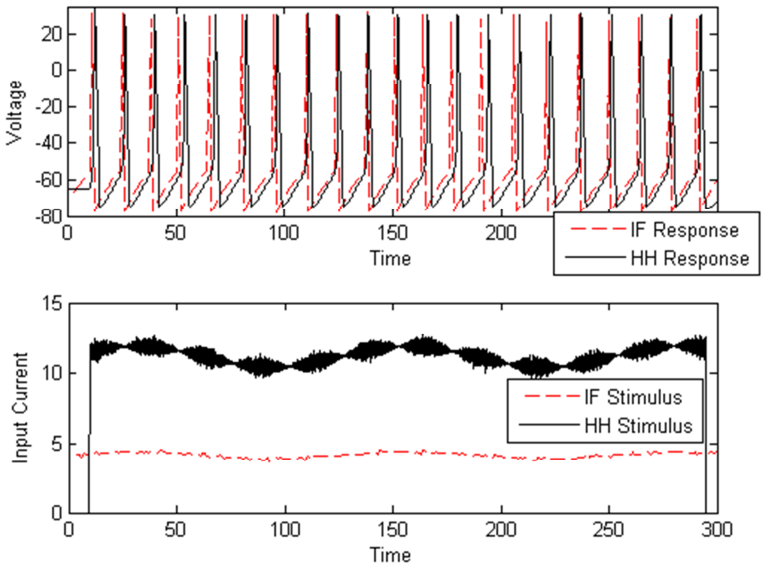

Fig. 5.1(d)

Figure 5.1: Responses of the IF (in dash) and HH (in bold) neuron to time-varying stimuli and periodic stimuli with varying noise. (a) injected stimulus having minimum noise, (b)injected stimulus with medium-high noise, (c) injected stimulus with medium-low noise, (d) injected stimulus with very high noise. In each of the sub-plots, the responses are plotted for their corresponding stimuli (below the responses). The neural responses plotted are generated for different neural stimuli. The corresponding stimuli are shown - bold for HH and dashed for the IF neuron.

	Γ	$\Gamma_{chaotic}$	$\%FT_{coinc}$	$\%A_{coinc}$	$\%N_{coinc}$
(a)	0.8016	0.4195	85.7143	61.9048	47.6190
(b)	0.7354	0.5712	80.9524	76.1905	61.9048
(c)	0.8016	0.5153	85.7143	71.4286	57.1429
(d)	0.5370	0.3805	66.6667	66.6667	42.8571

Table 5.1: The corresponding similarity for neural responses in fig. 5.1 is estimated by Γ and $\Gamma_{chaotic}$ for IF and HH neurons. The similarity estimated by $\Gamma_{chaotic}$ is consistent with the number of conditional coincidences. FT_{coinc}, A_{coinc} and N_{coinc} represent the number of firing time, amplitude and conditional coincidences respectively.

It is observed from table 5.1 that the similarity estimated by $\Gamma_{chaotic}$ is lower than Γ for (a), (b), (c) & (d). These values represent the comparative likeness between corresponding IF and HH neural responses. Γ represents the similarity based on firing time coincidences while $\Gamma_{chaotic}$ estimates similarity based on firing times and amplitudes. The percentage of firing time coincidences ($\%FT_{coinc}$), amplitude coincidences ($\%A_{coinc}$) and conditional coincidences (amplitude coincidences given firing times coincide) $\%N_{coinc}$ represented in table 5.1 show that the estimated similarity $\Gamma_{chaotic}$ is consistent with the percentage of

conditional coincidences. In (a), 85.7143% of the IF spikes coincide with corresponding HH spikes, only 61.9048% of them coincide with respect to amplitudes. Hence, the percentage of conditional coincidences is 47.6190. The corresponding similarity estimated by $\Gamma_{chaotic}$ is 0.4195. A similar relationship is seen for other neural response pairs. The results show that $\Gamma_{chaotic}$ correlates with the percentage of conditional coincidences ($\%N_{coinc}$) and is evident throughout table 5.1. These observations of $\Gamma_{chaotic}$ correlating with absolute coincidences are also seen in Chapter 4.

The HH neuron under self-sustained oscillations has fluctuations in the membrane voltage. This phenomenon cannot be accurately replicated by an IF neuron due to a reduction to a lower order. In some cases, injection of a time-varying stimulus can establish IO equivalence (i.e. both neurons fire at approximately similar times) between IF and HH neuron (Lazar, 2006). However, an IO equivalence has not been chosen so as to retain individuality between the IF and HH neuron. A time-varying periodic stimulus is known to induce chaotic dynamics in the HH neuron and the IF neuron can generate responses that are temporally similar. The results in this section outline that as the underlying dynamics are independent and distinct, the responses of the two neurons will be different. $\Gamma_{chaotic}$ considers amplitude fluctuations arising due to periodic stimuli therefore has lower similarity estimates than Γ. It is worthwhile to mention that Γ does differentiate between the responses, however, in the presence of chaotic oscillations an exact estimate of similarity is given by $\Gamma_{chaotic}$ as it considers additional temporal information.

5.4 Constant Current Stimulus and $\Gamma_{chaotic}$

$\Gamma_{chaotic}$ is formulated to estimate similarity of neural responses exhibiting chaotic oscillations generated by time-varying periodic stimuli. In this section, performance of $\Gamma_{chaotic}$ is evaluated for neural responses generated with a constant current stimuli. A constant current stimulus does not induce fluctuations in the membrane voltage hence, resulting in a steady state response. A constant current ($I_{constant}$) with noise (η) is injected into two HH neurons at independent times t_1 and t_1'. The corresponding neural

responses $R_1$and R_1' are compared using $\Gamma_{chaotic}$. The noise (η) has a Normal distribution with mean $\mu = 0$ and standard deviation $\sigma = 0.025$.

The injected current is slowly increased in strength from 8μA to 10μA to get neural responses for comparison. Similarity is estimated using $\Gamma_{chaotic}$ for each pair of responses. It is observed that $\Gamma_{chaotic}$ is unity for all pairs of neural responses indicating that each pair is an exact match. These results are consistent with Γ (Table 5.2)

The HH neurons fire at precise intervals with approximately the same amplitude (within a precision for similarity). For each simulation (fig. 5.2 a-c), the neural responses overlap such that they fall within the firing time precision of $\Gamma_{chaotic}$. All the corresponding spikes in each neural response coincide with respect to firing time and amplitude hence, the conditional coincidences equate to 100%, which correlates to $\Gamma_{chaotic} = 1$.

The results in table 5.2 indicate that $\Gamma_{chaotic}$ performs in consistence with Γ. These results indicate that in the absence of amplitude variations, $\Gamma_{chaotic}$ reduces to Γ.

	Stimulus Strength	Γ	$\Gamma_{chaotic}$
(a)	$8\mu A$	1	1
(b)	$9\mu A$	1	1
(c)	$10\mu A$	1	1

Table 5.2: Performance of $\Gamma_{chaotic}$ compared with Γ for HH neurons stimulated with a constant current stimulus. The strength of the stimulus is increased by $1\mu A$ from a-c. All spikes in the steady state responses of the HH neuron coincide with respect to firing times and amplitudes. Hence, conditional coincidences are 100%. This correlates to $\Gamma_{chaotic} = 1$.

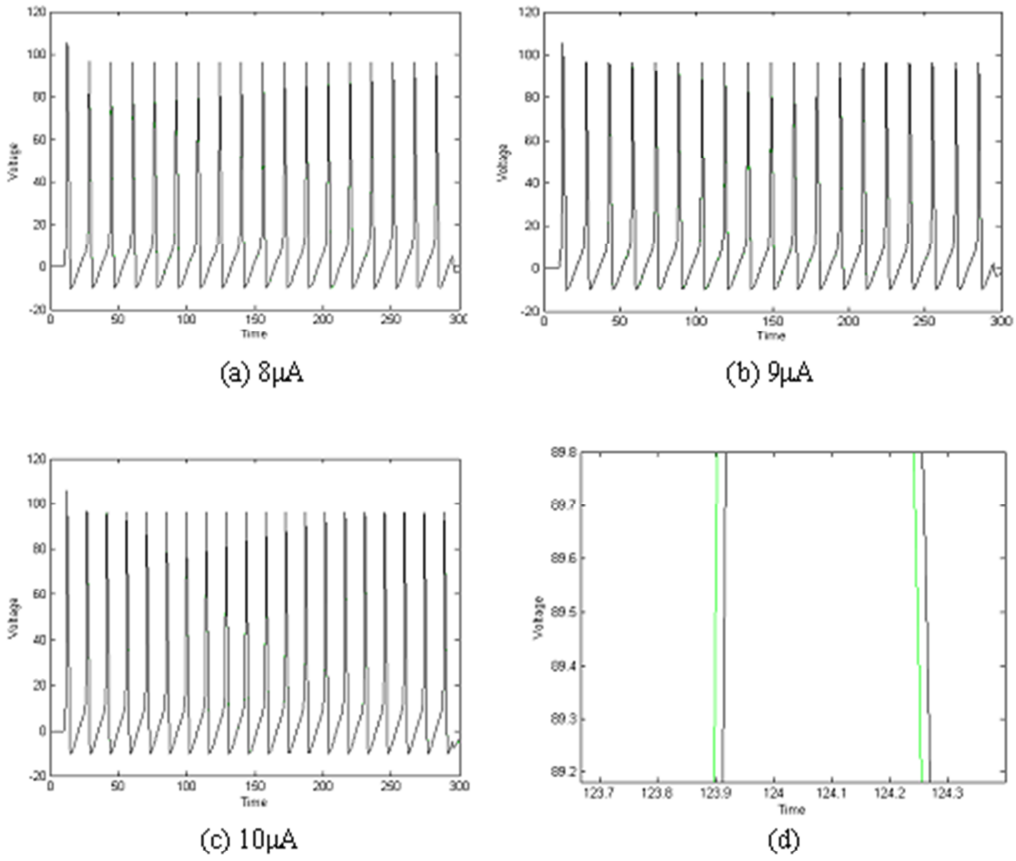

Figure 5.2: The responses of the two HH neurons to constant current stimulus. The responses of the neurons for stimulus 8μA-10μA are shown in (a), (b) & (c) respectively. The responses overlap to a high degree as indicated in (d).

5.5 Energy Content of a Spike Train and its role in Neural Response Differentiation

Chapters 3 and 4 explain the need for the formulation of $\Gamma_{chaotic}$ and outline the biological relevance of a neural activity exhibiting chaotic oscillations. The previous sections described the application of $\Gamma_{chaotic}$ to validate reduced-order neuron models and steady state neural responses. Due to the varying temporal nature of neural responses, there exists an '*absolute difference*' between them. This absolute difference is implemented as an application of Slepian's principle (Slepian, 1976) and is used as a benchmark to assess the similarity estimates of $\Gamma_{chaotic}$ and Γ.

Each neural response is a function of time, therefore, according to Slepian (Slepian, 1976), a neural response can be considered as a signal and two signals of time $f(t)$ and $g(t)$ are distinguishable if their difference has sufficient energy (E) i.e.

$$\int_{-\infty}^{\infty} |f(t) - g(t)|^2 > \varepsilon_{\min} \tag{5.10}$$

where, ε_{min} is the energy-difference minimum required for two neural responses to be distinguishable. Assuming that all responses are distinct and distinguishable i.e. any two neural responses are different from each other, it follows that their energy difference is greater than ε_{min}. This energy-difference minimum for differentiating two responses is not defined therefore a simple but realistic threshold ε_{min} for distinction is considered.

The principal square root of a non-negative real number is always less than the number itself (except if the number is less than 1). This principle serves in defining the energy-difference minimum. Let the energy-difference minimum ε_{min} be the square root of the energy difference between two neural responses (5.11).

$$\varepsilon_{\min} = \sqrt{\int_{-\infty}^{\infty} |f(t) - g(t)|^2} \tag{5.11}$$

This ensures that any two given spike trains are dissimilar from each other and ε_{min} acts as a threshold for differentiation. The only exception being a spike train compared to itself – where $f(t) = g(t)$ and therefore E $= \varepsilon_{min} = 0$. In Chapters 3 and 4, it is shown that two neural responses $f(t)$ and $g(t)$ are identical only if they are generated by the same stimulus. The minimum energy-difference required for two neural responses to be classified as distinct is given by ε_{min} which is normalised between 0 and 1.

5.5.1 Slepian's Principle – HH neurons

The results in Chapter 4 show that the similarity between neural responses exhibiting chaotic oscillations is well approximated by $\Gamma_{chaotic}$. This section investigates the

similarity estimates of $\Gamma_{chaotic}$ against the '*absolute difference*' in neural responses and whether $\Gamma_{chaotic}$ essentially captures the '*energy-difference minimum*' ε_{min}. The aim of this section is to outline and identify if $\Gamma_{chaotic}$ can determine similarity with an implicit consideration of Slepian's principle.

5.5.1.1 Energy Difference

The HH neurons (HH_1 and HH_{ref}) are stimulated by periodic stimuli (Park and Kim, 1996) and a variation in the ISI of the periodic stimuli generate neural responses across a broad range of ISI, as seen in Chapter 4.

HH_1 is stimulated by varying the ISI of the periodic stimulus between 13ms-15ms to generate various neural responses. HH_{ref} is stimulated by a periodic stimulus with ISI = 14ms (T_{ref}) to generate R_{ref14} and each HH_1 neural response is compared against R_{ref14}. The difference in the energy of each pair of neural responses is calculated using (5.10) and the threshold for differentiation 'ε_{min}' is determined using (5.11). Sample ε_{min} values for ISI varied between 13-15ms are shown in Table 5.3.

T(ms)	T_{ref} (ms)	ε_{min}
13.00	14.00	0.8649
13.25	14.00	0.7971
13.50	14.00	0.8074
13.75	14.00	0.7652
14.00	14.00	0
14.25	14.00	0.6303
14.50	14.00	0.8140
14.75	14.00	0.9357
15.00	14.00	1.0000

Table 5.3: Sample ε_{min} values for responses to stimuli generated with ISI varying between 13ms-15ms.

Table 5.3 shows the normalised energy-difference minimum ε_{min} in comparison with $\Gamma_{chaotic}$ and Γ. Any two neural responses are distinguishable if the difference between

their energies is greater than ε_{min}. It is observed that this ε_{min} is unique for each pair of ISI. It implies that each neural response is characterised by the stimulus ISI (T) as it influences the temporal pattern of the resulting neural responses. Thus, T remains intrinsic to response comparison.

In order for the neural responses generated by periodic stimuli having ISI $T = 14.25ms$ and $T_{ref} = 14ms$ to be distinguished, the difference between them needs to have sufficient energy i.e. greater than $\varepsilon_{min} = 0.6303$. If both $T = T_{ref}$, it implies that stimuli are identical. As discussed in Chapters 3 and 4, identical stimuli generate exactly matching neural responses and the *energy-difference* between these neural responses is zero therefore, $\varepsilon_{min} = 0$. Hence, the value of ε_{min} for $T = 14ms$ and $T_{ref} = 14ms$ is zero. $\varepsilon_{min} = 0$ indicates that the two neural responses have a zero *energy-difference* and they are an exact match.

Similarly, HH_1 is stimulated by varying the ISI (T) between 14ms-16ms (set II) and 15ms-17ms (set III) while the corresponding stimulus to HH_{ref} is fixed with $T_{ref} = 14ms$ (set II) and $T_{ref} = 15ms$ (set III). It is observed for each of the three sets, $\varepsilon_{min} = 0$ between two identical neural responses. Also, as all neural responses are assumed to be distinct, for dissimilar neural responses $\varepsilon_{min} \neq 0$. These results indicate that two neural responses with *'zero'* energy difference are an *'exact-match'* (fig. 5.3-5.5).

5.5.1.2 Evaluating similarity estimates of $\Gamma_{chaotic}$, ε_{min} and Γ

To evaluate the efficacy of $\Gamma_{chaotic}$ for any two neural responses, it should implicitly identify the difference in their energies, which should be greater than ε_{min}. As the similarity estimates from $\Gamma_{chaotic}$ and Γ are between 0 and 1, they are compared against the normalised value of ε_{min}. Slepian's principle is used to distinguish neural responses while $\Gamma_{chaotic}$ and Γ are similarity measures. Hence, for the purpose of evaluation, the dissimilarity indices for $\Gamma_{chaotic}$ and Γ are calculated.

Let $\Gamma_{chaotic}'$ and Γ' be the corresponding dissimilarity indices of $\Gamma_{chaotic}$ and Γ. The dissimilarity indices are obtained by subtracting the corresponding similarities from unity. For $\Gamma_{chaotic}'$ to correctly identify ε_{min}, the dissimilarity estimated by $\Gamma_{chaotic}'$ should be higher than ε_{min}. The dissimilarity indices and ε_{min} are calculated for each set of neural responses in which the ISI (T) is varied between 13ms-15ms (set I), 14ms-16ms (set II) and 15ms-17ms (set III).

The results show that $\Gamma_{chaotic}'$ identifies the energy-difference minimum ε_{min} for most pairs of neural responses across the three sets. It is discussed in Chapter 4 that $\Gamma_{chaotic}$ evaluates similarity more accurately than Γ as it uses both amplitude and firing time information to estimate similarity. Therefore, the dissimilarity index of $\Gamma_{chaotic}$ is more accurate than Γ estimating ε_{min}.

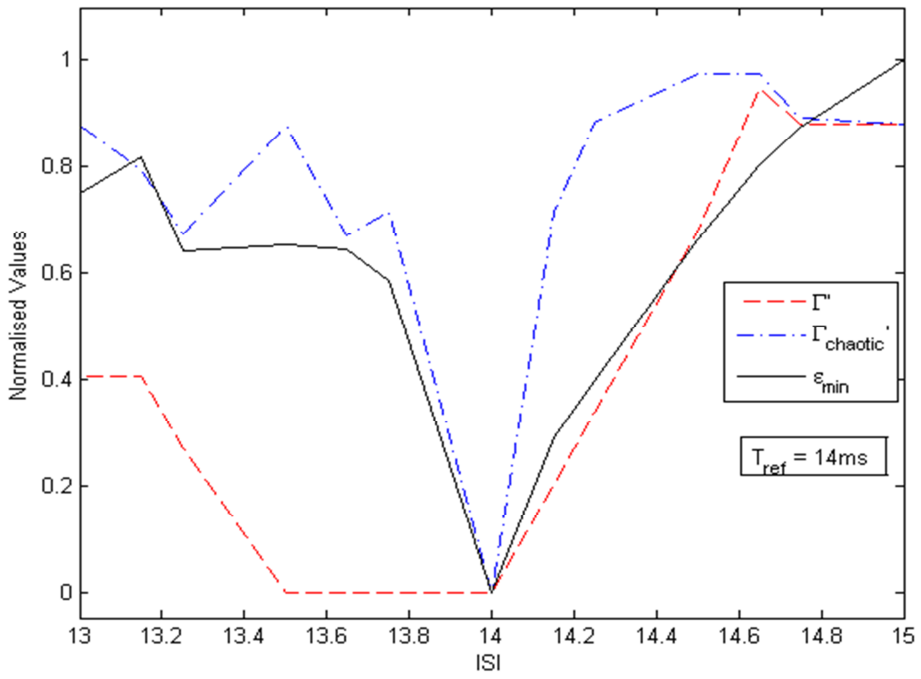

Figure 5.3: Performance of $\Gamma_{chaotic}'$ in comparison to normalised values of ε_min and Γ' for ISI varied between 13ms-15ms. ε_{min} represents the energy-difference minimum. $\Gamma_{chaotic}'$correctly identifies the dissimilarity in the neural responses. An exact match between neural responses is observed at ISI=14ms. This is also correctly identified by $\Gamma_{chaotic}' = 0$.

Figures 5.3-5.5 show that $\Gamma_{chaotic}'$ distinguishes neural responses with a higher degree of accuracy than Γ' and the plots of $\Gamma_{chaotic}'$ and Γ' are separated by the energy-difference

minimum ε_{min}. The dissimilarity between neural response pairs estimated by $\Gamma_{chaotic}{}'$ is higher than ε_{min} indicating that the neural response pairs are distinguishable. Also, it is seen that all the neural response pairs are dissimilar except when $\varepsilon_{min} = 0$. At $\varepsilon_{min} = 0$, the neural responses are an exact match and it is already established that $\Gamma_{chaotic}$ accurately identifies similarity. Hence, the corresponding dissimilarity index $\Gamma'_{chaotic} = 0$. It is discussed in Chapters 3 and 4 that for a single bipolar neuron, such as the HH, only identical stimuli can generate exactly matching neural responses. This result is consistent with understanding that all neural responses are distinct except if they are generated by the same or identical stimuli (Davies *et. al.*, 2006, Chechik *et. al.*, 2006).

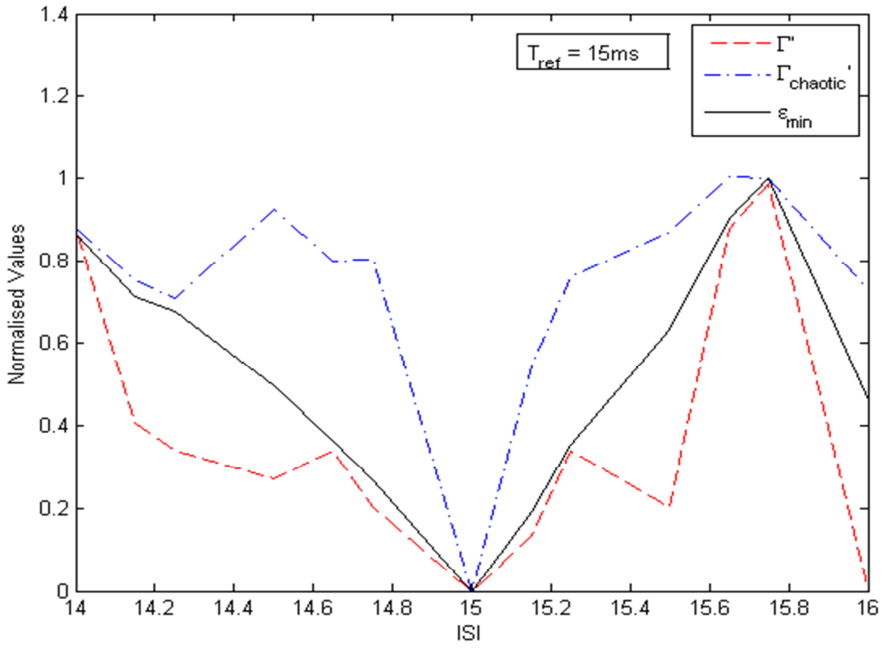

Figure 5.4: Performance of $\Gamma_{chaotic}$' in comparison to normalised values of ε_{min} and Γ' for ISI varied between 14ms-16ms. ε_{min} represents the energy-difference minimum. $\Gamma_{chaotic}$' correctly identifies the dissimilarity in the neural responses. An exact match between neural responses is observed at ISI=15ms. This is also correctly identified by $\Gamma_{chaotic}$' = 0. All dissimilar neural responses are correctly identified.

On the contrary, the dissimilarity estimated by Γ' is less than ε_{min}, which indicates that the minimum energy difference cannot be estimated by Γ'. As Γ is only utilises firing times of the neural spikes, it can be concluded that the energy-difference minimum ε_{min} cannot be determined based on firing time alone. $\Gamma_{chaotic}$ estimates similarity using firing times and

amplitudes of neural spikes and hence captures this threshold of differentiation. It is evident from the results that due to the firing-times limitation, Γ′ cannot capture ε_{min}.

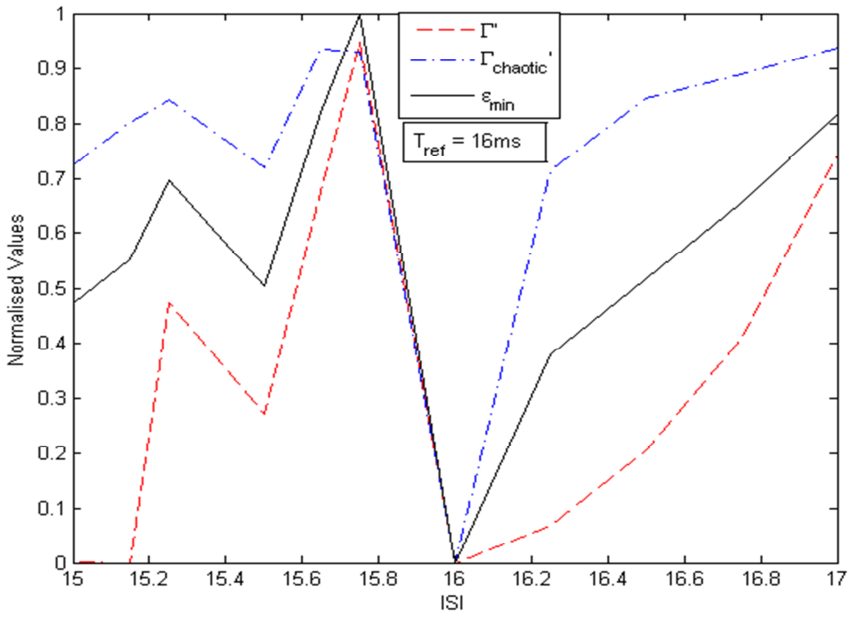

Figure 5.5: Performance of $\Gamma_{chaotic}$' in comparison to normalised values of ε_{min} and Γ' for ISI varied between 15ms-17ms. ε_{min} represents the energy-difference minimum. $\Gamma_{chaotic}$' correctly identifies the dissimilarity in most neural responses. An exact match between neural responses is observed at ISI=16ms. This is also correctly identified by $\Gamma_{chaotic}$' = 0.

In medical diagnosis where the temporal pattern of the neural response is crucial, such as Epilepsy (Kumar et. al., 2009; Milton and Jung, 2003), there remains a possibility of absolute difference between neural responses being utilised as a framework for comparison. $\Gamma_{chaotic}$ is therefore more applicable to estimate similarity of neural responses in presence of chaotic oscillations or when amplitudes fluctuate and estimating dissimilarity in accordance with the energy-difference minimum ε_{min} as defined by Slepian.

5.6 Chapter Summary

The complex nonlinearity of the HH neuron limits the understanding of its neural dynamics leading to reduced-order models of neurons, which aid mathematical analysis by simplifying the neural dynamics. This chapter considers stimulation of HH neurons with periodic stimuli and compares their responses with an IF neuron. Due to the periodic

nature of the stimulus, the HH neuron displays self-sustained oscillations, which are characterised by irregular firing times and fluctuating amplitudes. The IF neuron, due to a reduction in the nonlinearity of its dynamics, cannot model such chaotic oscillations.

In the presence of chaotic oscillations or fluctuations in the amplitudes of a neural response, both firing times and amplitudes reflect the true dynamics of the internal state of a neuron. Therefore, both firing times and amplitudes should feature in similarity estimation (Sarangdhar and Kambhampati, 2008a,b; Sarangdhar and Kambhampati, 2009). The similarity thus obtained by $\Gamma_{chaotic}$ correlates with the number of spikes that coincide with respect to both firing times and amplitudes. The results show that the similarity estimated by $\Gamma_{chaotic}$ is approximately equal to the number of conditional coincidences - amplitude coincidences given firing time coincidences (Sarangdhar and Kambhampati, 2010a,b). In addition, in the absence of chaotic oscillations, $\Gamma_{chaotic}$ reduces to Γ.

Two neural responses are distinguishable if the difference between their energies is greater than ε_{min} (Slepian, 1976). In other words, identical neural responses will have similar energies and hence $\varepsilon_{min} = 0$. If two neural responses are dissimilar, their energy-difference minimum $\varepsilon_{min} \neq 0$. Considering a simple but realistic ε_{min}, it is seen that the dissimilarity index $\Gamma_{chaotic}{}'$ distinguishes all neural responses in accordance with ε_{min}. On the other hand, the estimation of $\varepsilon_{min}$is rather less accurate using Γ' (dissimilarity index of Γ) as Γ is based only on firing times of neural spikes. The results suggest that both firing times and amplitude are required to capture ε_{min} .

It is worthwhile to mention that the energy-difference minimum ε_{min} considered in this chapter is simple realistic threshold. It is chosen such that each neural response can be unique and future work is aimed at establishing a relationship that can quantify ε_{min} in terms of neural response parameters.

6 Stimulus Reconstruction from a Hodgkin-Huxley Neural Response

6.1 Introduction

Neural responses are the fundamental expressions of any neural activity, its nature determines the information carried by a neural response. In majority of cases, the underlying stimulus that triggers this activity remains largely unknown. Recent studies to reconstruct the stimulus from a neural response show that the high non-linearity of neural dynamics renders analytical inversion of a neuron a challenging task (Abbott and Kepler 1990; Saggar *et. al.*, 2007; Lazar 2004; Lazar 2007a,b). This chapter presents a numerical solution rather than an analytical one to reconstruct stimuli from Hodgkin-Huxley (HH) neural responses. The stimulus is reconstructed by first retrieving the maximal conductances of the ionic gating channels and then numerically solving the Hodgkin-Huxley equations for the stimulus. By considering a numerical solution, the retrieval of neural dynamics is possible, hence, this reconstruction approach also retrieves the neural dynamics for which an analytical solution does not currently exist. The ability to reconstruct neural dynamics offers an advantage in understanding the timeline changes in the neural mechanism for brain disorders like Motor Neuron Disease (MND), Parkinson's Disease (PD) and Epilepsy. This chapter shows the reconstruction of constant-current and periodic stimuli along with the retrieval of neural dynamics using this approach. The simulations carried out in this chapter are explained in the form of an algorithm in Appendix A, section A.5.4.

6.2 Related Research on Stimulus Construction

A stimulus represents a trigger for a neural activity, which underlines any neural response. This relationship between a neural response and its stimulus has been studied in the recent years to understand the encoding and decoding mechanisms adopted by neurons (Panzeri et.al., 1999; Stanley and SeyedBoloori, 2001; Sanger, 2002; Kohn and Vieira, 2002; Nelken and Chechik, 2005; Cozzi et. al., 2006). Not much is known about how neurons specifically encode and decode information. It is thought that either the firing time or the rate of fire of a neuron carries specific neural response information (Rinzel 1985; Panzeri *et. al.*, 1999; Gabbiani and Metzner, 1999). On the other hand, research suggests that reconstruction of the stimulus from a neural response can aid our understanding of neural coding (Wilson, 1999a,b). The ability to reconstruct a stimulus hence offers to retrieve stimulus parameters that can help extend our understanding of neuronal encoding and decoding.

Research on input reconstruction has been carried out across many fields like digital filters, neural networks, algorithms and complexity, and digital signal processing (Das *et. al.*, 2006; Saggar *et. al.*, 2007; Stanley and SeyedBoloori, 2001; Stanley 2001; Lazar and Pnevmatikakis, 2009; Lazar 2007a,b; Lazar 2006; Lazar *et. al.*, 2006; Lazar 2004). Similar approach can be considered for stimulus reconstruction however, due to the high non-linearity of neural dynamics, it is very difficult to obtain an analytical solution that can recreate neural dynamics. Periodic signals, unlike aperiodic signals, can be recovered using conventional filters (Das *et. al.*, 2006). Artificial neural networks are used to treat the HH neuron as a black box and reconstruct the stimulus by learning the dynamics (Saggar *et. al.*, 2007). Other implementations use a reverse filter that predicts the sensory input from neuronal activity and recursive algorithms to reconstruct stimulus from an ensemble of neurons (Stanley and SeyedBoloori, 2001; Stanley 2001). The principles of Time Encoding and Decoding Machines for signal recovery have been explored to reconstruct a neural stimulus whereas, a more direct approach to recover stimulus

focuses to make the HH neuron Input-Output (IO) equivalent to an Integrate and Fire (IF) neuron (Lazar and Pnevmatikakis, 2009; Lazar 2007a,b; Lazar 2006; Lazar *et. al.*, 2006; Lazar 2004). These approaches establish a relationship between the neural response and the stimulus but are not designed to capture or retrieve the neural dynamics. In other words, they offer some starting point for stimulus reconstruction but it remains quite a challenge to analytically invert a neuron. However, it is possible to reconstruct stimulus from a neural response and retrieve neural dynamics using numerical approximations and small time-steps for integration; this offers a local solution to the problem of stimulus reconstruction.

This chapter aims to reconstruct constant-current and periodic stimuli by a) extracting the maximal conductances from a trace of neural response and b) solving the neural equations for the stimulus. To reconstruct the stimulus, it is imperative that linearization is carried out. The above approach is demonstrated in this chapter using a Hodgkin-Huxley (HH) neuron and Euler integration. This reconstruction involves solving the neural equations for a small time-step δ, such that the maximal conductances are extracted accurately. Also, the reconstructed stimulus matches the original stimulus accurately. As reconstruction of the stimulus involves solving the neural equations, this approach can replicate the neural dynamics, the time-dependent changes in the voltage-gated channels of Na^+, K^+ and Cl^-. This technique, though computationally iterative, offers a local solution to the problem of inverting a neural response (Sarangdhar and Kambhampati, 2010c, d, e).

6.3 Stimulus Reconstruction of HH neuron

Let $V(t)$ be the neural response of the HH neuron to a synaptic stimulus $I(t)$ with ionic conductances g_{Na}, g_K and g_L. Assuming that $I(t)$ is unknown and only the neural response $V(t)$ and the reversal potential V_{ion} are known, the aim is to reconstruct the stimulus $I'(t)$ such that $I(t)$ and $I'(t)$ are identical. The reversal potential is the membrane voltage at which there is no net flow of ions from one side of the membrane to the other. In order to reconstruct $I'(t)$, the conductance parameters of the ions need to be retrieved first.

Therefore the primary target is to retrieve g'_{Na}, g'_{K} and g'_{L} and based on the equations of the HH model, reconstruct $I'(t)$ without any information of $I(t)$.

6.3.1 Extracting the maximal conductances

The equations 2.11-2.23 from Chapter 2 show that the gating variables m, n and h only depend on the instantaneous voltage at time t. The instantaneous voltage at time t is given by

$$v(t) = v(0) + \frac{1}{C}\left[\begin{array}{l} \int_0^t I(t')dt' - g'_{Na}\int_0^t m^3(t')h(t')\cdot(v(t')-V_{Na})dt' \\ -g'_K\int_0^t n^4(t')\cdot(v(t')-V_K)dt' - g_L\int_0^t (v(t')-V_L)dt' \end{array}\right] \tag{6.1}$$

Reconstruction of the stimulus is based on accurate retrieval of the maximal conductances of the ion channels of the HH neuron. The three ionic conductances can be retrieved by re-writing equation (6.1) to form three linear equations in three unknowns (ionic conductances). The formulation of these equations is proposed as an algorithm by Shepardson (Shepardson 2009). Solving these equations will yield the conductances for Na^+, K^+ and Cl^-.

Consider a small voltage trace $v(t)$ of the HH neuron for time t and select three times t_i, $i = 1, 2, 3$. As the voltage trace $v(t)$ is known over all t, $v(t_i)$ is known for $i = 1, 2, 3$.

Let functions $f_j(t), j = 1,2,3$ be defined as

$$f_1(t) = -\frac{1}{C}\int_0^t m^3(t')h(t')\cdot(v(t')-V_{Na})dt' \tag{6.2}$$

$$f_2(t) = -\frac{1}{C}\int_0^t n^4(t')\cdot(v(t')-V_K)dt' \tag{6.3}$$

$$f_3(t) = -\frac{1}{C}\int_0^t (v(t') - V_L)dt' \tag{6.4}$$

(6.2-6.4) are obtained by splitting (6.1) for each ion channel (j) of the HH neuron.

Let $b(t)$ be defined as

$$b(t) = v(t) - v(0) - \int_0^t I(t')dt' \tag{6.5}$$

Hence combining (6.1-6.5), we have

$$b(t) = g'_{Na}\ f_1(t) + g'_K\ f_2(t) + g'_L\ f_3(t) \tag{6.6}$$

The aim is to retrieve the maximal conductances g'_{Na}, g'_K and g'_L. Let the conductances be represented by x_1, x_2 and x_3. If $\int_0^t I(t')dt'$ is a known analytic function, the value of $b(t)$ is known for all values of t. Hence, for a voltage trace $v(t)$ and external stimulus $I(t)$, approximations to the gating variables, m, n and h are obtained by integrating the HH equations. If m', n' and h' are the estimates of the gating variables and $f'_j(t)$ is the resultant approximation of $f_j(t)$, then retrieving the maximal conductances can be defined as a solution to the linear system

$$b(t_i) = \sum_{j=1}^{3} f'_j(t_i)x_j\ ,\ i = 1\ldots N \tag{6.7}$$

This is an *overdetermined* system of linear equations in the form $Ax = b$. An approximate solution can be obtained by using the entire set of voltages from $v(t)$ generated during the integration of the HH equations and treating (6.7) as a linear least squares problem.

Hence, the best fit solution in the linear least squares sense is obtained by solving

$$\min_x \sum_{i=1}^{N} \left(b(t_i) - \sum_{j=1}^{3} f'_j(t_i) x_j \right)^2 \tag{6.8}$$

If $A \epsilon \mathbb{R}^{N \times 3}$ is the matrix whose entries are $a_{i,j} = f'_j(t_i), i = 1 \dots N$ and $b \epsilon \mathbb{R}^N$, (6.5) can be rewritten as

$$\min_x \| Ax - b \|_2 \tag{6.9}$$

As the equations $Ax = b$ are linear in x, a solution is obtainable using linear regression.

6.3.2 Reconstructing the Stimulus

The approach defined above requires the knowledge of both voltage $v(t)$ and the external stimulus $I(t)$, for all time t. In principle, it is unrealistic to know the stimulus for all times t and in majority of biological cases, the stimulus $I(t)$ remains unknown. Therefore, retrieving the maximal conductances using the equations (6.2-6.9) is specific when all parameters are known.

In order to reconstruct the stimulus entirely without any knowledge of corresponding $I(t)$ for a neural response $V(t)$, a two-fold approach is adopted. As the type of the neuron and the reversal potential for Na^+, K^+ and Cl^- is known, this algorithm shows that the neural stimulus can be reconstructed without the knowledge of the original stimulus $I(t)$. The algorithm computes the approximate estimates of maximal conductances and uses these approximations to reconstruct the unknown neural stimulus.

The algorithm described below (6.2.2.1) shows that the reconstructed stimulus $I'(t)$ can be obtained from the voltage trace of a known neuron.

6.3.2.1 Algorithm for Stimulus Reconstruction and Neural Dynamics Retrieval

1) For a known neuron, record any neural response $V(t)$ whose stimulus, say $I(t)$, requires to be reconstructed

2) Inject a supra-threshold stimulus, $I_s(t_s)$ for a small time duration t_s

3) Record the corresponding voltage trace generated, $v_s(t_s)$

4) Retrieve the maximal conductances using $v_s(t_s)$, equations (6.2-6.9) and $I_s(t_s)$ as the external stimulus

5) Using the approximated maximal conductances, g'_{Na}, g'_K and g'_L, solve the HH equations using the recorded original neural response $V(t)$ and the stimulus as the only unknown to get the reconstructed stimulus $I'(t)$

6.3.2.2 Numerical Solution

The HH equations can be re-written as

$$\left.\begin{aligned} I'(t) = {} & g'_{Na}\, m'(t)^3 h'(t)(v(t) - V_{Na}) + g'_K\, n'(t)^4 (v(t) - V_K) \\ & + g'_L\, (v(t) - V_L) + C\,\frac{dv}{dt} \end{aligned}\right\} \tag{6.10}$$

where, g'_{Na}, g'_K and g'_L are the approximated maximal conductances calculated from $v_s(t_s)$ and m', n' and h' are the estimates of the gating variables m, n and h respectively.

As $V(t)$ is known for all times t, the rate of change of voltage ($\frac{dv}{dt}$) can be numerically approximated. The retrieved neural dynamics are given by the following equations

$$\frac{dm'}{dt} = -(\alpha_{m'} + \beta_{m'})m' + \alpha_{m'} \tag{6.11}$$

$$\frac{dh'}{dt} = -(\alpha_{h'} + \beta_{h'})h' + \alpha_{h'} \tag{6.12}$$

$$\frac{dn'}{dt} = -(\alpha_{n'} + \beta_{n'})n' + \alpha_{n'} \tag{6.13}$$

$$\alpha_{m'} = 0.1(V + 40)/[1 - e^{-(V+40)/10}] \tag{6.14}$$

$$\alpha_{h'} = 0.07e^{-(V+65)/20} \tag{6.15}$$

$$\alpha_{n'} = 0.01(V+55)/[1-e^{-(V+55)/10}] \tag{6.16}$$

$$\beta_{m'} = 4e^{-(V+65)/18} \tag{6.17}$$

$$\beta_{h'} = 1/[1+e^{-(V+35)/10}] \tag{6.18}$$

$$\beta_{n'} = 0.125e^{-(V+65)/80} \tag{6.19}$$

This approach provides a local solution for reconstructing the neural stimulus of a HH neuron by approximating the gating variables. In addition to retrieval of stimulus parameters, it also estimates the neural dynamics, which are important, which help identify the open-close mechanism of ionic gates. The estimation of neural dynamics from a neural response is key to understanding the effect of brain biochemistry on neural disorders.

6.4 Computational Results

The above algorithm to reconstruct an unknown stimulus is applied to the HH neuron. In the process of extracting the maximal conductance of the ionic channels, the algorithm also retrieves approximations of the gating variables m', n' and h' which represent the neural dynamics. This approach is scalable to accommodate any number of ion channels, therefore it can also be used for higher-level neurons e.g. Cortical neurons (Wilson 1999a,b; Wilson and Cowan, 1973; Wilson and Cowan, 1972).

6.4.1 Generating a Voltage Trace

Let I_S be a small supra-threshold step current that evokes an action potential. The resultant voltage trace v_S is sufficient to retrieve the maximal conductance values.

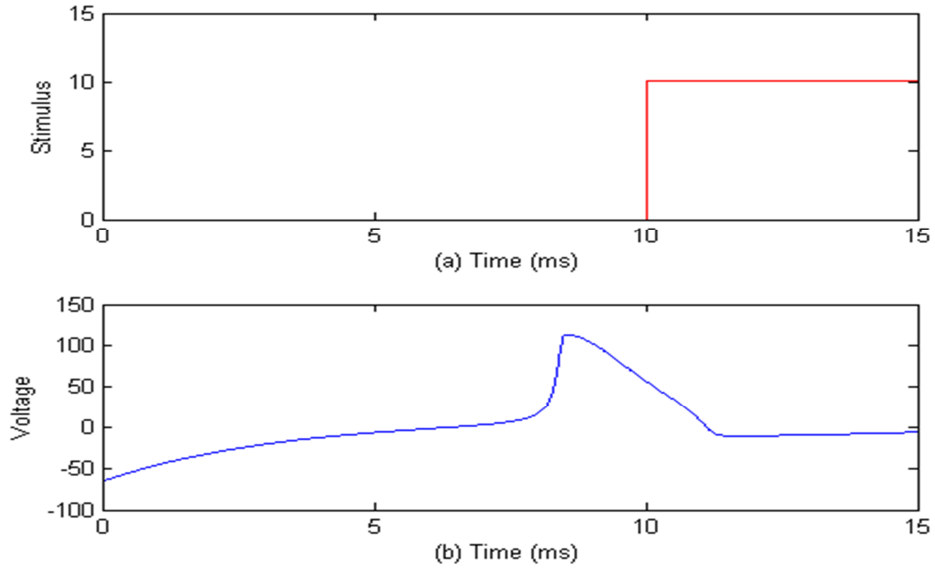

Figure 6.1: The voltage trace v_s generated by a small step-current I_s. This small trace of neural voltage is sufficient to retrieve the maximal conductances.

6.4.2 Retrieving Maximal Conductances

Given the voltage trace v_s and the corresponding external stimulus I_s, near approximation of the maximal conductance values can be obtained using equations (6.2-6.9). Let δ be the time-step of the Euler integration. It is observed that the accuracy of the approximated conductances is dependent on δ. The accuracy increases if the time-step of integration (δ) is close to 0. These approximated conductances are consistent with the observations of Shepardson (Shepardson, 2009). As (6.8) is an overdetermined system of linear equations, an exact solution cannot be obtained for all values of δ.

Original↓/Retrieved→	$\delta = 0.01$	$\delta = 0.001$	$\delta = 0.0001$
$g_{Na} = 120$	$g'_{Na} = 120.49$	$g'_{Na} = 120.05$	$g'_{Na} = 120$
$g_K = 36$	$g'_K = 36$	$g'_K = 36$	$g'_K = 36$
$g_L = 0.30$	$g'_L = 0.33$	$g'_L = 0.30$	$g'_L = 0.30$

Table 6.1: Retrieved maximal conductance values for various values of δ. The conductances are highly accurate as δ becomes close to 0.

The relative error of the approximations decreases as δ becomes close to 0.

δ	Relative error (ε)
0.01	0.0037
0.001	0.00038
0.0001	0

Table 6.2: The relative error ε decreases as δ becomes close to 0.

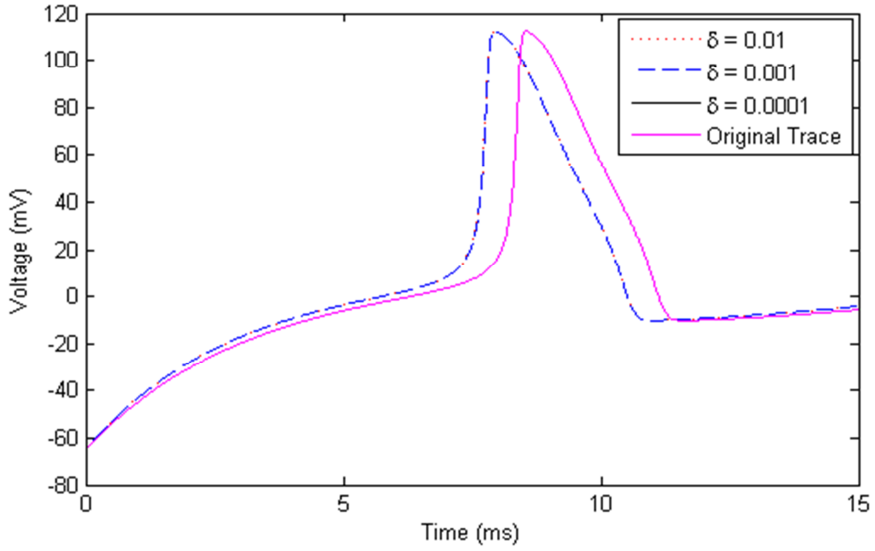

Fig. 6.2(a)

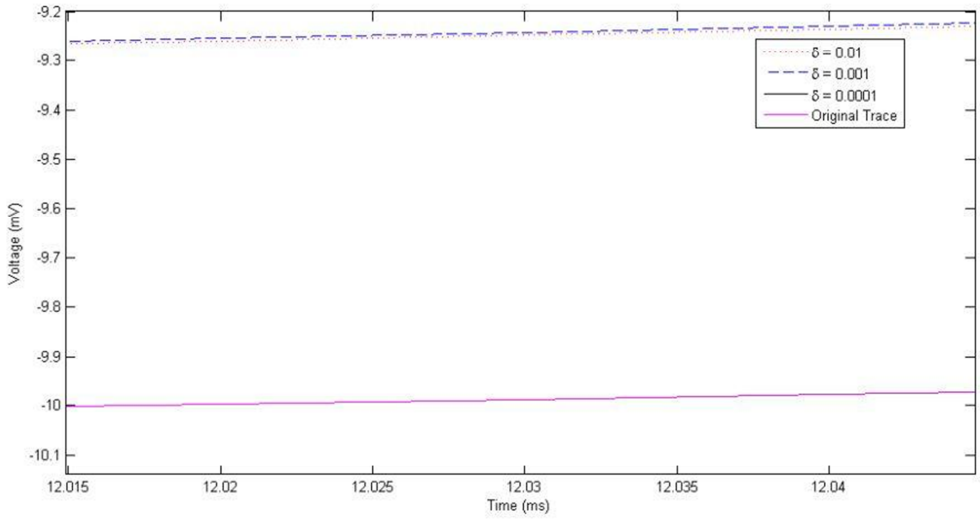

Fig. 6.2(b)

Figure 6.2: (a) The reconstructed voltage traces using the approximated maximal conductance values for different time-steps δ. (b) As δ becomes close to 0, the approximations approach the actual conductance values. For $\delta = 0.0001$, the approximated conductance values are equal to the original values. Hence the trace generated by $\delta = 0.0001$ overlaps with the original trace v_s which can be considered as $\delta = 0$. Due to the near exact overlap, the trace generated by $\delta = 0.0001$ and the original trace are indiscernible.

In order to assess the accuracy of the estimated maximal conductance values, the voltage trace is reconstructed using the approximated conductances from table 6.1. It is observed that the estimated maximal conductance values produce a good fit to the original trace v_s (fig. 6.2). A smaller time-step of integration (δ) gives accurate estimates of ionic conductances (table 6.2) which can replicate the actual neural voltage trace. The degree of overlap between the actual and predicted voltage traces (fig. 6.2) confirms that the accuracy of prediction is dependent on the choice of δ.

6.4.3 Stimulus Reconstruction

The retrieval of maximal conductance values and a good fit of the original voltage trace indicate that the approximations are nearly accurate. Using equations (6.10-6.19), stimulus reconstruction can be carried out by linearising the equations of the HH neuron.

6.4.3.1 Constant-Current Stimulus

Let us assume that the HH neuron is stimulated by an unknown step-current I_{step} such that it evokes a series of action potentials V_{step}. The aim is to recreate an approximation of the stimulus, I_{step}, to trace the trigger for the neural activity. In order to reconstruct I_{step}, the ionic conductance values need to be retrieved. The maximal conductances are approximated using the approach described in section 6.3.2 and the retrieved values for different integration time-step (δ) are shown in table 6.1. The stimulus is reconstructed using these retrieved conductance values for different values of δ (fig. 6.3 and fig.6.4). As the accuracy of retrieving conductance values depends on δ, the precision in the ability of reconstructing an unknown stimulus also depends on δ. This also indicates that a tiny change in ionic conductance effects a change in the neural dynamics, which is reflected in the response of the HH neuron.

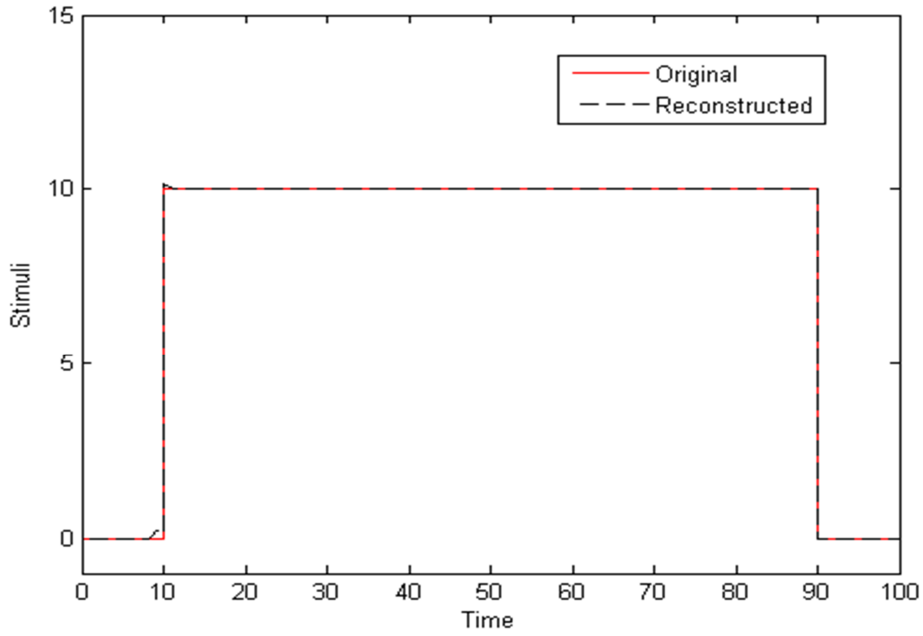

Figure 6.3: The reconstructed stimulus is good fit to the original stimulus. The original stimulus is very well approximated if chosen δ is close to 0, $\delta \sim 0.0001$.

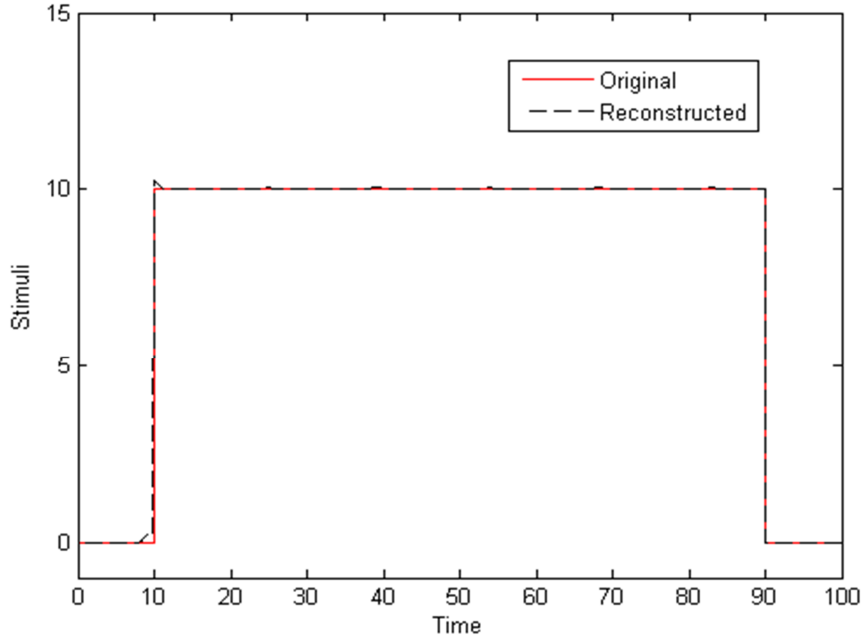

Figure 6.4: The approximated stimulus is less accurate if δ is higher, $\delta \sim 0.01$.

Results show that if the time-step of Euler integration is sufficiently small i.e. $\delta \sim 0.0001$, the maximal conductances can be accurately retrieved. The stimulus reconstructed using these maximal conductance values, is a near approximation of the original unknown stimulus, I_{step}.

6.4.3.2 Periodic Stimulus

If the HH neuron is stimulated by an unknown periodic stimulus $I_{periodic}$, the resultant neural response is $V_{periodic}$ and the temporal variations in $V_{periodic}$ are influenced by the nature of $I_{periodic}$. These temporal variations could result a change in the conductance values of the ion channels, difference in the potential (ion concentrations) across the membrane or a physical change in a neuron (Tuckwell, 1988). In either case, the approach detailed in section 6.3.2 is applicable even in the presence of periodic stimuli. Using the algorithm (6.3.2) the maximal conductance values are retrieved for different integration time-steps, δ (table 6.1) by generating a voltage trace (6.3.1). The unknown periodic stimulus can therefore be reconstructed using these retrieved maximal conductance values (6.10-6.19).

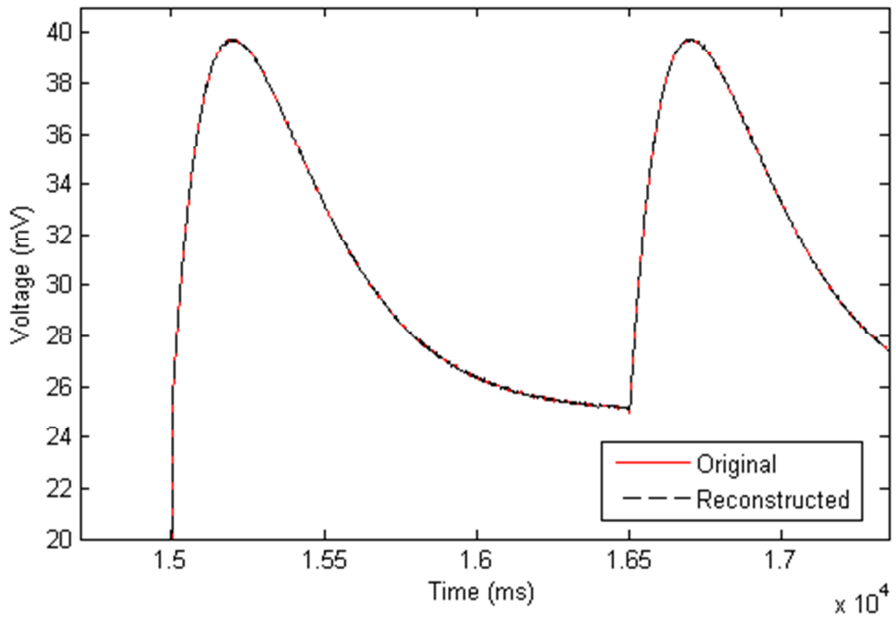

Figure 6.5: The reconstructed periodic stimulus for δ close to 0. For $\delta = 0.0001$, the reconstructed stimulus is a near-fit of the original stimulus.

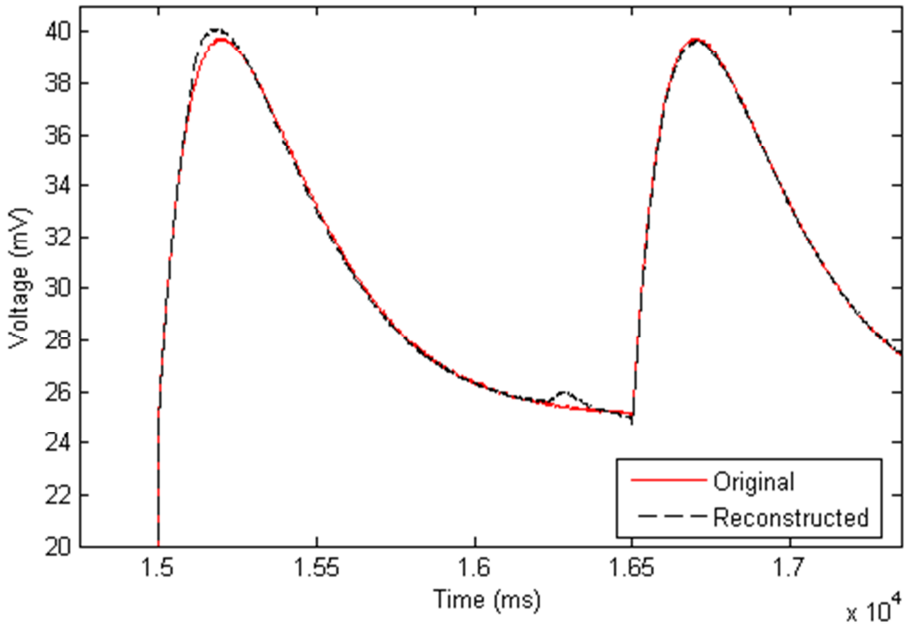

Figure 6.6: The approximation of the reconstructed stimulus becomes less accurate with an increase in δ ($\delta \sim 0.001$). The numerical approximation of the derivatives causes some jitters.

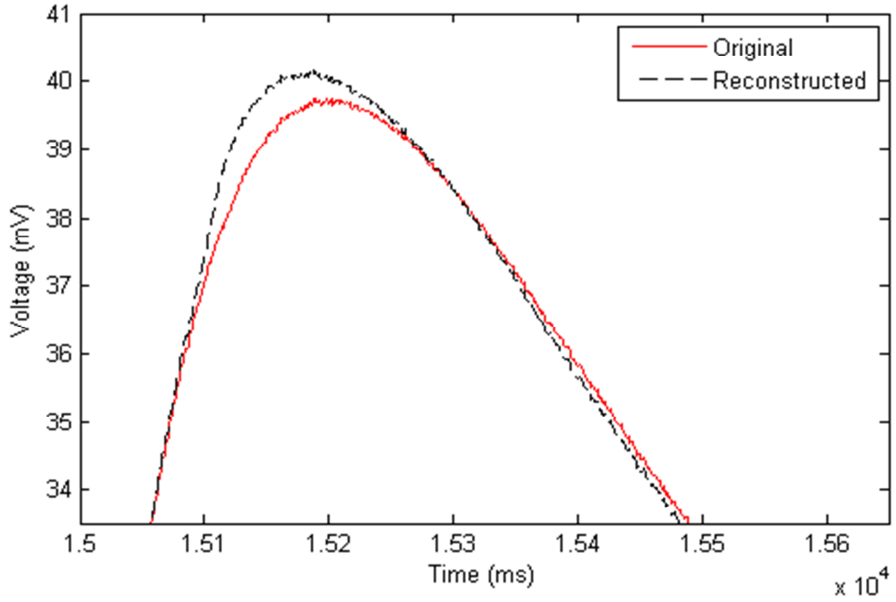

Figure 6.7: Due to the presence of noise in original stimulus, the reconstructed noise cannot be an exact match. The jitters are due to the numerical approximation of the rate of change of voltage. However, the reconstruction is very close to the original stimulus for δ close to 0.

It is observed that the unknown periodic stimulus can be predicted accurately if δ is small and close to 0 (fig. 6.5). The accuracy of the reconstructed stimulus is dependent on the δ hence at times the reconstruction can be time-consuming. However, this approach provides a local solution to reconstructing unknown stimuli using the knowledge about the computational model of a neuron. If the time-step of integration δ is large ($\delta \sim 0.01 -$

0.001), the approximation of the neural stimulus is less accurate (fig. 6.6 and fig. 6.7). It is observed that the prediction of the neural stimulus becomes less accurate due to the numerical approximations during the linearization of the HH equations.

6.4.4 Retrieval of Neural Dynamics

The study of neural dynamics is significant as they carry a lot of information about neural biochemistry and retrieval of neural dynamics can be of great help in assessing a neural disorder. One significant advantage in using this numerical approach to reconstructing neural stimulus is the ability to reconstruct the internal state of the neuron during the activity, which cannot be retrieved by a purely analytical approach (fig. 6.8).

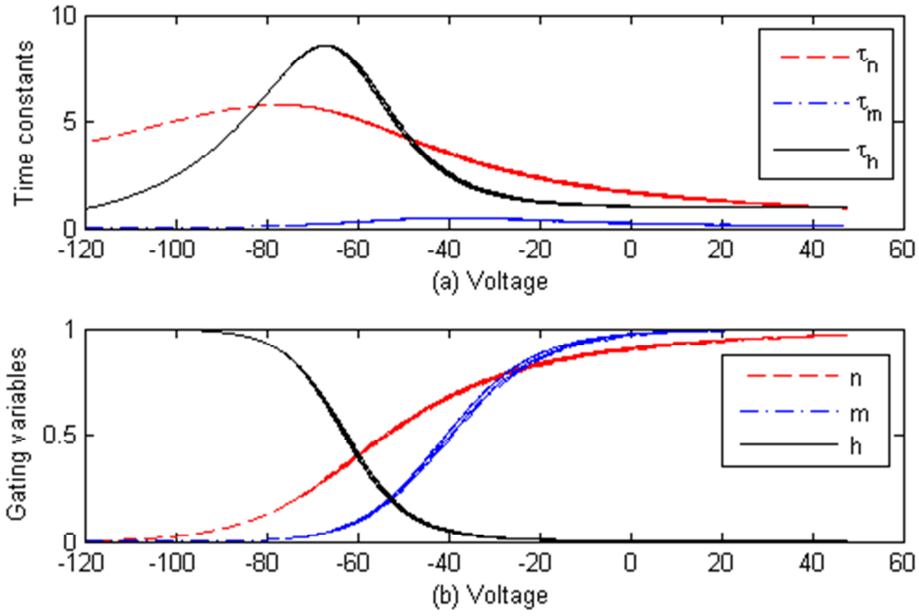

Figure 6.8: The reconstructed neural dynamics. This numerical solution can retrieve the gating variables m, n and h and their time constants τ_m, τ_n and τ_h.

The neural dynamics represent the open-close mechanism of the ion channels in a neuron. The HH neuron has three ion channels $Na^+, K^+$and Cl^-. The probability that a channel is open is defined by the variables m, n and h. The combined action of m and h controls Na^+ while the K^+ gates are controlled by n. The time constants of the three gating variables are defined by τ_m, τ_n and τ_h. Fig. 6.8 shows the reconstructed neural dynamics for the HH neuron stimulated by a periodic stimulus (section 6.3.3.2). It represents a timeline of the internal state of the neuron during a neural activity. For a neuron, which has undergone a

physical change due to attrition or deformation (e.g. Motor Neuron Disease) due to physical changes of pressure, the ionic conductance changes (Gonzalez de Aguilar et. al., 2007; Fischer and Glass, 2007; Tuckwell, 2003). The recreated neural dynamics of such neurons will exhibit a different open-close mechanism of the ion channels. More specifically, the time-constants of the gating variables will differ compared to a normally functioning fit neuron. Future work aims to quantify this difference by using a diseased neuron and studying the change in its ionic conductance over time.

6.4.4.1 Effect of Conductance Variation on Neural Dynamics

The effect of conductance variation is evident in the influx of ions passing through the ion channels and a change in conductance effectively affects the Nernst potential that governs the equilibrium of the neural membrane. The open-close mechanism of the ion channels adopted by such a neuron will differ compared to a similar-type neuron with different ionic conductance values. It can be said that the neural dynamics of a neuron are conductance-specific.

It is observed that a small variation in the ionic conductance can significantly change the neural dynamics. To exemplify this effect, consider the retrieved conductances for $\delta = 0.01$ in Table 6.1. The actual conductance values in mS/cm^2 are $g_{Na} = 120$, $g_K = 36$ and $g_L = 0.30$ while the retrieved values are $g'_{Na} = 120.49$, $g'_K = 36$ and $g'_L = 0.33$. This tiny variation from the actual values affects the gating variables m', n' and h' , which trace different timeline plots compared to the original gating variables m, n and h.

Let the subscript *D* represent a 'defect' in the neuron that caused the change in the conductance. If the retrieved dynamics described above are from a defective neuron, the change in the neural excitability is distinct (fig. 6.9). As the Na^+ conductance in the *defective* neuron is higher than the actual original conductance value, it is observed that the *m-gate* closes quicker than normal. This is indicated by the small time constant of m_D.

The variable m is responsible for the depolarization of the neuron. The change in the conductance indicates that the neuron depolarizes quicker than *normal* and therefore due to refractoriness, hyperpolarization occurs when $n - gate$ opens. However, as the conductance of the leakage is higher, the neuron has a faster hyperpolarization that the *normal* neuron. The cycle repeats for the entire time duration of neural stimulation. Hence, the corresponding firing times of these neurons will be different, and the amplitudes will be governed by their respective time constants τ_n and τ_{nD}, which determine the point of hyperpolarization of the action potential. It is evident that this tiny variation has a significant effect on the neural cycle (fig. 6.9).

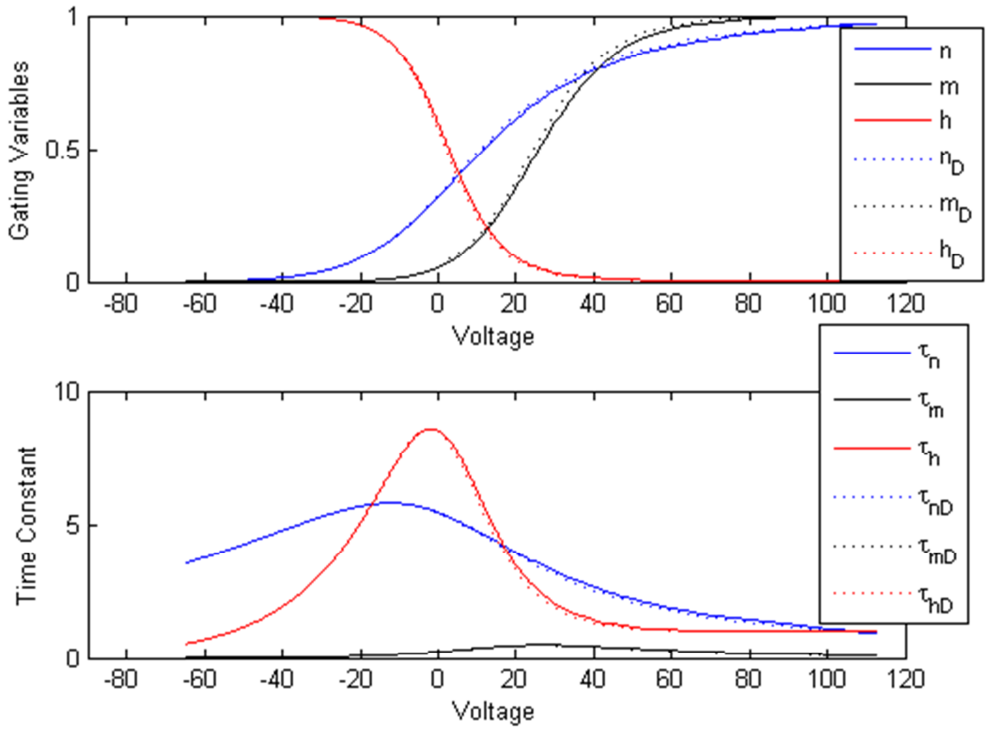

Figure 6.9: The effect of conductance variation on neural dynamics is demonstrated by a tiny change in the conductance of Na^+ and Cl^-. The subscript D represents the 'defect', which causes a change in the conductance of a neuron. The dotted lines show the effect of the variation in conductance on the gating variables and their time constants.

6.5 Chapter Summary

The neural dynamics of the HH neuron have been the subject of research for many years now. The dynamics put forth by Hodgkin and Huxley have been well studied and replicated by many researchers. In much the same way, inverting the HH neural equations

has attracted interest in recent years. The equations of the HH neuron are highly non-linear due to the incorporation of probability of the gating variables $m, n\ and\ h$, which regulate the open-close mechanism of ionic channels.

Previous research has addressed the problem of inverting this non-linear neuron by using digital filters, neural networks, algorithms and complexity, and digital signal processing. Other approaches point to the use of reconstruction algorithms, time encoding/decoding machines or an IF neuron. These approaches establish a relationship between the neural response and the stimulus but they are not designed to capture or retrieve the neural dynamics. The neural dynamics represent the timeline changes in the gating variables of the ion channels over the period of neural stimulation. It is therefore important to be able to retrieve dynamics from the response of a neuron, which can help to understand the changes in the internal state of a diseased neuron.

The approach described in this chapter provides a numerical solution to reconstruct an unknown neural stimulus. An unknown stimulus is shown to be reconstructed by

1) Recording any neural response $V(t)$ whose stimulus, say $I(t)$, requires to be reconstructed

2) Injecting a supra-threshold stimulus, $I_s(t_s)$ for a small time duration t_s

3) Recording the corresponding voltage trace generated, $v_s(t_s)$

4) Retrieving the maximal conductances using equations (6.2-6.9) and $I_s(t_s)$ as the external stimulus

5) Using the approximated maximal conductances, g'_{Na}, g'_{K} and g'_{L}, solve the HH equations using the recorded neural response $V(t)$ and the stimulus as the only unknown to get the reconstructed stimulus $I'(t)$

It is observed that the accuracy of maximal conductances retrieved by solving an overdetermined system of linear equations depends on the time-step (δ) of Euler integration. A small value of $\delta \sim 0.0001$ can reproduce almost exact maximal conductances. The accurate conductance values help reconstruct a near-fit approximation of the original stimulus. Due to the nature of numerical approximation and the inherent non-linearity in the neural dynamics, the reconstructed stimulus shows some jitters. In addition, it is noticed that if the original stimulus carries any noise, an exact match of the stimulus cannot be reconstructed. However, the reconstructed stimulus still matches the original stimulus to a high degree of accuracy. The choice of δ is very important and there is a trade-off between computational time and accuracy. The accuracy increases with a decrease in δ (Sarangdhar and Kambhampati, 2010c, d, e). Since the physiological neural responses recorded in labs are continuous signals, sampling or discretising these signals to a sufficiently small $\delta \sim 0.0001$ is realisable.

The approached described here can reconstruct very good approximations of the original stimuli. The results show that the unknown periodic and constant current stimuli are well approximated by this reconstruction method. It is also worth mentioning that although establishing an IO relationship can provide some information of the stimulus parameters, the current approach can accurately reconstruct the neural dynamics in addition to an unknown stimulus. This ability of neural dynamics retrieval is significant to study the timeline changes in the conductance of ion channels of a diseased neuron. Future work is focused on studying these variations in the conductances in higher order models of mammalian neurons.

7 Conclusions

This thesis contributes towards the development of a framework for the understanding and prediction of early onset of neural disorders based on a computational study of the neural biophysics. The responses obtained by stimulating a neuron depend on the biochemistry while prediction of an onset requires the comparison of neural responses in order to understand changes in the underlying biochemistry. Understanding the onset of a neural disorder requires the study of neural biophysics, voltage-dependent activation-deactivation of ion channels and their effect on neural responses. More specifically, the study requires understanding

1) the deviation of neural spiking from normalcy that results from changes in ionic concentrations effected by disorders, which can be done using neural response comparison

2) the exact changes in the biochemistry governed by the ion concentrations and conductance of ion channels.

Studying *a particular neural disorder and its biophysics* is a future objective. Thus, the framework developed in this thesis helps the understanding of such an onset by

- developing a similarity measure for neural response comparison
- developing an algorithm for reconstructing the unknown neural stimulus
- and retrieving the neural dynamics that show voltage-gated changes of ion channels

The deviation of neural spiking patterns from normalcy results either from a change in the underlying neurobiochemistry or the stimulus, both of which can be traced using the approaches described in this thesis.

7.1 Research Contributions

The *effect of the temporal nature of a stimulus on a neural response highlights the requirement of a new similarity measure* as physiological observations show the existence of more types of stimuli such as periodic, excitatory and inhibitory besides constant-current stimuli. The neural responses evoked by these types of stimulations are distinct in comparison with steady state neural responses generated by constant-current stimuli. Neural response comparison carried out using similarity estimation approach used for steady state responses yields false positives due to implicit assumptions about the neural dynamics. For instance, excitatory and inhibitory stimuli have distinct functional roles in the nervous system and differ in the nature of electrical excitability (Brazier, 1977; Chapter 3, section 3.2.2). These stimuli also have different shape and form; hence, they cannot generate identical responses. Therefore, a false positive for an inhibitory-excitatory neural response pair, which indicates that the two responses are identical and generated by similar stimuli, is not physiologically relevant. As the ion channel activation-deactivation of the neural membrane depends on the potential difference created by the external stimulation, the nature of the stimulus imparts a distinct firing pattern to a neuron (see Chapter 2 and Chapter 3). The existence of false positives may affect the detection of onset by missing the deviation from normalcy.

The *formulation of the new similarity measure* Γ_{chaotic} is based on the temporal nature of the neural response rather than just firing times of spikes. The consideration of amplitude variation in addition to firing time information ensures that false positives are eliminated and neural responses with temporal deviations beyond physiological precision are classified as distinct (see Chapter 4). The *similarity estimated by* Γ_{chaotic} *correlates with the total number of coincidences in corresponding neural responses*; hence, Γ_{chaotic} is

mathematically realisable. This further establishes that classification of neural responses with temporal variations requires consideration of amplitude coincidences in addition to firing times coincidences.

Establishing similarity between neural responses using $\Gamma_{chaotic}$, as discussed in Chapters 3-5, identifies whether the neuron had identical or non-identical stimulation. In a physiological setting, this stimulus is largely unknown apart from the knowledge that it is supra-threshold. The voltage-gated ion channels responsible for the neural excitability exhibit timeline changes and present a valuable source of information about the neural spiking and biochemistry that results in an action potential. In particular, the ability to retrieve and understand these changes from the neural response will be beneficial towards understanding neural disorders. *An algorithm to reconstruct unknown stimuli and retrieval of the neural dynamics* of a Hodgkin-Huxley (HH, see Chapter 2) neuron is described in Chapter 6. The HH neuron has sodium, potassium and chloride ion channels that regulate the action potential and represents the spiking mechanism of most neurons in the nervous system. The models of cortical neurons (such as the Wilson model) are based on the physiology of HH neuron and have two additional ion currents compared to the HH neuron (see Chapter 2), which makes this approach scalable to neurons of higher complexity. The results show that the accuracy of the reconstructed stimulus and retrieved neural dynamics depends on the time step of integration δ. It is observed that the accuracy of prediction increases if δ is small. The neural responses obtained physiologically are continuous signals and sampling the signal with a small δ makes this algorithm scalable to physiological observations.

Thus, by observing the similarity estimate given by $\Gamma_{chaotic}$ one can determine the degree of deviation of a neural response from normalcy. In addition, by using the approach defined in Chapter 6, it is possible to reconstruct a near approximation of the stimulus, the changes in ion conductances and the exact timeline variations in the voltage-dependent ion channels.

7.2 Discussion and Future Work

7.2.1 Studying Neural Disorder using a Computational Neural Model

The transition of a neuron from a healthy to a diseased or unhealthy state follows the trajectory of gradual decay. This course of transition in commonly observed for individual neurons in most disorders like Motor Neuron Diseases (MND), Parkinson's Disease (PD) and Alzhiemer's Disease (AD). At disease onset, the biochemistry of a neuron starts to drift from normalcy and it is reflected by a change in neural spiking and its function, which can be observed in the neural dynamics (Strange, 1992). Estimating the extent of this drift from normalcy is possible by studying the responses using the similarity measure, $\Gamma_{chaotic}$, developed in Chapter 4. This approach helps to estimate the gradual decay by comparing neural responses observed at successive stages of degeneration. Studying such neural responses and recreating the neural biophysics can contribute towards understanding and predicting onset of neural disorders. Using the approach to reconstruct stimuli, which is discussed in Chapter 6, it is possible to reconstruct the stimulation while retrieving the neural dynamics. This retrieval of neural dynamics recreates the timeline changes in the gating variables of the ion channels over the period of neural stimulation. This provides the researcher to study the internal function of a neuron over the course of degeneration, which could help understanding disease-onset clinically and possibly provide new ideas in medicine. It is also worthwhile to mention that studying the recreated neural dynamics can also reveal the effect of stimulation on certain ion channels. Also, in a network of neurons, this approach can be applied to locate a failing pathway by adopting an iterative application of the above process. It is expected that this computational ability to identify the early onset can help to prolong the life of a neuron by determining biochemical changes that initiate degeneration and timely clinical intervention.

7.2.2 Rate of Fire and Information Content

Studies of neural spiking activity have focused on firing times of neural spikes because it is thought that the information in a neural response could be encoded in either the firing

times or the firing rate (Rinzel, 1985; Gabbiani *et. al.*, 1999; Panzeri *et. al.*, 1999; Bialek *et. al.*, 1991). The results in Chapter 3, section 3.5 show that a change in the ISI of periodic stimulation does not change the rate of fire of the neuron. Based on the current study, it might be argued that these neural responses have the same information content; however, this thought on information content and rate of fire has not been quantified so far. This thesis demonstrates that similarity between neural responses can be determined using firing time and amplitude coincidences while the rate of fire is used to calculate the coincidence by chance (see Chapter 4, section 4.3.2). In addition, it must be noted that irrespective of the rate of fire, model validation is carried out using coincidence factor (Kistler and Gernster, 2002; Kistler *et. al.*, 1997; Jolivet *et. al.*, 2004). This opens the possibility for future work on establishing the nature of information encoded in the neural responses generated by periodic stimuli. The information content can reveal the similarity between the neural responses and more specifically, answer if biological precisions of 2ms and 2mV conform to that of information content.

7.2.3 Stimulus Reconstruction of Mammalian Neocortical Neurons

The computational model of a mammalian neocortical neuron is an extension of the biophysics of the HH neuron (see Chapter 2, section 2.6.1) with an addition of calcium and calcium mediated potassium currents. The stimulus reconstruction and neural dynamics retrieval algorithm described in Chapter 6 can be extended to this neuronal model by scaling equation 6.1. Studying the timeline changes in the cortical neurons may help to understand neural disorders and the effect of drug concentrations on cortical spiking. Future work aims to scale up this research by implementing a population of cortical neurons coupled together via synapses to replicate a biological pathway.

7.3 Concluding Remarks

It is conceivable that the neuron, which is a constitutional and fundamental unit of the nervous system, represents a neural disorder to some extent. Classically, a network of neurons is collectively responsible for a neural activity however; an individual neuron

presents equal importance towards the proper functioning of the network. This thesis addresses some limitations with existing approaches and proposes a new and improved approach for identifying similarity between neural responses. In a broader context, this thesis aims to help predict the onset of a neural disorder by way of stimulus reconstruction and neural dynamics retrieval. This retrieved information can be of immense importance towards the understanding of neural disorders.

This thesis considers some of the existing debates in computational neuroscience such as rate of fire of a neuron and information content of a neural response while raising the possibility of future work on understanding the nature of information encoded in neural responses leading to neural communication. The research presented in this thesis contributes in part towards the field of computational neuroscience by implementing scalable approaches to address existing limitations with respect to neural response comparison, stimulus reconstruction and neural dynamics retrieval. It is expected that during the course of the future work, the approaches described in this thesis will be applied to neural models of higher complexity and necessary modifications based on scalability to be implemented as required.

Bibliography

Abbott LF, Kepler TB (1990). Model Neurons: From Hodgkin Huxley to Hopfield. *Statistical Mechanics of Neural Networks*, Edited by Garrido L, 5-18.

Agüera y Arcas B, Fairhall AL (2003). What causes a Neuron to Spike? *Neural Computation* 15, 1789-1807.

Agüera y Arcas B, Fairhall AL, Bialek W (2003). Computation in a Single Neuron: Hodgkin and Huxley Revisited. *Neural Computation* 15, 1715-1749.

Aihara K, Matsumoto G, Ikegaya Y (1984). Periodic and Non-periodic Responses of a Periodically Forced Hodgkin-Huxley Oscillator. *Journal of Theoretical Biology*, 109, 249-269.

Arbib MA (1995). *The Handbook of Brain Theory and Neural Networks*. Cambridge, Massachusetts, MIT Press.

Bialek W, Rieke F, de Ruyter van Steveninck RR, Waland D (1991). Reading a Neural Code. *Science* 252, 1854-1857.

Bokil HS, Pesaran B, Andersen RA, Mitra PP (2006). A Method for Detection and Classification of Events in Neural Activity. *IEEE Transactions on Biomedical Engineering*, Vol. 53, No. 8, 1678-1687.

Brazier MAB (1977). *Electrical Activity of the Nervous System*. 4th ed. The Williams and Wilkins Company, Baltimore.

Brazier MAB ed. (1979). *Brain Mechanisms in Memory and Learning: From Single Neuron to Man*. Raven Press, New York.

Brooks VB. (1986). *The Neural Basis of Motor Control*. Oxford University Press, New York.

Chechik G, Anderson MJ, Bar-Yosef O, Young ED, Tishby N, Nelken I (2006). Reduction of Information Redundancy in the Ascending Auditory Pathway. *Neuron* 51, 359-368.

Cisi RRL, Kohn AF (2008). From Neuronal Ionic Channels to Muscle Control: A Web-based Simulator and its Application to Teaching. In *World Congress on Engineering 2008 : The 2008 International Conference of Systems Biology and Bioengineering*, London, U.K. 2-4 July 2008, **Vol. 2**, pp 1662-1665.

Cozzi L, D'Angelo P, Sanguineti V (2006). Encoding of time-varying stimuli in populations of cultured neurons. *Biological Cybernetics*, 94: 335-349.

Craver CF (2007). *Explaining the Brain: Mechanisms and the Mosaic unity of Neuroscience*. Clarendon Press, Oxford.

Das A, Folland R, Stocks NG, Hines EL (2006). Stimulus reconstruction from neural spike trains: Are conventional filters suitable for both periodic and aperiodic stimuli? *Signal Processing*, 86 (7), 1720-1727.

Davies RM, Gerstein GL, Baker SN (2006). Measurement of Time-Dependent Changes in the Irregularity of Neural Spiking. *Journal of Neurophysiology*, 96:906-918.

De Wilde P (1997). *Neural Network Models*. 2nd ed.. Springer Verlag, London.

Diba K, Koch C, Segev I (2006). Spike Propagation in dendrites with stochastic ion channels. *Journal of Computational Neuroscience*, 20: 77-84.

Dimitrov AG, Gedeon T (2006). Effects of stimulus transformations on estimates of sensory neuron selectivity. *Journal of Computational Neuroscience*, 20: 265-283.

Eccles JC (1964). *The Physiology of Synapses*. 1st ed. Springer.

EruptingMind (2010). Neurons in the Brain. http://www.eruptingmind.com/types-of-neurons/ Accessed 21st November 2010.

Eulo J (2008). How the brain governs behaviour. My College Class Notes. http://mycollegenotes.wordpress.com/2008/05/ Accessed November 2010.

Fischer LR, Glass JD (2007). Axonal Degeneration in Motor Neuron Disease. *Neurodegenerative Diseases*, 4: 431-442.

FitzHugh R (1961). Impulses and physiological states in models of nerve membrane. *Biophys. J*, 1, 445-466.

Foran E, Trotti D. (2009). Glutamate Transporters and the Excitotoxic Path to Motor Neuron Degeneration in Amyotrophic Lateral Sclerosis. *Antioxidants and redox signalling*, 11(7): 1587-602.

Fourcaud-Trocmé N, Hansel D, van Vreeswijk C, Brunel N (2003). How Spike Generation Mechanisms Determine the Neuronal Response to Fluctuating Inputs. *The Journal of Neuroscience*, 23(37): 11628-11640.

Gabbiani F, Metzner W (1999). Encoding and Processing of Sensory Information in Neuronal Spike Trains. *The Journal of Biology*, 202, 1267-1279.

Gernster W, Kistler W (2002). *Spiking Neuron Models: Single Neurons, Populations , Plasticity*, Cambridge University Press.

Goldman DE (1943). Potential, Impedance and Rectification in Membranes. *The Journal of General Physiology*, 37-60.

Gonzalez de Aguilar JL, Echaniz-Laguna A, Fergani A, René F, Meininger V, Loeffler JP, Dupuis L (2007) . Amyotrophic Lateral Sclerosis: All Roads Lead to Rome. *Journal of Neurochemistry*, 101, 1153-1160.

Guttman R, Feldman L, Jakobsson E (1980). Frequency Entrainment of Squid Axon Membrane. *Journal of Membrane Biology*, 56, 9-18.

Guckenheimer J, Labouriau IS (1993). Bifurcation of the Hodgkin and Huxley Equations: A New Twist. *Bulletin of Mathematical Biology*, Vol. 55, No. 5, pp. 937-952.

Hasegawa H (2000). Responses of a Hodgkin-Huxley neuron to various types of spike-train inputs. *Physical Review E*, Vol. 61, No. 1.

Hasegawa H (2008). Information conveyed by neuron populations – Firing rate, fluctuations and synchrony. *Neuroquantology*, Vol. 6 (2), 105-118.

Hayashi H, Ishizuka S, Hirakawa K (1985). Chaotic responses of the pacemaker neuron. *J. Phys. Soc. Jpn*., 54, 2337.

Hebb DO (1949). *The Organization of Behaviour: a neuropsychological theory*. New York. Wiley.

Herbst JA, Gammeter S, Ferrero D, Hahnloser RHR. (2008). Spike sorting with Hidden Markov Models. *Journal of Neuroscience Methods*. 174, 126-134.

Hille B (1992). *Ionic Channels of Excitable Membranes*. 2nd ed. Massachusetts: Sinauer Associates, Inc.

Hindmarsh JL, Rose RM (1984). A model of neuronal bursting using three coupled first order differential equations. *Proceedings of the Royal Society of London B*, 221, 87-102.

Hodgkin AL, Huxley AF (1952). A quantitative description of membrane current and its application to conduction and excitation in nerve. *J. Physiol*. 117:500–544.

Hodgkin AL, Katz B (1949). The effect of sodium ions on the electrical activity of the giant axon of the squid. *J. Physiol. (London)* 108:37-77.

Hodgkin AL (1976). Chance and design in Electrophysiology: An informal account of certain experiments on nerve carried out between 1934 and 1952. *J. Physiol. (London)* 236:1-21.

Holden AV (1987). *Chaos.* Manchester: Manchester University Press.

Hollet H (2008). *The Nervous System*. http://heatherhollettbiol3500.blogspot.com/ Accessed October 2010.

Hubert JP, Delumeau JC, Glowinski J, Prémont J, Doble A. (1994). Antagonism by riluzole of entry of calcium evoked by NMDA and veratridine in rate cultured granule cells: evidence for a dual mechanism of action. *Br. J. Pharmacol*. 113 (1): 261–267.

Izhikevich EM (2003). Simple Model of Spiking Neurons. *IEEE Transactions on Neural Networks* Vol. 14 (6), 1569-1572.

Izhikevich EM (2006). Polychronization: Computation with Spikes. *Neural Computation* 18, 245-282.

Izumi Y, Kaji R. (2007). Clinical trials of ultra-high-dose methylcobalamin in ALS. *Brain Nerve*. 59 (10): 1141-1147.

Joeken S, Schwegler H (1995). Predicting spike train responses in neuron models; in M.Verleysen (ed.), *Proceedings of the 3rd European Symposium on Artificial Neural Networks* 1995, Brussels, Belgium, April 19-21, 1995, pp 93-98.

Jolivet R, Lewis TJ, Gerstner W (2004). Generalized Integrate-and-Fire Models of Neuronal Activity Approximate Spike Trains of a Detailed Model to a High Degree of Accuracy. *Journal of Neurophysiology* 92: 959-976.

Kambhampati C, Sarangdhar M, Poolsawad N (2010). Dysphonia Measures in Parkinson's Disease and their use in prediction of its progression. *International Conference on Knowledge Engineering and Ontology Development* (Article in print).

Kaplan D, Glass L (1995). *Understanding Non Linear Dynamics*. Springer, New York.

Kaske A, Maass W (2006). A model for the interaction of oscillations and pattern generation with real-time computing in generic neural microcircuit models. *Neural Networks*, Vol. 19, 600-609.

Kepecs A, Lisman J (2003). Information encoding and computation with spikes and bursts. *Network: Comput. Neural Syst.* 14, 103-118.

Kepler TB, Abbott LF, Marder E (1992). Reduction of conductance-based neuron models. *Biological Cybernetics*, 66, 381-387.

Kingsley RE (2000). *Concise Text of Neuroscience*, 2nd Ed. Lippincott Williams & Wilkins, USA.

Kistler WM, Gerstner W, Leo van Hemmen J (1997). Reduction of the Hodgkin-Huxley Equations to a Single-Variable Threshold Model. *Neural Computation* 9: 1015-1045.

Klein DJ, Simon JZ, Depireux DA, Shamma SA (2006). Stimulus-invariant processing and spectrotemporal reverse correlation in primary auditory cortex. *Journal of Computational Neuroscience*, 20: 111-116.

Koch C ed., Segev I ed. (1989). *Methods in Neuronal Modelling: From Synapses to Networks*. MIT Press, Massachusetts.

Kohn AF (2005). Cross-correlation between EMG and center of gravity during quiet stance: theory and simulations. *Biological Cybernetics*, 93, 382-388.

Kohn AF, Vieira MF (2002). Optimality in the encoding/decoding relations of motoneurones and muscle units. *Biosystems*, 67: 113-119.

Kumar A, Gupta K, Vyas P, Boolchandani D, Sonania R, Dube A (2009). Chaotic Neural Dynamics as Evinced from Scalp Electroencephalography (EEG). *Nature Precedings*. http://hdl.handle.net/10101/npre.2009.2784.1.

Lazar AA, Pnevmatikakis EA (2009). Reconstruction of Sensory Stimuli Encoded with Integrate-and-Fire Neurons with Random Thresholds. *EURASIP Journal on advances in Signal Processing*. Article no. 682930.

Lazar AA (2007a). Information representation with an ensemble of Hodgkin-Huxley neurons. *Neurocomputing*, Vol. 70 (10-12), 1764-1771.

Lazar AA (2007b). Recovery of Stimuli Encoded with Hodgkin-Huxley Neurons, *Computational and Systems Neuroscience Meeting, COSYNE 2007, Salt Lake City, UT, February 22-25*.

Lazar, AA (2006). Time encoding machines with multiplicative coupling, feedforward, and feedback. *IEEE Transactions on Circuits and Systems II – Express Briefs*. Vol. 53 (8), 672-676.

Lazar AA, Simonyi EK, Toth LT(2006). A Real-Time Algorithm for Time Decoding Machines. *14th European Signal Processing Conference*, September, 2006.

Lazar AA (2004). Time encoding with an integrate-and-fire neuron with a refractory period. *Neurocomputing*, Vol.58, 53-58.

Levitan IB, Kaczmarek LK (1997). *The Neuron: Cell and Molecular Biology*. 2nd ed. Oxford University Press, New York.

Li X, Ascoli GA (2006). Computational simulation of the input-output relationship in hippocampal pyramidal cells. *Journal of Computational Neuroscience*, 21:191-209.

Luk WK, Aihara K (2000). Synchronization and sensitivity enhancement of the Hodgkin-Huxley neurons due to inhibitory inputs. *Biological Cybernetics*. 82, 455-467.

Lundström I (1974). Mechanical Wave Propagation on Nerve Axons. *Journal of Theoretical Biology*, 45, 487-499.

Matsumoto G, Aihara K, Ichikawa M, Tasaki A (1984). Periodic and Nonperiodic responses of membrane potentials in squid giant axons during sinusoidal current simulations. *Journal of Theoretical Neurobiology*, 3, 1-14.

Matsumoto G, Kim K, Ueda T, Shimada J (1980). Electrical and Computer Simulations upon the Nervous Activities of Squid Giant Axons at and around the State of Spontaneous Repetitive Firing of Action Potentials. *J. Phys. Soc. Jpn*., 49, 906.

McCulloch W, Pitts W (1943). A Logical Calculus of the Ideas Immanent in Nervous Activity. *Bulletin of Mathematical Biophysics*, Vol. 5, pp. 115-133.

Mezzarane RA, Kohn AF (2009). A method to estimate EMG crosstalk between two muscles based on the silent period following an H-reflex. *Medical Engineering & Physics 31* pp. 1331-1336.

Milton J, Jung P (2003). *Epilepsy as a Dynamic Disease*. Springer, New York.

Morris C, Lecar H (1981). Voltage Oscillations in the barnacle giant muscle fiber. *Biophys J.* 35(1): 193–213.

Nagumo JS, Arimoto S, Yoshizawa S (1962). An active pulse transmission line simulating a nerve axon. *Proceedings of IRE*, 50, 2061-2070.

Nelken I, Chechik G (2005). Encoding Stimulus Information by Spike Numbers and Mean Response Time in Primary Auditory Cortex. *Journal of Computational Neuroscience*, 19, 199-221.

Nicholls JG, Martin AR, Wallace BG (1992). *From Neuron to Brain: A Cellular and Molecular Approach to the function of the Nervous System*. 3rd ed. Massachusetts: Sinauer Associates, Inc.

Nogradi A, Szabo A (2008). Transplantation of embryonic neurones to replace missing spinal motoneurones. *Restorative Neurology and Neuroscience*,Vol. 26 (2-3) pp 215-223.

Offner FF. (1974). Solution of the Time-dependent Ionic Diffusion Equation. *Journal of Theoretical Biology*, 45, 81-91.

Panzeri S, Schultz SR, Treves A, Rolls ET (1999). Correlations and the encoding of information in the nervous system. *Proc. R. Soc. Lond. B* 266, 1001-1012.

Park MH, Kim S (1996). Analysis of Phase Models for two Coupled Hodgkin-Huxley Neurons. *Journal of the Korean Physical Society*, Vol. 29, No. 1, pp. 9-16.

Patestas MA, Gartner LP (2006). *A textbook of Neuroanatomy*. Blackwell Science Ltd. UK.

Peters A, Palay SL, Webster HD (1991). *The Fine Structure of the Nervous System*. 3rd ed. New York: Oxford University.

Ramón y Cajal S (1899). *Comparative study of the sensory areas of the human cortex*. Harvard University.

Rinzel J (1985). Excitation dynamics: insights from simplified membrane models. Theoretical Trends in Neuroscience Federal Proceedings, Vol. 44, No. 15, 2944-2946.

Rinzel J (1990). Discussion: Electrical excitability of cells, theory and experiment: Review of the Hodgkin-Huxley foundation and an update. *Bulletin of Mathematical Biology*, Vol. 52, 1/2, 5-23.

Sabbatini R.M.E. (2003). Neurons and Synapses: The History of its Discovery. *Brain and Mind Magazine*, 17. Accessed October 23, 2010.

Saggar M, Mericli T, Andoni S, Miikkulainen R (2007). System identification for the Hodgkin-Huxley model using artificial neural networks. *IEEE International Joint Conference on Neural Networks Orlando, FL, AUG 12-17*, 2239-2244.

Sakshat Virtual Labs. Amrita Vishwa Vidyapeetham University. *Simple Neuron Model - the HH neuron*. http://sakshat.amrita.ac.in/VirtualLab/ accessed October 2010.

Sanger TD (2002). Decoding Neural Spike trains: Calculating the probability that a spike train and an external signal are related. *Journal of Neurophysiology*, 87: 1659-1663.

Sarangdhar M, Kambhampati C (2008a). Spiking Neurons: Is coincidence-factor enough to compare responses with fluctuating membrane voltage? *In World Congress on Engineering 2008 : The 2008 International Conference of Systems Biology and Bioengineering*, London, U.K. 2-4 July 2008, **Vol. 2**, pp 1640-1645.

Sarangdhar M, Kambhampati C (2008b). Spiking Neurons and Synaptic Stimuli: Determining the Fidelity of Coincidence-Factor in Neural Response Comparison. *Engineering Letters*, Volume **16** Issue 4, pp 512-517.

Sarangdhar M, Kambhampati C (2009). Spiking Neurons and Synaptic Stimuli - Neural Response Comparison using Coincidence-Factor. *In Advances in Electrical Engineering and Computational Science*. Edited by Gelman L, Balkan N, Ao S. Published by Springer.

Sarangdhar M, Kambhampati C (2010a). Chaotic Oscillations in a Hodgkin-Huxley Neuron – Quantifying Similarity Estimation of Neural Responses *In World Congress on Engineering 2010: The 2010 International Conference of Systems Biology and Bioengineering*, London, U.K. 30 June-2 July 2010, Vol. 1, pp 589-594.

Sarangdhar M, Kambhampati C (2010b). Quantification of Similarity using Amplitudes and Firing times of a Hodgkin-Huxley Neuron. *In Electrical Engineering and Applied Computing* (Article in Print).

Sarangdhar M, Kambhampati C (2010c). Stimulus Reconstruction from a Hodgkin-Huxley Neural Response- A Numerical Solution. *In World Congress on Engineering 2010: The 2010*

International Conference of Systems Biology and Bioengineering, London, U.K. 30 June-2 July 2010, Vol. 1, pp 627-632.

Sarangdhar M, Kambhampati C (2010d). Chaotic Oscillations in Hodgkin-Huxley Neural Dynamics: Stimulus Reconstruction and Neural Dynamics Retrieval. *In Electrical Engineering and Applied Computing* (Article in Print).

Sarangdhar M, Kambhampati C (2010e). A numerical model for neural stimulus reconstruction. *Engineering Letters* (Article in Print).

Shepardson D (2009). *Algorithms for inverting Hodgkin-Huxley type neuron models*. PhD diss., Georgia Institute of Technology. http://www.aco.gatech.edu/doc/Shepardson _thesis.pdf, accessed November 2009.

Silani V, Cova L, Corbo M, Ciammola A, Polli E (2004). Stem-cell therapy for Amyotrophic Lateral Sclerosis. *Lancet*, Vol. 364 (9429), pp 200-202.

Slepian D (1976). On Bandwidth. *Proceedings of the IEEE*, 64(3): 292-300.

Stanley GB, SeyedBoloori A (2001). Decoding in neural systems: Stimulus reconstruction from nonlinear encoding. *Proceedings of the 23rd Annula International Conference of the IEEE Engineering in Medicine and Biology Society*, Vols 1-4, Vol. 23, 816-819.

Stanley GB (2001). Recursive stimulus reconstruction algorithms for real-time implementation in neural ensembles. *Neurocomputing*, 38, 1703-1708.

Strange PG (1992). *Brain Biochemistry and Brain Disorders*. Oxford University Press, New York.

Trappenberg TP (2002). *Fundamentals of Computational Neuroscience*. Oxford University Press, New York.

Tuckwell HC (1988). *Introduction to Theoretical Neurobiology - Vol. 1, Linear Cable Theory and Dendritic Structure*. Cambridge University Press, Cambridge.

Mann MD (2008). *Properties of Excitable Membranes: The Spike*. The Nervous System in Action. http://www.unmc.edu/physiology/Mann/mann3b.html Accessed December 2009.

Vieira MF, Kohn AF (2007). Compartmental models of mammalian motoneurons of types S, FR and FF and their computer simulation. *Computers in Biology and Medicine*, 37, 842-860.

Wang XJ, Buzsáki G (1996). Gamma Oscillation by Synaptic Inhibition in a Hippocampal Interneuronal Network Model. *The Journal of Neuroscience*, 16(20): 6402-6413.

Wilson HR (1999a). S*pikes, Decisions and Actions – The dynamical foundations of neuroscience*. Oxford University Press Inc., New York.

Wilson HR (1999b). Simplified dynamics of human and mammalian neocortical neurons. *J. Theoretical Biol.* Vol. 200 (4), 375-388.

Wilson HR, Cowan JD (1973). A mathematical theory of the functional dynamics of cortical and thalamic nervous tissue. *Kybernetik*, 13, 55-80.

Wilson HR, Cowan JD (1972). Excitatory and inhibitory interactions in localized populations of model neurons. *Biophysical Journal*, 12, 1-24.

Wong J (2009). The Pursuit of Happiness. *The Science Creative Quarterly*. http://www.scq.ubc.ca/the-pursuit-of-happiness-aka-it-appears-that-the-writer-wrote-about-bananas-after-eating-a-few-too-many/ Accessed November 2010.

Appendices

A Neuron Design

A.1 Sofware Platform

Matlab™ (versions 7.1-7.6) was used as the software platform for the computational simulations in this thesis. The choice of Matlab was based on its efficiency, speed, memory allocation and numeric data handling and prior experience of scripting in Matlab. A PC with Windows XP operating on a Pentium IV 3GHz processor and 4GB of RAM was used for this research.

A.2 Design

The computational design of the neuron is defined by its ion concentrations, physiological and biochemical properties as described in literature (Hodgkin and Huxley, 1952; Hasegawa, 2000; Trappenberg, 2002).

A.3 Implementation

The neuron simulations, implemented as a time series, follow the norm to compute neural responses for various stimuli. The output neural voltage was computed over a time-window with iterations every 0.01ms. A sample code that shows the computation of neural output is shown below:

```
%Matlab code simulation of the Hodgkin Huxley Model
%Experiment conducted as Hideo Hasegawa - Responses of a Hodgkin Huxley
%neuron to various types of spike-train inputs
clear; % clears the workspace
```

```
clf; % clears the figures
% Maximal conductance (in units of mS/cm^2);1=K+, 2= Na+, 3= Leakage;
g(1)=36;
g(2)=120;
g(3)=0.3;
% Equilibrium potential for ions
E(1)=-77;
E(2)=50;
E(3)=-54.5;
% Initialization of variables
I_ext=0;
V=-10;
x=zeros(1,3);
x(3)=1;
t_rec=0;
% Time step for Integration
dt=0.01;
% Integration with Euler Method
for t=-30:dt:100
   if t==10; I_ext=10+random('Normal',0,0.025); end % turn on external current at t=10
   if t==295; I_ext=0;  end % turn off external current at t=40
   %alpha functions used in the model
   alpha(1)=0.01*(V+55)/(1-exp(-(V+55)/10));
   alpha(2)=0.1*(V+40)/(1-exp(-(V+40)/10));
   alpha(3)=0.07*exp(-(V+65)/20);
   %beta functions used in the model
   beta(1)=0.125*exp(-(V+65)/80);
   beta(2)=4*exp(-(V+65)/18);
   beta(3)=1/(1+exp(-(V+35)/10));
%time constant Tau_x and the equilibrium value x_infty
   tau=1./(alpha+beta);
   x_infty=alpha.*tau;
   %Integration with Euler Method
   x=(1-dt./tau).*x+dt./tau.*x_infty;
```

```
    %Calculate the actual conductance g with given n,m,h
    gnmh(1)=g(1)*x(1)^4;
    gnmh(2)=g(2)*x(2)^3*x(3);
    gnmh(3)=g(3);
    %The internal ion current
    I=gnmh.*(V-E);
    %Update the membrane voltage
    V=V+dt*(I_ext-sum(I));
    %Record some variables for plotting after equilibration
    if t>=0;
      t_rec=t_rec+1;
      x_plot(t_rec)=t;
      y_plot(t_rec)=V;
    end
  end % the end of the time loop
  plot(x_plot,y_plot); xlabel('Time'); ylabel('Voltage');
```

This Matlab™ script computes the neural voltage over a 130ms time-window. The neuron enters into an asymptotic state within the first few milliseconds, which is required for the steady-state analysis of the gating variables.

A.4 Testing

The neural response is a plot of the neural voltage against time (fig. A.1). The script in section A.3 generates the plot given below, which identifies the correct implementation of the neuron. See Trappenberg (2002) for identical results.

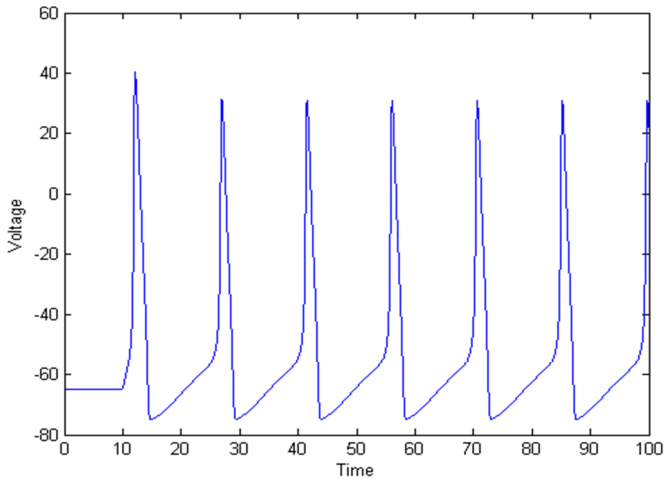

Figure A.1: The neural voltage for a constant-current stimulus shows that neuron exhibiting alternating depolarized (upward rise)-hyperpolarized (downward slope) states.

A.5 Algorithms

The algorithms for computational simulations in each chapter are listed as individual sections below. These algorithms explain the logical approach used to perform *in silico* experiments.

A.5.1 Chapter 3

1) Start

2) Stimulate two identical Hodgkin-Huxley (HH) neurons H_1 and H_2, using synaptic periodical stimuli P_1 (variable ISI) and P_2 (fixed ISI).

3) Record corresponding neural responses R_1 and R_2.

4) Estimate similarity using neural firing times (coincidence factor).

5) Plot coincidence factor against the ISI of P_1.

6) Repeat steps 2-5 across the time window. The objective is to get a plot of similarity estimates using the coincidence factor approach, where the coincidence factor for each pair of neural responses is plotted against the ISI of P_1. As the ISI of P_2 is fixed across the entire time window, the plot is consistent for all P_1 stimuli.

7) End.

A.5.2 Chapter 4

1) Start

2) Stimulate two identical Hodgkin-Huxley (HH) neurons H_1 and H_2, using synaptic periodical stimuli P_1 (variable ISI) and P_2 (fixed ISI).

3) Record corresponding neural responses R_1 and R_2.

4) Estimate similarity using both amplitude and firing time coincidences ($\Gamma_{chaotic}$).

5) Plot $\Gamma_{chaotic}$ against the ISI of P_1. Compare this estimate of similarity against the corresponding estimate given by coincidence factor in Chapter 3.

6) Repeat steps 2-5 across the time window. The objective is to get a plot of similarity estimates using the coincidence factor and $\Gamma_{chaotic}$, which will aid comparison between corresponding similarities for a pair of neural responses.

7) End.

A.5.3 Chapter 5

A.5.3.1 : Model Validation

1) Start

2) Stimulate an IF neuron by a supra-threshold stimulus as in eq. (5.8).

3) Stimulate an HH neuron by a synaptic stimulus as given by eq. (5.9).

4) Compare the responses of the IF and HH neuron using a) coincidence factor (Γ) and b) $\Gamma_{chaotic}$.

5) Repeat steps 2-4 by varying the noise in the stimuli.

6) End

A.5.3.2 : Constant current stimulus and $\Gamma_{chaotic}$

1) Start

2) Stimulate two identical Hodgkin-Huxley (HH) neurons H_1 and H_2, using constant current stimuli with strength 8μA.

3) Compare the responses of the two neurons using a) coincidence factor (Γ) and b) $\Gamma_{chaotic}$.

4) Repeat steps 2 and 3 by increasing the strength of the stimuli by 1μA .

5) End

A.5.3.3 : Energy Content

1) Start

2) Stimulate two identical Hodgkin-Huxley (HH) neurons H_1 and H_2, using synaptic periodical stimuli P_1 (variable ISI) and P_2 (fixed ISI).

3) Record corresponding neural responses R_1 and R_2.

4) Calculate the Energy Difference Minimum (ε_{min}) using eq. (5.10).

5) Repeat steps 2-4 across the time window. This, according to Slepian's principle, gives the minimum difference in the energy required to classify the two neural responses as distinct.

6) End

A.5.4 Chapter 6

1) Start

2) For a known neuron, record any neural response $V(t)$ whose stimulus, say $I(t)$, requires to be reconstructed

3) Inject a supra-threshold stimulus, $I_s(t_s)$ for a small time duration t_s

4) Record the corresponding voltage trace generated, $v_s(t_s)$

5) Retrieve the maximal conductances using $v_s(t_s)$, equations (6.2-6.9) and $I_s(t_s)$ as the external stimulus

6) Using the approximated maximal conductances, g'_{Na}, g'_K and g'_L, solve the HH equations using the recorded original neural response $V(t)$ and the stimulus as the only unknown to get the reconstructed stimulus $I'(t)$.

7) End

B Binary Clustering

Two independent supra-threshold stimulating currents (10μA/cm2 + a random value from a Gaussian distribution with zero mean and standard deviation 0.025, fig. 1) injected into the HH neuron generate neural responses (fig. 2). The ion conductances of the neuron are as listed below.

	Max. conductance (mS/cm2)	Reversal Potential (mV)
Potassium (K)	36	12
Sodium (Na)	120	115
Leakage (Cl)	0.3	10.613

Table 1: The maximal conductances and reversal potentials of the ion channels.

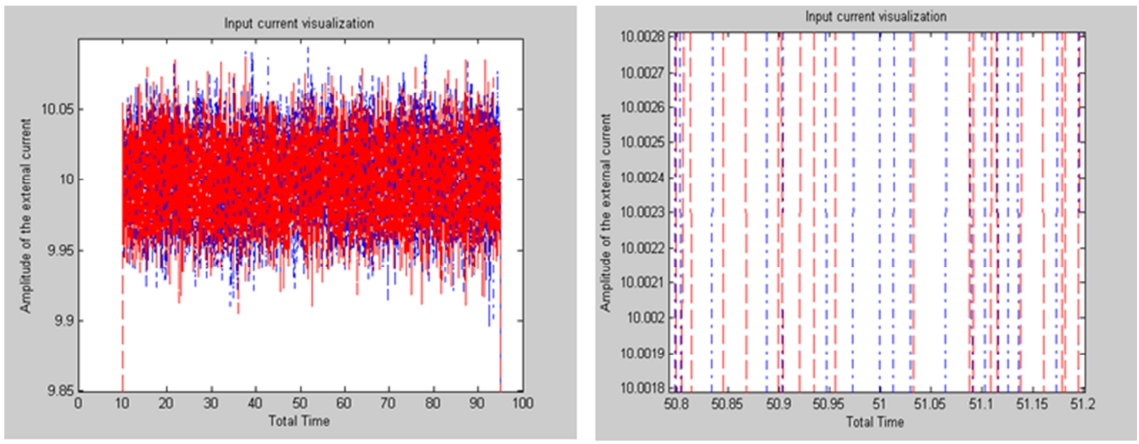

Figure 1: The left panel shows the two currents superimposed with Current 1 dash-dotted (blue) and Current 2 is dashed (red). The right panel shows a magnified version of a section in the left panel. Notice how distinct the two currents are. Both currents are turned on at time t = 10ms and turned off at t = 85ms.The two currents generate two independent spike trains as shown in fig. 2.

The neural responses evoked by these similar stimuli are shown below in fig.2

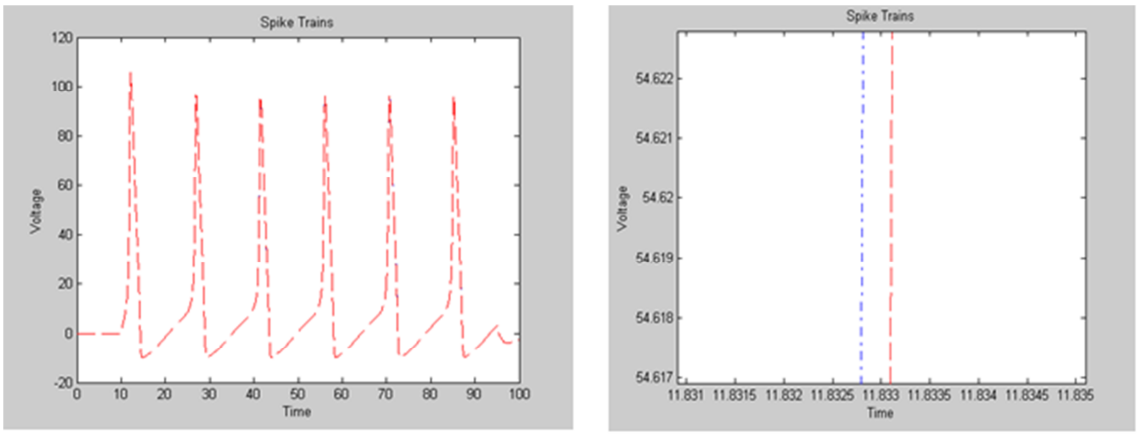

Figure 2: Identical stimuli generate similar neural responses. The neural responses superimposed (left panel) show a high degree of overlap (right panel). The difference in firing times is approximately 0.0006ms

B.1 Cluster Formation

The amplitudes (Amp in mV) and the firing times (Fir in ms) for the two neural responses shown in fig. 2 are

Amp1 = [105.6974 96.4448 96.0727 96.0438 96.039 96.0427]

Amp2 = [105.6962 96.4472 96.0737 96.0486 96.0422 96.0369]

Fir1 = [1210 2696 4154 5610 7066 8522]

Fir2 = [1210 2696 4154 5610 7066 8522]

Normalising the values by using a standard approach

$$Z = \frac{X - mean(X)}{standard\ deviation\ (X)} \quad (1)$$

where X is the input vector, gives a centred scaled version of X, known as the Z-scores of X.

Table 2 shows the original and the normalised values of the spike amplitudes and the neural firing times.

Spikes	Original Values					Normalised Values			
	Amp1	Fir1	Amp2	Fir2		Amp1	Fir1	Amp2	Fir2
1	105.6974	1210	105.6962	1210		2.0396	-1.3416	2.0395	-1.3416
2	96.4448	2696	96.4472	2696		-0.3270	-0.7978	-0.3267	-0.7978
3	96.0727	4154	96.0737	4154		-0.4222	-0.2643	-0.4222	-0.2643
4	96.0438	5610	96.0486	5610		-0.4296	-0.2685	-0.4287	-0.2685
5	96.039	7066	96.0422	7066		-0.4308	0.8012	-0.4303	0.8012
6	96.0427	8522	96.0369	8522		-0.4299	1.3340	-0.4317	1.3340

Table 2: Transformation spike points to a normalised scale

The spike points are represented as Objects in space. The spike train set for each train is represented as a two-dimensional array of amplitudes and firing times.

B.2 Spike Train Set 1

X_1 = [2.0395 -1.3416;-0.3270 -0.7978;-0.4222 -0.2643;-0.4296 -0.2685;-0.4308 0.8012;-0.4299 1.3340]

The Euclidean distance between each of these Objects is given by

$$d_{rs}^2 = (x_r - x_s)(x_r - x_s)' \quad (2)$$

where x_r and x_s represent the spike points and the matrix Y_1 with each element represents the distance between a pair of objects.

Y_1 =

Columns 1 through 8

2.4282 2.6871 2.6922 3.2702 3.6410 0.5419 0.5392 1.6024

Columns 9 through 15

2.1343 0.0085 1.0655 1.5983 1.0697 1.6025 0.5328

The value in the first column, 2.4282, is the distance of spike point 1 from spike point 2, the value in column 2 is the distance between spike point 1 and spike point 3 and so on. The following matrix will give a clear picture of the individual distances between the spike points.

ans =

	1	2	3	4	5	6
1	0	2.4282	2.6871	2.6922	3.2702	3.6410
2	2.4282	0	0.5419	0.5392	1.6024	2.1343
3	2.6871	0.5419	0	0.0085	1.0655	1.5983
4	2.6922	0.5392	0.0085	0	1.0697	1.6025
5	3.2702	1.6024	1.0655	1.0697	0	0.5328
6	3.6410	2.1343	1.5983	1.6025	0.5328	0

The distance between spike point 1 and itself is zero. Similarly, the distance between spike point 5 and spike point 6 is 0.5328 (5th row and 6th column)

B.2.1 Formation of Clusters

Once the proximity between the spike points in the data set has been computed, the spike points can be grouped into clusters using the nearest neighbour approach as follows

$$d(r,s) = \min(dist(x_{ri}, x_{sj})), i \in (1,..., n_r), j \in (1,...n_s) \quad (3)$$

where, n_r is the number of spike points in cluster r and n_s is the number of spike points in cluster s, and x_{ri} is the i^{th} object in cluster r.

The matrix Z_1 depicts the cluster information

$Z_1 =$

3.0000 4.0000 0.0085

5.0000 6.0000 0.5328

2.0000 7.0000 0.5392

8.0000 9.0000 1.0655

1.0000 10.0000 2.4282

Cluster formation takes place systematically. Column 1 and 2 are the spike points, which have been linked whereas column 3 represents the distance between them. Spike points 3 and 4 are grouped together. This cluster is numbered as 7. Spike points 5 & 6 are linked together by 0.5328. This cluster is numbered as 8 and so on. When two objects are clustered into a new cluster, it must assign the cluster a new unique index value starting with the value *m+1*, where *m* is the number of objects in the original data set. The *nearest neighbour* approach is adopted to calculate the distances between old and new clusters.

B.2.2 Plotting the Cluster Tree

The hierarchical, binary cluster tree created above is most easily understood when viewed graphically. In fig. 3, the numbers along the horizontal axis represent the indices of the objects/spike-points in the original data set. The links between objects are represented as upside-down U-shaped lines. The height of the U indicates the distance between the objects. For example, the link representing the cluster containing objects 3 and 4 has a height of 0.0085. The link representing the cluster that groups object 2 together with objects 3, 4, and 2, (which are already clustered as object 9) has a height of 0.5392. The height represents the distance computed between objects 2 and 8.

B.2.3 Evaluating Cluster Information

After linking the objects in a data set into a hierarchical cluster tree, it is required to verify that the distances (that is, heights) in the tree reflect the original distances accurately and investigate the natural divisions that exist among links between objects. This can be understood by determining the cophenetic correlation coefficient and inconsistency coefficient.

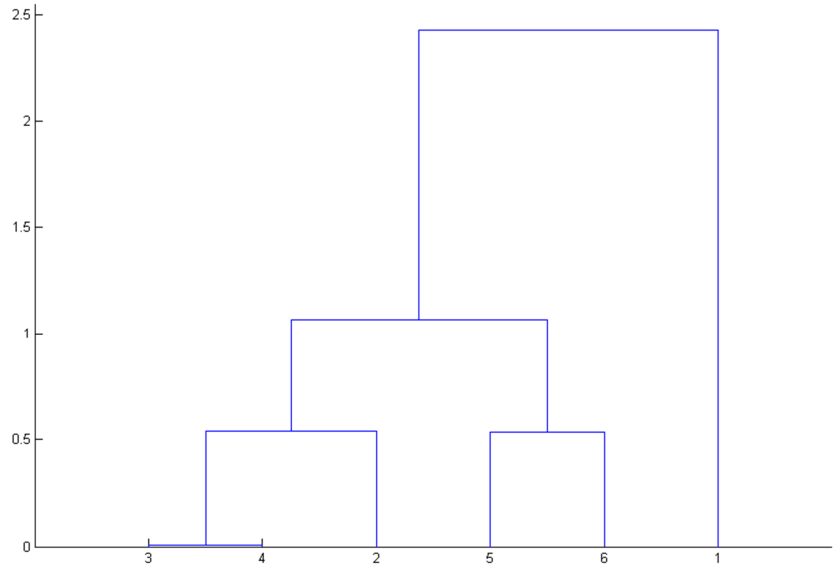

Figure 3: Cluster information for spike train 1

In a hierarchical cluster tree, any two objects in the original data set are eventually linked together at some level. The height of the link represents the distance between the two clusters that contain those two objects. This height is known as the cophenetic distance between the two objects. One way to measure how well the cluster tree generated reflects the data is to compare the cophenetic distances with the original distance data generated. If the clustering is valid, the linking of objects in the cluster tree should have a strong correlation with the distances between objects in the distance vector. The *cophenet* function in MATLAB compares these two sets of values and computes their correlation, returning a value called the cophenetic correlation coefficient. The closer the value of the cophenetic correlation coefficient is to 1, the more accurately the clustering solution reflects your data.

```
C1=cophenet(Z1,Y1)

C1 =

   0.9362
```

This shows that the clustering solution is very accurate. One way to determine the natural cluster divisions in a data set is to compare the height of each link in a cluster tree with the heights of neighbouring links below it in the tree. A link that is approximately the same height as the links below it indicates that there are no distinct divisions between the objects joined at this level of the hierarchy. These links are said to exhibit a high level of consistency, because the distance between the objects being joined is approximately the same as the distances between the objects they contain. On the other hand, a link whose height differs noticeably from the height of the links below it indicates that the objects joined at this level in the cluster tree are much farther apart from each other than their components were when they were joined. This link is said to be inconsistent with the links below it.

In cluster analysis, inconsistent links can indicate the border of a natural division in a data set. The relative consistency of each link in a hierarchical cluster tree can be quantified and expressed as the inconsistency coefficient. This value compares the height of a link in a cluster hierarchy with the average height of links below it. Links that join distinct clusters have a low inconsistency coefficient; links that join indistinct clusters have a high inconsistency coefficient.

To generate a listing of the inconsistency coefficient for each link in the cluster tree, use the *inconsistent* function in MATLAB By default, the inconsistent function compares each link in the cluster hierarchy with adjacent links that are less than two levels below it in the cluster hierarchy, known as the depth of the comparison. The objects at the bottom of the cluster tree, called leaf nodes, that have no further objects below them, have an inconsistency coefficient of zero. Clusters that join two leaves also have a zero inconsistency coefficient.

I1 =

0.0085	0	1.0000	0
0.5328	0	1.0000	0
0.2738	0.3752	2.0000	0.7071
0.7125	0.3058	3.0000	1.1546
1.7469	0.9635	2.0000	0.7071

The inconsistent function returns data about the links in an (m-1)-by-4 matrix, whose columns are described in table 3. In the sample output, the first row represents the link between objects 3 and 4. This cluster is assigned the index 7. Because both 3 and 4 are leaf nodes, the inconsistency coefficient for the cluster is zero. The second row represents the

link between objects 5 and 6, both of which are also leaf nodes. This cluster is assigned the index 8.

Column	Description
1	Mean of the heights of all the links included in the calculation
2	Standard deviation of all the links included in the calculation
3	Number of links included in the calculation
4	Inconsistency coefficient

Table 3: Description of columns returned by the inconsistent function in MATLAB

The third row evaluates the link that connects these two clusters, objects 2 and 7. (This new cluster is assigned index 9 in the linkage output). Column 3 indicates that two links are considered in the calculation. Column 1 represents the mean of the heights of these links. The inconsistent function uses the height information output by the linkage function to calculate the mean. Column 2 represents the standard deviation between the links. The last column contains the inconsistency value for these links, 0.7071. It is the difference between the current link height and the mean, normalized by the standard deviation:

(0.5392 - 0.2738) / 0.3752

ans =

0.7071

B.3 Spike Train 2 – Cluster Formation

The spike train set for the train is

$X_2 =$ [2.0395 -1.3416;-0.3267 -0.7978;-0.4222 -0.2643;-0.4287 -0.2685;-0.4303 0.8012;-0.4317 1.3340]

The distance matrix Y_2 is

$Y_2 =$

0	2.4279	2.6871	2.6914	3.2698	3.6422
2.4279	0	0.5420	0.5390	1.6024	2.1344
2.6871	0.5420	0	0.0077	1.0655	1.5983
2.6914	0.5390	0.0077	0	1.0697	1.6025
3.2698	1.6024	1.0655	1.0697	0	0.5328
3.6422	2.1344	1.5983	1.6025	0.5328	0

The matrix Z_2 that depicts the cluster information

$Z_2 =$

3.0000	4.0000	0.0077
5.0000	6.0000	0.5328
2.0000	7.0000	0.5390
8.0000	9.0000	1.0655
1.0000	10.0000	2.4279

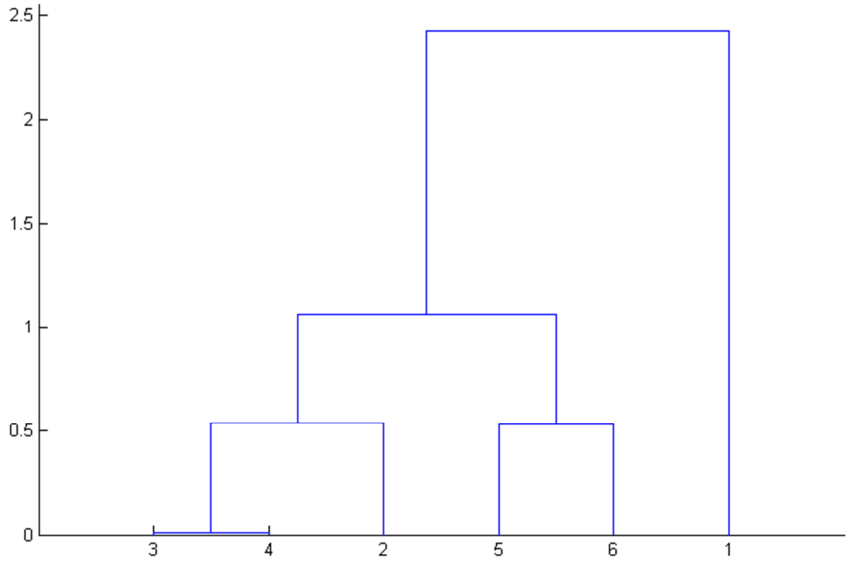

Figure 4: Cluster information for spike train 2

B.3.1 Cophenetic correlation coefficient for Spike Train 2

C2=cophenet(Z2,Y2)

C2 =

0.9361

This shows that the clustering solution is very accurate. Also, C2 is very close to spike train 1's cophenet correlation coefficient.

B.3.2 Inconsistency Coefficient

I2 =

0.0077	0	1.0000	0
0.5328	0	1.0000	0
0.2734	0.3757	2.0000	0.7071
0.7125	0.3058	3.0000	1.1546
1.7467	0.9633	2.0000	0.7071

This is same as I1 (inconsistency coefficient for spike train1). This shows a similarity between the two spike trains. In addition, the same spike points are grouped together in clusters for both the trains.

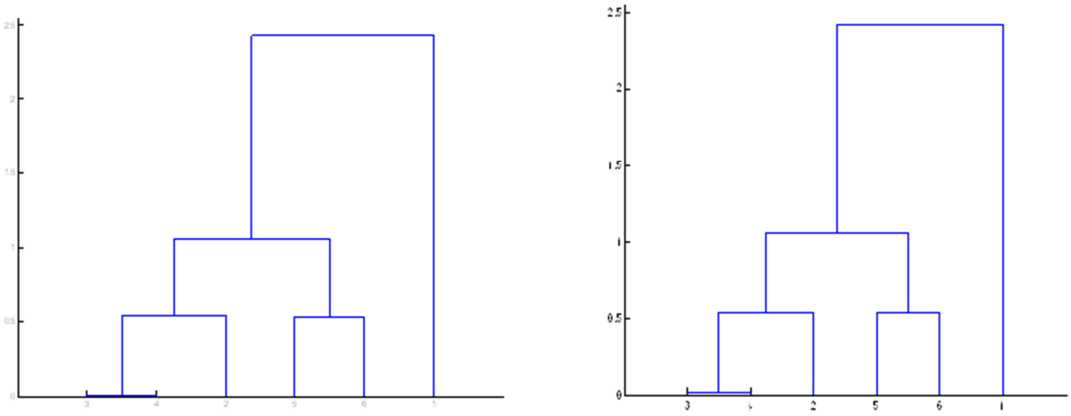

Figure 5: Clustering information for spike trains 1 & 2 indicating almost identical features.

The table below shows the spike points/objects used to form clusters for both the spike trains. The same spike points are used for clustering indicating a similarity in the spike train.

	Spike train 1			Spike train 2	
Spike points used to form clusters	3	4		3	4
	5	6		5	6
	2	7 {3 & 4}		2	7 {3 & 4}
	8 {5 & 6}	9 {2 & 7}		8 {5 & 6}	9 {2 & 7}
	1	10 {8 & 9}		1	10 {8 & 9}

Table 4: Cluster Solution and Linkages